europhysicsnews

SPECIAL ISSUE & DIRECTORY

Nonextensive statistical mechanics: new trends, new perspectives

36/6
2005

November/December 2005
Institutional subscription price:
99 euros per year

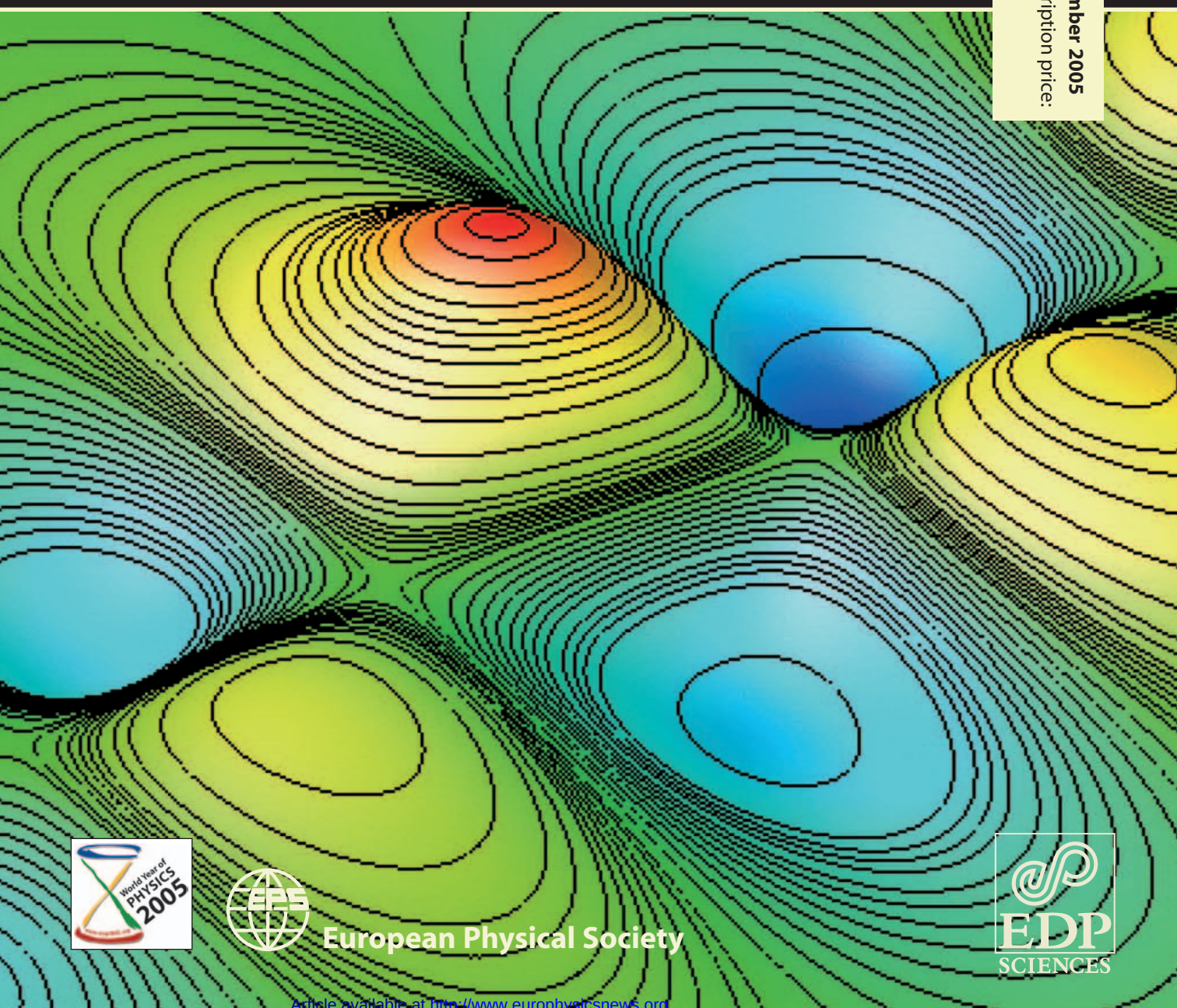

European Physical Society

EDP SCIENCES

Article available at http://www.europhysicsnews.org

europhysicsnews

Volume 36 Number 6
November/December 2005

Cover picture: Fingering is a generic phenomenon that results from the destabilization of the interface between two fluids with different mobilities. But before any fingering pattern becomes visible, precursor phenomena can be detected by measuring local fluctuations whose spatial structure appears of a landscape of *q*-Gaussian "hills and wells" (simulation by P. Grosfils).
See the article by B.M. Boghosian and J.P. Boon p.192

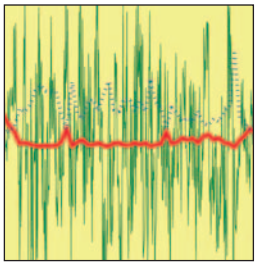

▲ PAGE 189

Atmospheric turbulence and superstatistics

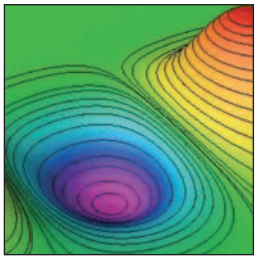

▲ PAGE 192

Lattice Boltzmann and nonextensive diffusion

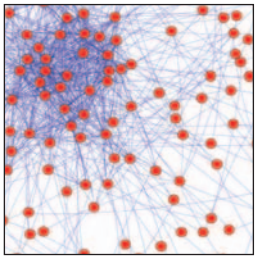

▲ PAGE 218

Nonextensive statistical mechanics and networks

FEATURES

185 Special issue overview: nonextensive statistical mechanics: new trends, new perspectives
Jean Pierre Boon and Constantino Tsallis

186 Extensivity and entropy production
Constantino Tsallis, Murray Gell-Mann and Yuzuru Sato

189 Atmospheric turbulence and superstatistics
C. Beck, E.G.D. Cohen and S. Rizzo

192 Lattice Boltzmann and nonextensive diffusion
Bruce M. Boghosian and Jean Pierre Boon

194 Relaxation and aging in a long-range interacting system
Francisco A. Tamarit and Celia Anteneodo

197 Noise induced phenomena and nonextensivity
Horacio S. Wio

202 Nonextensive thermodynamics and glassy behaviour
Andrea Rapisarda and Alessandro Pluchino

206 Complexity of seismicity and nonextensive statistics
Sumiyoshi Abe, Ugur Tirnakli and P.A. Varotsos

208 S_q entropy and self-gravitating systems
A.R. Plastino

211 Nuclear astrophysical plasmas: ion distribution functions and fusion rates
Marcello Lissia and Piero Quarati

214 Critical attractors and q-statistics
A. Robledo

218 Nonextensive statistical mechanics and complex scale-free networks
Stefan Thurner

221 Nonextensive statistical mechanics: implications to quantum information
A.K. Rajagopal and R.W. Rendell

224 Entropy and statistical complexity in brain activity
A. Plastino and O.A Rosso

228 Long-range memory and nonextensivity in financial markets
Lisa Borland

NEWS, VIEWS AND ACTIVITIES

231 Conferences in 2006

232 Pictures from EPS 13

234 Directory

contents

europhysicsnews

europhysicsnews is the magazine of the European physics community. It is owned by the European Physical Society and produced in cooperation with EDP Sciences. The staff of EDP Sciences are involved in the production of the magazine and are not responsible for editorial content. Most contributors to **europhysicsnews** are volunteers and their work is greatly appreciated by the Editor and the Editorial Advisory Board.
europhysicsnews is also available online at: **www.europhysicsnews.com**

Editor **Claude Sébenne** EMAIL: Claude.Sebenne@impmc.jussieu.fr

Science Editor **George Morrison** EMAIL: g.c.morrison@bham.ac.uk

Executive Editor **David Lee** EMAIL: d.lee@uha.fr

Graphic Designer **Xavier de Araujo** EMAIL: designer@europhysnet.org

Directeur de la publication **Jean-Marc Quilbé,** EDP Sciences

36/6
2005
November/December 2005
Institutional subscription price:
99 euros per year

Schedule

Six issues will be published in 2005. The magazine is distributed in the second week of January, March, May, July, September, November. A directory issue with listings of all EPS officials is published once a year.

Editorial Advisory Board

Chairman George Morrison
Members Alexis Baratoff, Giorgio Benedek, Marc Besançon, Carlos Fiolhais, Bill Gelletly, Frank Israel, Thomas Jung, Karl-Heinz Meiwes-Broer, Jens Olaf Pepke Pedersen, Jerzy Prochorow, Jean-Marc Quilbé, Christophe Rossel, Claude Sébenne, Wolfram von Oertzen

Production and Advertising

Agnès Henri

Address EDP Sciences
17 avenue du Hoggar, BP 112,
PA de Courtabœuf,
F-91944 Les Ulis Cedex A • France
Tel +33 169 18 75 75 • **Fax** +33 169 28 84 91
Web www.edpsciences.org

Printer Printer Rotofrance • Lognes, France
Dépôt légal: Novembre 2005

Subscriptions

Individual Ordinary Members of the European Physical Society receive **europhysicsnews** free of charge. Members of EPS National Member Societies receive Europhysics News through their society, except members of the Institute of Physics in the United Kingdom and the German Physical Society who receive a bimonthly bulletin. The following are subscription prices available through EDP Sciences. **Institutions** 99 euros (VAT included, European Union countries); 99 euros (the rest of the world). **Individuals** 58 euros (VAT included, European Union countries); 58 euros (the rest of the world). Contact subscribers@edpsciences.com or visit www.epdsciences.com

ISSN 0531-7479
ISSN 1432-1092 (electronic edition)

EPS Executive Committee

President	Ove Poulsen, *Aarhus*
Vice-President	Martin C.E. Huber, *Villigen*
Secretary	Peter Melville, *London*
Treasurer	Maria Allegrini, *Pisa*
Members	Gerardo Delgado Barrio, *Madrid*
	Berndt Feuerbacher, *Cologne*
	Paul Hoyer, *Helsinki*
	Hennie Kelder, *Eindhoven*
	Maciej Kolwas, *Warsaw*
	Anne-Marie Levy, *Copenhagen*
	Zenonas Rudzikas, *Vilnius*

EPS Secretariat

Secretary General	David Lee
Administrative Secretary	Sylvie Loskill
Accountant	Pascaline Padovani
EPS Conferences	Patricia Helfenstein
	Ophélia Fornari
Computer Engineer	Ahmed Ouarab
Graphic Designer	Xavier de Araujo
Europhysics Letters	Yoanne Sobieski
	Gina Gunaratnam
	Alexandre Berthereau

Address EPS • 6 rue des Frères Lumière
BP 2136 • F-68060 Mulhouse Cedex • France
Tel +33 389 32 94 40 • **Fax** +33 389 32 94 49
Web www.eps.org

The Secretariat is open 08.00–17.00 CET except weekends and French public holidays.

EDP Sciences

Managing Director Jean-Marc Quilbé

Address EDP Sciences
17 avenue du Hoggar, BP 112,
PA de Courtabœuf,
F-91944 Les Ulis Cedex A • France
Tel +33 169 18 75 75 • **Fax** +33 169 28 84 91
Web www.edpsciences.org

Foreword

It is our pleasure to welcome Jean Pierre Boon and Constantino Tsallis as guests Editors for the present Special Issue of Europhysics News on "Nonextensive Statistical Mechanics". They did a great job not only in selecting an impressive set of distinguished authors but also in writing the introductory Editorial and in each being a co-author of one of the contributions. The subject is difficult and could not go without a higher proportion of equations than usual in EPN: our thanks go to the EPN designer who had to face a heavier task than usual. It is sometimes necessary to address arduous developments to cover recent progress in Physics. This time, EPN will ask its readers to make an effort. It is always rewarding. The guests Editors were so efficient that the collected material passes largely the size of a standard EPN issue. We are grateful to the Publisher for accepting to accommodate all the articles in a single volume. It will make of this Special Issue the general reference work on "nonextensive statistical mechanics". Back to the usual mix of wide-ranging Features and News next time!

The Editors

Special issue overview Nonextensive statistical mechanics: new trends, new perspectives

Jean Pierre Boon [1] *and Constantino Tsallis* [2,3]
[1] *CNLPCS, Campus Plaine – CP 231 Université Libre de Bruxelles, B-1050 Bruxelles, Belgium*
[2] *Santa Fe Institute, 1399 Hyde Park Road, Santa Fe, New Mexico 87501, USA*
[3] *Centro Brasileiro de Pesquisas Fisicas, Xavier Sigaud 150, 22290-180 Rio de Janeiro-RJ, Brazil*

Boltzmann-Gibbs (BG) statistical mechanics is one of the monuments of contemporary physics. It establishes a remarkably useful bridge between the mechanical microscopic laws and classical thermodynamics. It does so by advancing a specific connection, $S_{BG} = -k\sum_{i=1}^{W} p_i \ln p_i$ in its discrete version, of the entropy a la Clausius with the microscopic states of the system. However, the *BG* theory is not universal. It has a delimited domain of applicability, as any other human intellectual construct. Outside this domain, its predictions can be slightly or even strongly inadequate. No surprise about that. That theory centrally addresses the very special stationary state denominated *thermal equilibrium.* This macroscopic state has remarkable and ubiquitous properties, hence its fundamental importance. The deep foundation of this state and of 27-year-old Boltzmann's famous *Stosszahlansatz* ("molecular chaos hypothesis") in 1871 lie on nonlinear dynamics, more specifically on *strong* chaos, hence mixing, hence ergodicity. However many important phenomena in natural, artificial, and even social systems do not accomodate with this simplifying hypothesis. This is particularly frequent in physical sciences as well as in biology and economics, where *non-equlibrium* stationary states are the common rule. Then, at the microscopic dynamical level, strong chaos is typically replaced by its *weak* version, when the sensitivity to the initial conditions grows not exponentially with time, but rather like a power-law.

A question then arises naturally, namely: *Is it possible to address some of these important - though anomalous in the BG sense - situations with concepts and methods similar to those of BG statistical mechanics?* Many theoretical, experimental and observational indications are nowadays available that point towards the affirmative answer. A theory which appears to satisfactorily play that role is *nonextensive statistical mechanics* and its subsequent developments. This approach, first proposed in 1988, is based on the generalization of the *BG* entropy by the expression

$$S_q = k\sum_{i=1}^{W} p_i \ln_q(1/p_i) \equiv k\frac{1-\sum_{i=1}^{W} p_i^q}{q-1}$$

with index $q \in \mathcal{R}$ and $S_1 = S_{BG}$, i.e. the *BG* theory is contained as the particular case $q = 1$ (see the Box). S_q shares with S_{BG} a variety of thermodynamically and dynamically important properties. Among these we have *concavity* (relevant for the thermodynamical stability of the system), *experimental robustness* (technically known as Lesche-stability, and relevant for the experimental reproducibility of the results), *extensivity* (relevant for having a natural matching with the entropy as introduced in classical thermodynamics), and *finiteness of the entropy production per unit time* (relevant for a variety of real situations where the system is striving to explore its microscopic phase space in order to ultimately approach some kind of stationary state). This is quite important because it is not easy to find entropic functionals that simultaneously and generically satisfy these four properties. Renyi entropy, for instance, is known to be an interesting form for characterizing multifractals. But it seems inadequate for thermodynamical purposes. Indeed, Renyi entropy satisfies concavity only in the interval $0 < q \leq 1$, and violates, for $q \neq 1$, all the other three properties mentioned above. The extensivity of S_q deserves a special mention. Indeed, if we compose

BASIC QUANTITIES
q-exponential : $\exp_q(x) \equiv [1+(1-q)x]^{\frac{1}{1-q}} \longrightarrow_{q\to 1} e^x$
q-logarithm : $\ln_q(x) \equiv \frac{x^{1-q}-1}{1-q} \longrightarrow_{q\to 1} \ln x$
Boltzmann-Gibbs entropy : $S_{BG} \equiv -k\sum_{i=1}^{W} p_i \ln p_i$
q-entropy : $S_q \equiv k\frac{1-\sum_{i=1}^{W} p_i^q}{q-1} = k\sum_{i=1}^{W} p_i \ln_q(1/p_i) = -k\sum_{i=1}^{W} p_i^q \ln_q p_i \longrightarrow_{q\to 1} S_{BG}$
Escort distribution : $P_i \equiv p_i^q / \sum_{j=1}^{W} p_j^q$
Ensemble q-average : $\langle A\rangle_q \equiv \sum_{i=1}^{W} A_i P_i = \sum_{i=1}^{W} A_i p_i^q / \sum_{j=1}^{W} p_j^q$

◄ **Box:** The two basic functions that appear in Nonextensive Statistical Mechanics are the q-exponential and the q- logarithm with $\ln_q(\exp_q x) = \exp_q(\ln_q x) = x$. They are simple generalizations of the usual exponential and logarithmic functions which are retrieved by performing a $|1-q| << 1$ expansion. Similarly the q-entropy generalizes the standard Boltzmann-Gibbs entropy. The escort distribution is a generalization of the usual ensemble averaging function to which it reduces for $q = 1$.

subsystems that are (explicitly or tacitly) probabilistically *independent,* then S_{BG} is *extensive* whereas S_q is, for $q \neq 1$, *nonextensive.* This fact led to its current denomination as "nonextensive entropy". However, if what we compose are subsystems that generate a nontrivial (strictly or asymptotically) scale-invariant system (in other words, with important global correlations), then it is generically S_q for a particular value of $q \neq 1$, *and not* S_{BG}, which is *extensive.* Asking whether the entropy of a system is or is not extensive *without indicating the composition law of its elements,* is like asking whether some body is or is not in movement *without indicating the referential with regard to which we are observing the velocity.*

The overall picture which emerges is that Clausius thermodynamical entropy is a concept which can accomodate with more than one connection with the set of probabilities of the microscopic states. S_{BG} is of course one such possibility, S_q is another one, and it seems plausible that there might be others. The specific one to be used appears to be univocally determined by the microscopic dynamics of the system. This point is quite important in practice. If the microscopic dynamics of the system is known, we can in principle determine the corresponding value of q from first principles. As it happens, this precise dynamics is most frequently unknown for many natural systems. In this case, a way out that is currently used is to check the functional forms of various properties associated with the system and then determine the appropriate values of q by fitting. This has been occasionally a point of – understandable but nevertheless mistaken – criticism against nonextensive theory, but it is in fact common practice in the analysis of many physical systems. Consider for instance the determination of the eccentricities of the orbits of the planets. *If* we knew all the initial conditions of all the masses of the planetary system and had access to a colossal computer, we could in principle, by using Newtonian mechanics, determine a priori the eccentricities of the orbits. Since we lack that (gigantic) knowledge and tool, astronomers determine those eccentricities through fitting. More explicitly, astronomers adopt the mathematical form of a Keplerian ellipse as a first approximation, and then determine the radius and eccentricity of the orbit through their observations. Analogously, there are many complex systems for which one may reasonably argue that they belong to the class that is addressed by nonextensive statistical concepts, but whose microscopic (sometimes even mesoscopic) dynamics is inaccessible. For such systems, it appears as a sensible attitude to adopt the mathematical forms that emerge in the theory, e.g. q-exponentials, and then obtain through fitting the corresponding value of q and of similar characteristic quantities.

Coming back to names that are commonly used in the literature, we have seen above that the expression "nonextensive entropy" can be misleading. Not really so the expression "nonextensive statistical mechanics". Indeed, the many-body mechanical systems that are primarily addressed within this theory include long-range interactions, i.e., interactions that are *not* integrable at infinity. Such systems clearly have a total energy which increases quicker than N, where N is the number of its microscopic elements. This is to say a total energy which indeed is nonextensive.

Acknowledgements

The present special issue of Europhysics News is dedicated to a hopefully pedagogical presentation, to the physics community, of the main ideas and results supporting the intensively explored and quickly evolving nonextensive statistical mechanics. The subjects that we have selected, have been chosen in order to provide a general picture of its present status in what concerns both its foundations and applications. It is our pleasure to gratefully acknowledge all invited authors for their enthusiastic participation.

Extensivity and entropy production

*Constantino Tsallis [1,2], Murray Gell-Mann [1] and Yuzuru Sato [1 * 1]*
Santa Fe Institute, 1399 Hyde Park Road, Santa Fe, New Mexico 87501, USA
[2] Centro Brasileiro de Pesquisas Fisicas, Xavier Sigaud 150, 22290-180 Rio de Janeiro-RJ, Brazil
** tsallis@santafe.edu, mgm@santafe.edu, ysato@santafe.edu*

In 1865 Clausius introduced the concept of entropy, S, in the context of classical thermodynamics. This was done, as is well known, without any reference to the microscopic world. The first connection between these two levels of understanding was proposed and initially explored one decade later by Boltzmann and then by Gibbs. One of the properties that appear naturally within the Clausius conception of entropy is the extensivity of S, i.e., its proportionality to the amount of matter involved, which we interpret, in our present microscopic understanding, as being proportional to the number N of elements of the system. The Boltzmann-Gibbs entropy $S_{BG} \equiv -k\sum_{i=1}^{W} p_i \ln p_i$ (discrete version, where W is the total number of microscopic states, with probabilities $\{p_i\}$, and where k is a positive constant, usually taken to be k_B). S_{BG} satisfies the Clausius prescription under certain conditions. For example, if the N elements (or subsystems) of the system are probabilistically independent, i.e., $p_{i_1,i_2,\ldots,i_N} = p_{i_1}p_{i_2}\ldots p_{i_N}$, we immediately verify that $S_{BG}(N) = NS_{BG}(1)$. If the correlations within the system are close to this ideal situation (e.g., local interactions), extensivity is still verified, in the sense that $S_{BG}(N) \propto N$ in the limit $N \to \infty$. There are however more complex situations (that we illustrate later on) for which S_{BG} is not extensive. The question then arises: *Is it possible, in such complex cases, to have an extensive expression for the entropy in terms of the microscopic probabilities?* The general answer to this question still eludes us. However, for an important class of systems (e.g., asymptotically scale-invariant), one such entropic connection is known, namely

$$S_q = k\frac{1-\sum_{1=1}^{W} p_i^q}{q-1} \quad (q \in \mathcal{R};\ S_1 = S_{BG})\,. \qquad (1)$$

(N = 0)	1	1
(N = 1)	π_{10} π_{11}	1/2 1/2
(N = 2)	π_{20} π_{21} π_{22}	1/3 1/6 1/3
(N = 3)	π_{30} π_{31} π_{32} π_{33}	3/8 5/48 5/48 0
(N = 4)	π_{40} π_{41} π_{42} π_{43} π_{44}	2/5 3/40 1/20 0 0

▲ **Table:** *Left:* Most general set of joint probabilities for N equal and distinguishable binary subsystems for which only the number of states 1 and of states 2 matters, not their ordering. *Right:* Triangle with $\epsilon = 0.5$ and $d = 2$ constructed by modifying the Leibnitz-triangle. In general $q_{sen} = 1-(1/d)$. For $N = 5, 6, \ldots$ a full triangle emerges (on the right side) all the elements of which vanish. For any finite N, the Leibnitz rule is not exactly satisfied, but it becomes asymptotically satisfied for $N \to \infty$. See details in [3].

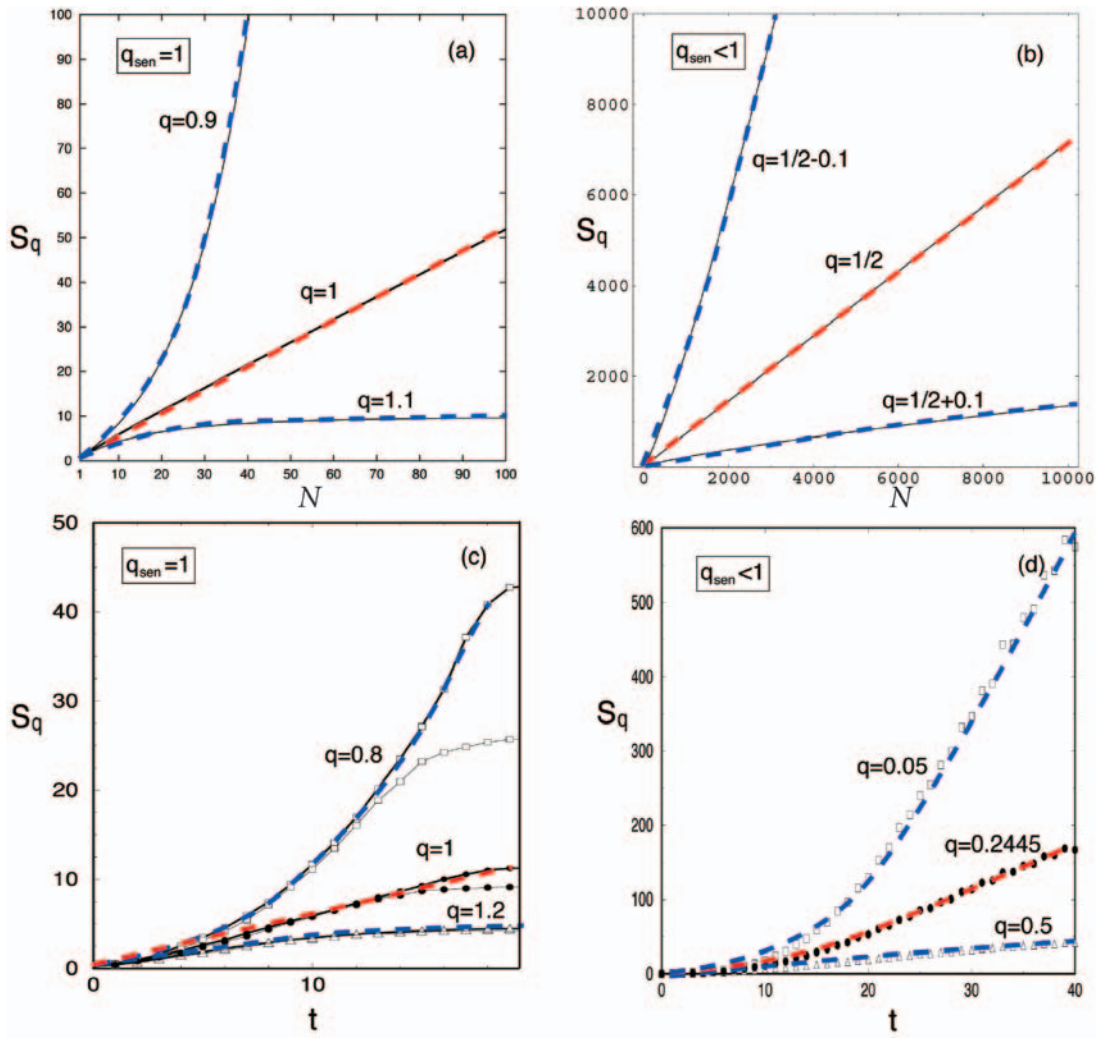

◄ **Fig. 1:** Size-dependence of S_q for probabilistically locally (a) or globally (b) correlated systems (see [3] for details). Time-dependence of S_q for strong (c) and weak (d) chaos (see [4] for details). All the actual data are in black. The coloured dashed lines are visual aids.

This expression was proposed in 1988 [1] as a possible basis for a generalization of Boltzmann- Gibbs statistics currently referred to as *nonextensive statistical mechanics* (see [2] for a set of minireviews). In such a theory the energy is typically nonextensive whether or not the entropy is.

Let us illustrate, for both $q = 1$ and $q \neq 1$, the extensivity of S_q in some examples [3]. Consider a system composed of N identical and distinguishable subsystems (or elements). Let us assume for simplicity that each of those elements corresponds to a probabilistic binary variable which takes values 1 and 2. The joint probabilities of such a system can be represented as in Table I with

$\sum_{n=0}^{N} \frac{N!}{(N-n)!\,n!}\, \pi_{N,n} = 1$ ($\pi_{N,n} \in [0, 1]; N = 1, 2, 3, \ldots; n = 0, 1, \ldots, N$).

Let us impose the scale-invariant constraint $\pi_{N,n} + \pi_{N,n+1} = \pi_{N-1,n}$ ($n = 0, 1, \ldots, N-1; N = 2, 3, \ldots$) . Hereafter we refer to this relation as the *Leibnitz rule.* Indeed, it is satisfied by the *Leibnitz triangle:* $(\pi_{10}, \pi_{11}) = (1/2, 1/2)$, $(\pi_{20}, \pi_{21}, \pi_{22}) = (1/3, 1/6, 1/3)$, $(\pi_{30}, \pi_{31}, \pi_{32}, \pi_{33}) = (1/4, 1/12, 1/12, 1/4)$, etc. By inserting these probabilities into expression (1) we can calculate $S_q(N)$ as shown in Fig.1(a). We see that S_q is *extensive only for* $q = 1$. This characterizes a typical *Boltzmannian system.* Let us now consider the probabilities in the table. They have been constructed by starting with Leibnitz triangle, then gradually introducing a zero probability triangle on its "right" side as indicated in Table I [3]. The total measure associated is then redistributed on a strip on the "left side" whose width is d. The distribution is such that $\pi_{N0} \gg \pi_{N1} \gg \ldots$, the discrepancies becoming larger as $N \to \infty$. It can be shown [3] that this system satisfies the Leibnitz rule not strictly but only asymptotically, i.e., for $N \to \infty$. If we now calculate $S_q(N)$ we get the result shown in Fig. 1(b). We see that now S_q is *extensive only for* $q = 1/2$. In fact, for a large class of probability sets, S_q is extensive only for a special value of q, from now on denoted q_{sen} for reasons that will soon become clear (*sen* stands for *sensitivity*). The property $S_q(A + B)/k = [S_q(A)/k] + [S_q(B)/k] + (1 - q)[S_q(A)/k][S_q(B)/k]$, which led to the term "nonextensive entropy", is valid *only* if the subsystems A and B are explicitly or tacitly assumed to be probabilistically independent.

We shall now address a completely different problem, namely that of *entropy production per unit time.* The system now is a specific one, classical and following deterministic nonlinear dynamics. In particular its value of N is fixed. We consider the $D(N)$-dimensional phase space, and denote by W_0 its Lebesgue measure. We then make a partition of it into small cells whose linear size is ϵ. The total number $W(N) \gg 1$ of cells (designated by $i = 1, 2, \ldots, W(N)$) is given by $W(N) \propto W_0/\epsilon^{D(N)}$ with $D(N) \propto N$ ($N \to \infty$). If the phase space is a $D(N)$-dimensional hypercube, then $W(N) = W_0/\epsilon^{D(N)}$. If the system is a classical Hamiltonian one, then $D(N) \sim 2\, d_s N$ ($N \to \infty$), where $d_s \equiv$ *space dimension.*

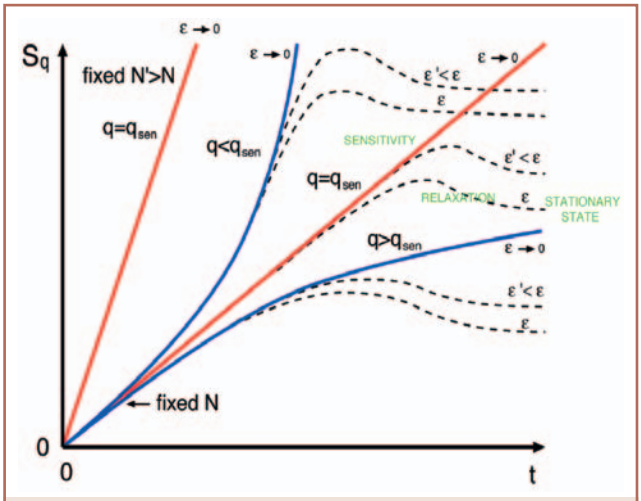

▲ **Fig. 2:** Schematic time-dependence of S_q for various degrees of fine-graining ϵ. We are disregarding in this scenario the influence of possible averaging over initial conditions that might be necessary or convenient.

We choose one of those cells and in it we randomly pick $M \gg 1$ initial conditions. As time t (assumed discrete, i.e., $t = 0, 1, 2, \ldots$) evolves, these M points spread around into $\{M_i(t)\}$ with $\sum_{i=1}^{W(N)} M_i(t) = M$. We can then define a set of probabilities $\{p_i(t)\}$ by $p_i \equiv M_i(t)/M$. With these probabilities we can calculate $S_q(N, t; \epsilon, M)$ for that particular initial cell. Then, depending on our focus, we may or may not average over all or part of the possible initial cells (both situations have been analyzed in the literature). We consider now two different cases, namely *strong chaos* (i.e., the maximal Lyapunov exponent is *positive*), and *weak chaos* (i.e., the maximal Lyapunov exponent vanishes). Both are illustrated in Figs. 1(c) and 1(d) for a very simple system, namely the logistic map $x_{t+1} = 1 - a x_t^2$ with $0 \le a \le 2$, and $-1 \le x_t \le 1$. For infinitely many values of the control parameter a (e.g., $a = 2$), we have strong chaos (this is the case in Fig. 1(c) with $a = 2$). But for other (infinitely many) values of a, we have weak chaos (this is the case in Fig. 1(d) with $a = 1.401155\ldots$). As we can see, it is quite remarkable how strongly similar all four figures 1 are. This suggests the following *conjecture:*

$$\lim_{M\to\infty} S_{q_{sen}}(N, t, \epsilon, M) \sim A N s_{q_{sen}}(t, \epsilon) \quad (t = 0, 1, 2, \ldots; t >> 1;\ N >> 1)\,, \quad (2)$$

as schematised in Fig. 2. (A is a positive constant.) We emphasize that this conjecture is built to some extent upon observations made on the time-dependence of *low*-dimensional systems, such as the logistic map and similar dissipative maps ([5] and references therein) as well as two-dimensional conservative maps [6]. Whether similar behavior indeed holds for the time-dependence of *high*-dimensional dissipative or Hamiltonian systems with $N \gg 1$ obviously remains to be checked.

Conjecture (2) has two consequences. The first of them is that, since by definition of $_{q_{sen}}$ it is $\lim_{\epsilon\to 0} S_{q_{sen}}(t, \epsilon) \sim K_{q_{sen}} t$, we have that $\lim_{\epsilon\to 0} \lim_{M\to\infty} S_{q_{sen}}(N, t; \epsilon, M) \sim A K_{q_{sen}} N t$. This means, interestingly enough, that N and t play similar roles. The second consequence concerns the case when we have a fine but *finite* graining ϵ, for example that imposed by quantum considerations. Then we typically expect the expressions $\lim_{N\to\infty} \lim_{t\to\infty} \lim_{M\to\infty} \frac{S_{q_{sen}}(N, t, \epsilon, M)}{Nt}$ and $\lim_{t\to\infty} \lim_{N\to\infty} \lim_{M\to\infty} \frac{S_{q_{sen}}(N, t, \epsilon, M)}{Nt}$ to coincide for typical $q = 1$ systems, and to differ for more complex systems ($q \neq 1$), as might well be the case for long-range-interacting Hamiltonians [7].

Let us illustrate, for a one-dimensional map, an important property associated with Eq. (2). The sensitivity ξ to the initial conditions is defined through $\xi \equiv \lim_{\Delta x(0)\to 0} \Delta x(t)/\Delta x(0)$, where $\Delta x(0)$ is the discrepancy of two initial conditions. For a wide class of one-dimensional systems we have the upper bound $\xi = e_{q_{sen}}^{\lambda_{q_{sen}} t}$, where $e_q^x \equiv [1+(1-q)x]^{1/(1-q)}$ ($e_1^x = e^x$), and $\lambda_{q_{sen}}$ a q-generalised Lyapunov coefficient . The property we referred to is that the entropy production per unit time $K_{q_{sen}}$ satisfies $K_{q_{sen}} = \lambda_{q_{sen}}$ [8]. This generalises, for $q \neq 1$, a relation totally analogous to the Pesin identity, which plays an important role in strongly chaotic systems (i.e., $q_{sen} = 1$). It is clear that K_q is a concept closely related to the so called Kolmogorov-Sinai entropy. They frequently, but not always, coincide. As we have shown, S_q can, for either $q = 1$ or $q \neq 1$, be extensive under suitable conditions and lead to a finite entropy production per unit time. Other important properties are satisfied, such as *concavity* and *Lesche-stability* (or *experimental robustness*) [9]. Moreover, the celebrated uniqueness theorems of Shannon and of Khinchine have also been q-generalised [10,11], and the same has been done with central procedures such as the Darwin-Fowler steepest descent method [12]. In short, a consistent mathematical structure is in place suggesting that the Boltzmann-Gibbs theory can be satisfactorily extended to deal with a variety of complex statistical mechanical systems. Since the first physical application [13] (to stellar polytropes), nonextensive statistical mechanics and its related concepts have made possible applications to very many natural and artificial systems, from turbulence to high energy and condensed matter physics, from astrophysics to geophysics, from economics to biology and computational sciences (e.g., signal and image processing). Recently, connections with scale-invariant networks, quantum information, and a possible q-generalisation of the central limit theorem [14,15] have been advanced as well. In some of these problems, when the precise dynamics is known, the indices q are in principle computable from first principles. In others, when neither the microscopic nor the mesoscopic dynamics is accessible, only a phenomenological approach is possible, and then q is determined through fitting. An interesting determination of this kind was recently carried out in the solar wind as observed by Voyager 1 in the distant heliosphere [16]. Indeed, the q-triplet that had been conjectured was fully determined for the first time in a physical system. The overall scenario which emerges is indicated in Fig. 3.

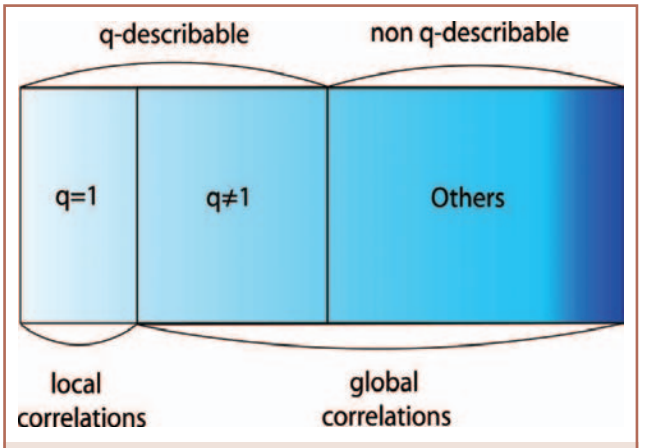

▲ **Fig. 3:** Scenario within which nonextensive statistical mechanics is located (see [3] for more details) [18].

There is a plethora of open problems, as can be easily guessed. Both at the level of the foundations (e.g., the dynamical origin [17]) and at that of specific applications. The fact that some basic questions are not yet fully understood even for Boltzmann-Gibbs statistics does not make the task easy. As an illustration of an important open problem let us mention *long-range-interacting* Hamiltonians. Although many favorable indications are available in the literature, it is still unknown, strictly speaking, if and how the present theory is applicable, and what is the value of q as a function of the range of the forces and of the space dimension. Solutions of problems such as this one are obviously very welcome. Let us finally mention that related or even more general approaches than the present one are already available in the literature. Such is the case of the Beck-Cohen superstatistics and the Kaniadakis statistics, that have already shown interesting specific applications.

Acknowledgement

Y. Sato has benefited from a Postdoctoral Fellowship at the Santa Fe Institute.
C.Tsallis has benefited from sponsoring by SI International and AFRL.
M. Gell-Man was supported by the C.O.U.Q. Foundation and by Insight Venture Management.

References

[1] C. Tsallis, *J. Stat. Phys.* **52**, 479 (1988).

[2] M. Gell-Mann and C. Tsallis, eds., *Nonextensive Entropy - Interdisciplinary Applications,* (Oxford University Press, New York, 2004). For a regularly updated bibliography see http://tsallis.cat.cbpf.br/biblio.htm.

[3] C. Tsallis, M. Gell-Mann and Y. Sato, *Proc. Natl. Acad. Sc. USA* **102**, 15377 (2005).

[4] V. Latora, M. Baranger, A. Rapisarda and C. Tsallis, *Phys. Lett. A* **273**, 97 (2000).

[5] E. Mayoral and A. Robledo, *Phys. Rev. E* **72**, 026209 (2005).

[6] G. Casati, C. Tsallis and F. Baldovin, *Europhys. Lett.* **72**, 355 (2005).

[7] V. Latora, A. Rapisarda and C. Tsallis, *Phys. Rev. E* **64**, 056134 (2001).

[8] F. Baldovin and A. Robledo, *Phys. Rev. E* **69**, 045202(R) (2004).

[9] S. Abe, *Phys. Rev. E* **66**, 046134 (2002).

[10] R.J.V. dos Santos, *J. Math. Phys.* **38**, 4104 (1997).

[11] S. Abe, *Phys. Lett. A* **271**, 74 (2000).

[12] S. Abe and A.K. Rajagopal, *J. Phys. A* **33**, 8733 (2000).

[13] A.R. Plastino and A. Plastino, *Phys. Lett. A* **174**, 384 (1993).

[14] C. Tsallis, *Milan J. Math.* **73**, 145 (2005).

[15] L.G. Moyano, C. Tsallis and M. Gell-Mann, cond-mat/0509229 (2005).

[16] L.F. Burlaga and A.F. Vinas, *Physica A* **356**, 375 (2005).

[17] E.G.D. Cohen, *Pramana* **64**, 635 (2005).

[18] The case of standard critical phenomena deserves a comment. The *BG* theory explains, as is well known, a variety of properties as close to the critical point as we want. If we want, however, to describe certain discontinuities that occur *precisely at the critical point* (e.g. some fractal dimensions connected with the $d_s = 3$ Ising and Heisenberg ferromagnets at T_c), we need a different theoretical approach.

Atmospheric turbulence and superstatistics

C. Beck [1], E.G.D. Cohen [2] and S. Rizzo [3]
[1] School of Mathematical Sciences, Queen Mary, University of London, Mile End Road, London E1 4NS, United Kingdom
[2] The Rockefeller University, 1230 York Avenue, New York, New York 10021, USA
[3] ENAV S.p.A, U.A.A.V. Firenze, Italy

In equilibrium statistical mechanics, the inverse temperature β is a constant system parameter – but many nonequilibrium systems actually exhibit spatial or temporal temperature fluctuations on a rather large scale. Think, for example, of the weather: It is unlikely that the temperature in London, New York, and Firenze is the same at the same time. There are spatio-temporal temperature fluctuations on a rather large scale, though locally equilibrium statistical mechanics with a given fixed temperature is certainly valid. A traveller who frequently travels between the three cities sees a 'mixture' of canonical ensembles corresponding to different local temperatures. Such type of macroscopic inhomogenities of an intensive parameter occur not only for the weather but for many other driven nonequilibrium systems as well. There are often certain regions where some system parameter has a rather constant value, which then differs completely from that in another spatial region. In general the fluctuating parameter need not be the inverse temperature but can be any relevant system parameter. In turbulent flows, for example, a very relevant system parameter is the local energy dissipation rate ϵ, which, according to Kolmogorov's theory of 1962 [1], exhibits spatio-temporal fluctuations on all kinds of scales. Nonequilibrium phenomena with macroscopic inhomogenities of an intensive parameter can often be effectively described by a concept recently introduced as 'superstatistics' [2]. This concept is quite general and has been successfully applied to a variety of systems, such as hydrodynamic turbulence, atmospheric

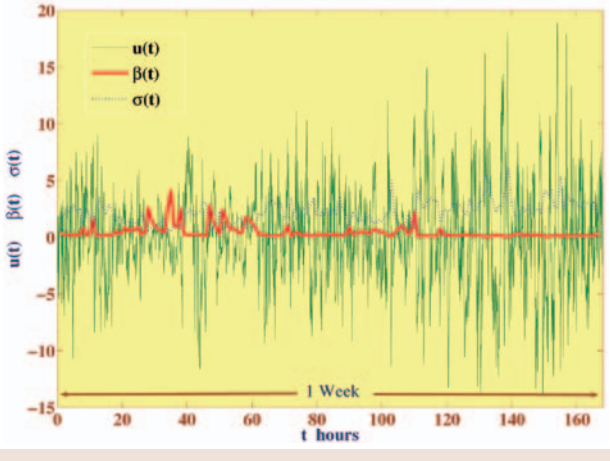

▲ **Fig. 1:** Time series of a temporal wind velocity difference $u(t)$ ($\delta = 60$ min) recorded by anemometer A every 5 min for one week (green line) and the corresponding parameter $\beta(t)$ (red line), as well as the corresponding standard deviation $\sigma(t)$ (blue dotted line), both for a 1 hour window.

features

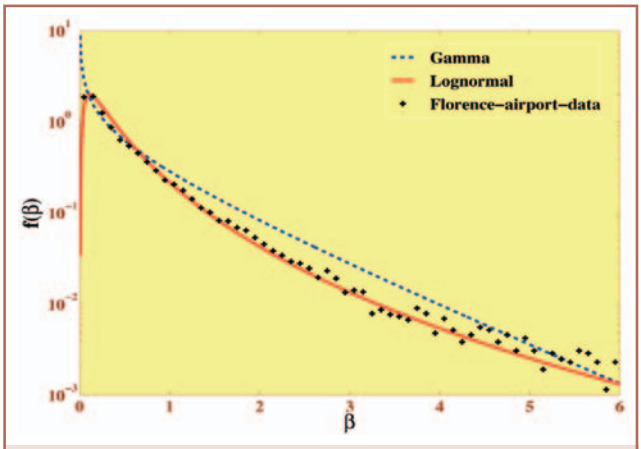

▲ **Fig. 2:** Rescaled probability density of the fluctuating parameter β, as obtained for the Florence airport data. Also shown is a Gamma distribution (dashed blue line) and a lognormal distribution (solid red line) sharing the same mean and variance as the data. The data are reasonably well fitted by the lognormal distribution.

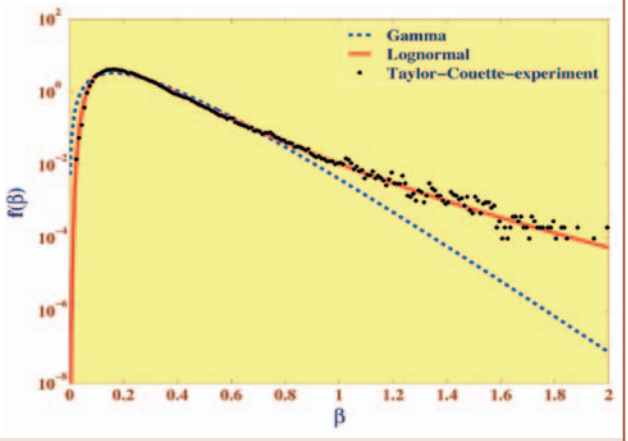

▲ **Fig. 3:** Probability density of the local variance parameter β as extracted from a time series of longitudinal velocity differences measured in a turbulent Taylor-Couette flow at Reynolds number Re = 540000 [8]. A lognormal distribution yields a good fit.

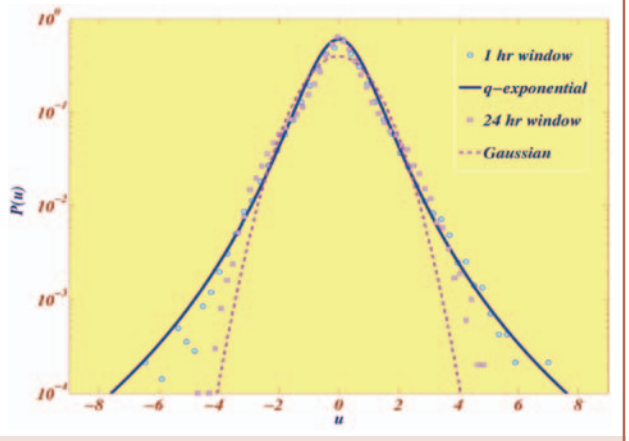

▲ **Fig. 4:** Probability density $p(u)$ of temporal wind velocity differences as observed at the airport.

turbulence, pattern formation in Rayleigh-Benard flows, cosmic ray statistics, solar flares, networks, and models of share price evolution [3]. For a particular probability distribution of large-scale fluctuations of the relevant system parameter, namely the Gamma-distribution, the corresponding superstatistics reduces to Tsallis statistics [4], thus reproducing the generalized canonical distributions of nonextensive statistical mechanics by a plausible physical mechanism based on fluctuations.

In this article we want to illustrate the general concepts of superstatistics by a recent example: atmospheric turbulence. Rizzo and Rapisarda [5, 6] analysed the statistical properties of turbulent wind velocity fluctuations at Florence Airport. The data were recorded by two head anemometers A and B on two poles 10 m high a distance 900 m apart at a sampling frequency of 5 minutes. Components of spatial wind velocity differences at the two anemometers A and B as well as of temporal wind velocity differences at A were investigated.

Analysing these data, two well separated time scales can be distinguished. On the one hand, the temporal velocity difference $u(t) = v(t + \delta) - v(t)$ (as well as the spatial one) fluctuates on the rather short time scale τ (see Fig. 1). On the other hand, we may also look at a measure of the average activity of the wind bursts in a given longer time interval, say 1 hour, where the signal behaves approximately in a Gaussian way. The variance of the signal $u(t)$ during that time interval is given by $\sigma^2 = \langle u^2 \rangle - \langle u \rangle^2$, where $\langle \ldots \rangle$ means taking the average over the given time interval. We then define a parameter $\beta(t)$ by the inverse of this local variance (i.e. $\beta = 1/\sigma^2$). β depends on time t, but in a much slower way than the original signal. Both signals are displayed in Fig. 1. One clearly recognizes that the typical time scale T on which β changes is much larger than the typical time scale τ where the velocity (or velocity difference) changes.

Dividing the wind flow region between A and B into spatial cells, so that air flows from one cell to another, one assumes that each cell is characterized by a different value of the local variance parameter β, which plays a similar role as the inverse temperature in Brownian motion and fluctuates on the relatively long spatio-temporal scale T. As mentioned before, one can then distinguish two well separated time scales for the wind through the cells: a short time scale τ which allows velocity differences u to come to local equilibrium described by local Gaussians $\sim \exp[-\beta \frac{1}{2} u^2]$, and a long time scale T, which characterizes the long time secular fluctuations of β over many cells. Similar fluctuations of a local variance parameter are also observed in financial time series, e.g. for share price indices, and come under the heading 'volatility fluctuations' [7].

A terrestrial example would be a Brownian particle of mass m moving from cell to cell in an inhomogeneous fluid environment characterized by an inverse temperature β which varies slowly from cell to cell. The two time scales are then the short local time scale τ on which the Brownian particle reaches local equilibrium and a long global time scale over which β changes significantly. If the particle moves for a sufficiently long time through the fluid then it samples, in the cells it passes through, values of β distributed according to a probability density function $f(\beta)$, which leads to a resulting long-term probability distribution $p(v)$ to find the Brownian particle in the fluid with velocity v given by $p(v) \sim \int e^{-\frac{\beta}{2} m v^2} f(\beta) d\beta$. This is like a superposition of two statistics in the sense that $p(v)$ is given by an integral over local statistics given by the local equilibrium Boltzmann statistics convoluted with the statistics $f(\beta)$ of the β occurring in the Boltzmann statistics. In other words, it is a 'statistics of a statistics' or a superstatistics.

Returning now to the atmospheric experiment, it is this superstatistics which is employed here to analyse the wind data.

However, there is a fundamental difference in the interpretation of the corresponding variables: First of all, the variable v (the velocity of the Brownian particle) corresponds to the longitudinal velocity *difference* in the flow (either spatial or temporal), not the velocity itself. Secondly, since we are analyzing turbulent velocity fluctuations and not thermal ones, the parameter β is a local variance parameter of the macroscopic turbulent fluctuations and hence it does not have the physical meaning of an inverse temperature as given by the actual temperature at the airport. Rather, it is much more related to a suitable power of the local energy dissipation rate ϵ. The fluctuations of the variance parameter β can be analysed using time windows of different lengths. Rizzo and Rapisarda carried this out for two time series of interest: for the temporal fluctuations of the wind velocity component (in the x-direction) as recorded at the anemometer A and also the spatial fluctuations as given by the longitudinal wind velocity differences between the anemometers A and B. The probability distribution of β as obtained for the temporal case is shown in Fig. 2 for a time window of 1 hour. For comparison, the dashed (blue) line shows a Gamma or χ^2-distribution function, which is of the general form $f(\beta) \sim \beta^{c-1} e^{-\beta/b}$, with b and c appropriate constants. The solid (red) line represents a lognormal distribution function which is of the general form $f(\beta) \sim (1/\beta s) \exp[-(\log(\beta/\mu))^2/(2s^2)]$, with μ and s appropriate constants. Apparently, the data are reasonably well fitted by a lognormal distribution (note that a different conclusion was reached by Rizzo and Rapisarda in [5, 6]) We see that our result for atmospheric turbulence is similar to laboratory turbulence experiments on much smaller space and time scales, such as a turbulent Taylor-Couette flow as generated by two rotating cylinders. For Taylor-Couette flow it has been shown [8] that β is indeed lognormally distributed, see Fig. 3.

In general, for a given nonequilibrium system the probability density of the parameter β is ultimately determined by the underlying spatio-temporal dynamics of the system under consideration.

The Gamma distribution results if β can be represented by a **sum** of n independent squared Gaussian random variables X_i^2 (with $i = 1; \ldots; n$) with mean zero, i.e. $\beta = \sum_{i=1}^{n} X_i^2 > 0$. The constants c and b above are related to n.

The lognormal distribution results if β is due to a multiplicative cascade process, i.e. if it can be represented by a **product** of n independent positive random variables ξ_i, i.e. $\beta = \prod_{i=1}^{n} \xi_i$ or $\log \beta = \sum_{i=1}^{n} \log \xi_i$. Due to the Central Limit Theorem, under suitable rescaling the latter sum will become Gaussian for large n. But if $\log \beta$ is Gaussian this means that β is lognormally distributed.

We notice that the difference between the Gamma distribution and the lognormal distribution is essentially that of an additive versus a multiplicative definition of β. So far there is no theory of turbulence, but following Kolmogorov [1], the mechanism of the turbulent motion of the fluid is critically determined by the transfer mechanism of the energy dissipation between neighboring cells and between different spatial scales in the flow. A multiplicative cascade process is expected to lead to a lognormally distributed β. It seems that the above mentioned transfer mechanism for energy dissipation is similar for turbulent wind fluctuations and laboratory turbulence, which are performed under very different conditions. The spatial scale of environmental turbulence as measured at the airport is much larger than in the laboratory, moreover the Reynolds number fluctuates for the wind measurements, whereas in the laboratory experiments it is controlled.

The probability density $p(u)$ of longitudinal wind velocity differences u (either temporal or spatial) as measured at the airport has strong deviations from a Gaussian distribution and it exhibits prominent ('fat') tails (see Fig. 4). In superstatistical models one can understand these tails simply from a superposition of Gaussian distributions whose inverse variance β fluctuates on a rather large spatio-temporal scale. In the long-term run one has $p(u) \sim \int_0^\infty f(\beta) e^{-\frac{1}{2}\beta u^2} d\beta$, and generically these types of distributions $p(u)$ exhibit broader tails than a Gaussian.

For the special case that $f(\beta)$ is a Gamma distribution the integral can be explicitely evaluated, and one ends up with the generalized canonical distributions (q-exponentials) of nonextensive statistical mechanics, i.e. $p(u) \sim (1+\tilde{\beta}(q-1)\frac{1}{2}u^2)^{-\frac{1}{q-1}}$, where $\tilde{\beta}$ is proportional to the average of β and q is an entropic parameter [2, 4]. These distributions asymptotically decay with a power law. For other $f(\beta)$ (such as the lognormal distributions relevant in our case), the integral cannot be evaluated explicitly, and more complicated behaviour arises. However, it can be shown that for sharply peaked distributions $f(\beta)$ a q-exponential for $p(u)$ is often a good approximation provided $|u|$ is not too large [2].

Quite generally, the superstatistics approach also gives a plausible physical interpretation to the entropic index q. One may generally define

$$q = \frac{\langle \beta^2 \rangle}{\langle \beta \rangle^2}$$

where $\langle \beta \rangle = \int f(\beta)\beta d\beta$ and $\langle \beta^2 \rangle = \int f(\beta)\beta^2 d\beta$ denote the average and second moment of β, respectively. Clearly, if there are no fluctuations in β at all but β is fixed to a constant value β_0, one has $\langle \beta^2 \rangle = \langle \beta \rangle^2 = \beta_0^2$, hence in this case one just obtains $q = 1$ and ordinary statistical mechanics arises. On the other hand, if there are temperature fluctuations (as in most nonequilibrium situations) then those are effectively described by $q > 1$. For the special case that $f(\beta)$ is a Gamma-distribution, the q obtained by eq. (1) coincides with Tsallis' entropic index q (up to some minor correction arising from the local β-dependent normalization constants). But the superstatistics concept is more general in that it also allows for other distributions $f(\beta)$, as for example the lognormal distribution observed in Fig. 2 and 3. General superstatistics can lead to a variety of distributions $p(u)$ with prominent ('fat') tails, i.e. not only power laws but, for example, also stretched exponentials tails and much more. The atmospheric turbulence data seem roughly consistent with Kolmogorov's general ideas of a lognormally distributed fluctuating energy dissipation rate, as are the laboratory turbulence data. In that connection comparison with long range oceanic measurements of a similar kind as the atmospheric wind experiments discussed here might be instructive, testing yet larger scales.

features

References

[1] A.N. Kolmogorov, *J. Fluid Mech.* **13**, 82 (1962)

[2] C. Beck and E.G.D. Cohen, *Physica* **322A**, 267 (2003)

[3] C. Beck, G. Benedek, A. Rapisarda, and C. Tsallis (eds.), *Complexity, Metastability and Nonextensivity,* (World Scientific, Singapore, 2005)

[4] C. Tsallis, *J. Stat. Phys.* **52**, 479 (1988)

[5] S. Rizzo and A. Rapisarda, in *Proceedings of the 8th Experimental Chaos Conference,* Florence, AIP Conf. Proc. **742**, 176 (2004) (cond-mat/0406684)

[6] S. Rizzo and A. Rapisarda, in *Complexity, Mestasbility and Nonextensivity,* (eds.) C. Beck, G. Benedek, A. Rapisarda, and C. Tsallis (World Scientific, Singapore, 2005), 246

[7] J.-P. Bouchard and M. Potters, *Theory of Financial Risk and Derivative Pricing,* Cambridge University Press, Cambridge (2003)

[8] C. Beck, E.G.D. Cohen, and H.L. Swinney, cond-mat/0507411 8

Lattice Boltzmann and nonextensive diffusion

Bruce M. Boghosian [1] *and Jean Pierre Boon* [2] *
[1] *Mathematics Department, Tufts University, Medford, MA 02155*
[2] *Physics Department, Université Libre de Bruxelles, B-1050 Bruxelles, Belgium*
* *bruce.boghosian@tufts.edu, jpboon@ulb.ac.be*

Statistical physics today is arguably in much the same situation that Euclidean geometry found itself in the early nineteenth century. Over the last decade, an increasing body of evidence has indicated that denying a certain postulate of statistical physics – the extensivity of the entropy – results not in a contradiction, but rather in an entirely new family of mathematically consistent variants of the statistical physics developed by Boltzmann and Gibbs (see Editorial).

The mathematical formulation of these variants begins with a generalization of the definition of the entropy in terms of the microscopic state probabilities of the system under study (see Box 1 in the Editorial). A family of such entropies has been posited, parametrized by a single positive number q, such that the usual Boltzmann- Gibbs formulation is recovered when $q = 1$. More precisely, whereas the Boltzmann-Gibbs entropy is expressed in terms of the logarithm function, nonextensive variants are expressed in terms of a q-deformed logarithm (defined in Box 1) to which application of l'Hôpital's rule confirms reduction to the ordinary logarithm as $q \to 1$. Remarkably, many fundamental results of statistical physics, such as the Maxwell relations and Onsager reciprocity, are "q-invariant"; that is, they hold for any statistical physics in the family. Other results, such as the Fluctuation-Dissipation Theorem and the compressible Navier-Stokes equations for viscous fluid dynamics, must be modified by the addition of terms that vanish when $q = 1$.

Entropic Lattice Boltzmann Models

In the late 1980's and early 1990's, it was realized that lattice kinetic models could be used to great advantage in the construction of new algorithms for computational fluid dynamics [1]. These are models wherein particles hop about on a regular spatial lattice in discrete time steps according to deterministic rules, with velocities restricted to the lattice vectors, and with collisions conserving mass and momentum. Unlike particles in a continuum fluid, whose velocities take on values in $\mathbb{R}^3$, the velocity space of a lattice kinetic model consists of a finite set of points. Hydrodynamic quantities – such as mass density and momentum density – may be obtained from such a discrete-velocity distribution by a finite sum, rather than an integral.

It is possible to construct Boltzmann equations for the single-particle distribution function for lattice fluids. At first, researchers restricted their attention to Boltzmann equations for microscopic models of discrete-velocity particles, but it was then realized that lattice Boltzmann equations for discrete-velocity fluids could be constructed with idealized collision operators that did not correspond to any underlying particulate model [2]; even a single relaxation time operator – *à la* Bhatnagar-Gross-Krook (BGK) – replacing the full collision operator, could be used for this purpose [3] giving rise to so-called lattice BGK equation: $f_j(r + v_j\Delta t, t + \Delta t) - f_j(r, t) = \tau^{-1}(f_j(r, t) - f^{equil})$, where f_j is the single-particle distribution function for velocity v_j, position r, and time t.

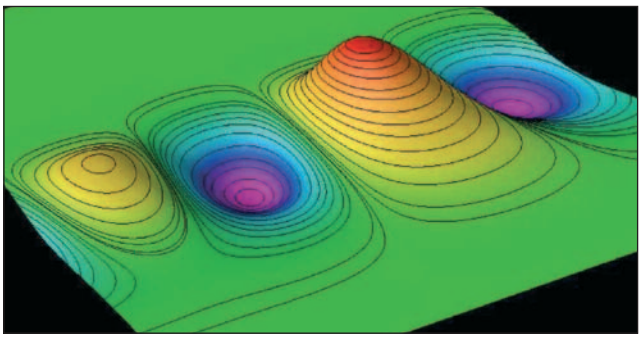

▲ **Fig. 1:** Concentration fluctuations field in the onset of fingering between two miscible fluids (flow direction South-East) showing landscape of q-Gaussian "hills and wells" (color code indicating highest positive values (red) to largest negative values (magenta) of c). These structures identify the existence of precursors to the fingering phenomenon as they develop before any fingering pattern can be seen.

Lattice Boltzmann equations derived from underlying microscopic dynamical models with detailed balance possess a discrete-space-time analog of Boltzmann's celebrated H-Theorem, which establishes that when the system evolves towards equilibrium it will reach a state of maximum entropy. That is – in mathematical terms – it is possible to identify a Lyapunov function for the dynamics. From the point of view of the lattice Boltzmann equation as a physical model, this maintains an important property possessed by the continuum Boltzmann equation. However lattice BGK models are not based on any underlying microscopic dynamical model, and one of the properties lost in the transition from lattice models with a microscopic basis to lattice models without one was the H-Theorem. The effort to modify the lattice BGK model so that it has an H-Theorem led to the proposal of so-called *entropic lattice Boltzmann models* in the late 1990's. These models begin by positing an H function of trace form, depending on the single-particle distribution function, and by dynamically adjusting the relaxation time in the BGK operator to ensure that this H function does not increase.

Researchers then focussed efforts on finding the most general class of entropic lattice Boltzmann model that would produce correct macroscopic behavior, i.e. give rise to the Navier-Stokes equations in the hydrodynamic limit [4]. These analyses restrict attention to collision operators of BGK form, but with *variable* relaxation time. They do not specify the precise form of the H function; rather, they assume that H is of trace form $H(t) = \sum_{\mathbf{r}}\sum_j h(f_j(\mathbf{r}, t))$, where the outer sum is over the lattice and the inner sum is over the finite set of velocities, without specifying the form of the function h. Boltzmann's H function would correspond to the choice $h(f) = f \ln f$, but that assumption is not made here. Of course the form of the equilibrium distribution function will depend on the choice of h. Remarkably, it is possible to carry out the entire Chapman-Enskog analysis for the above-described model without ever specifying h. This results in the Navier-Stokes equations with an extra factor multiplying the advective term, $\mathbf{v}\cdot\nabla\mathbf{v}$. This extra factor depends on h and its first two derivatives. The Galilean invariance of the Navier-Stokes equations depends on there being no such extra factor multiplying the advective term. The convective derivative operator is Galilean invariant. The above-described extra factor breaks that Galilean invariance. The

breaking of Galilean invariance is not completely unexpected – after all, the lattice itself constitutes a preferred Galilean reference frame, and this problem had been noted in earlier microscopic particulate lattice models of hydrodynamics. But now, however, it is straightforward to restore Galilean invariance; we need only demand that this extra factor be equal to one. Since the extra factor depends on h and its first two derivatives, this results in a second-order nonlinear ordinary differential equation for h, whose solution is $h(f) = f \ln_q f$, where $\ln_q$ is precisely the q-logarithm function [5] used in nonextensive statistical physics!

What this analysis shows is that lattice hydrodynamics provides an example of a statistical mechanical system from which the q-deformed functional form arises naturally, and can be demonstrated from first principles. It should be emphasized that Boltzmann's H function is not the entropy! The entropy is a functional of the N-body distribution function, whereas Boltzmann's H function is a functional of the single-particle distribution function. Nevertheless, it is striking that just as the natural logarithm function appears in Boltzmann's entropy (see Box 1) and in Boltzmann's H function, the q-deformed logarithm function appears in the nonextensive entropy, and in the H function for an entropic lattice Boltzmann model. It is however important to acknowledge that an entropic lattice Boltzmann model is not a natural physical system, but a highly idealized model system (that has found importance in numerical analysis). The analysis described above suggests that either the fragmentation of space into a regular lattice, or the reduction of velocity space to a finite set of points, or perhaps both, has resulted in the natural appearance of the q-deformed logarithm. It may be that similar fragmentation of phase space, possibly due to loss of ergodicity – wherein time averages are not equal to phase space averages – gives rise to the appearance of this same functional form in the entropy of certain complex systems.

Nonextensive diffusion as nonlinear response

One of the characteristic features of nonextensive statistical mechanics is the appearance of non-exponential distribution functions with power-law tails and there has been considerable interest in the question of how such non-exponential distributions might arise from first principle consideration [6]. For the diffusion processes, power-law distributions follow, in a generic manner, from a generalization of classical statistical mechanics linear response theory. Suppose we are interested in the diffusion of a tracer particle in a fluid. We then consider the probability $f(\mathbf{r}, t; \mathbf{r}_0, 0)$ to find the diffuser at point $\mathbf{r}$ at time t given that it starts at point r_0 at time 0. This distribution function – but, instead of probabilities, we could as well speak of the concentration of a diffusing species (as in the example below) – as we know from linear response theory, obeys the advection-diffusion equation.

Now if one makes the key assumption that the current is not simply described by gradients in the distribution function, but rather by gradients in the distribution raised to some power, one can proceed essentially along the same lines of reasoning as in classical response theory, and obtain a *generalized diffusion equation*

$$\frac{\partial}{\partial t} f(\mathbf{r}, t; \mathbf{r}_0, 0) = \frac{\partial}{\partial \mathbf{r}} \cdot \mathbf{v}(\mathbf{r}, t) f(\mathbf{r}, t; \mathbf{r}_0, 0) + \frac{\partial}{\partial \mathbf{r}} \cdot \mathsf{D}(t) \cdot \frac{\partial}{\partial \mathbf{r}} f^{\alpha}(\mathbf{r}, t; \mathbf{r}_0, 0) \; .$$

What makes this equation a generalized diffusion equation is the power $\alpha \neq 1$, and the generalized Einstein relation connecting the diffusion coefficient D to the underlying microscopic dynamics and corresponding distribution function.

The generalized equation can be viewed as a classical diffusion equation with an effective diffusion coefficient $\mathsf{D}_\alpha = \alpha \mathsf{D} f^{\alpha-1}$. Since it is quite common to introduce concentration-dependent and density-dependent diffusion coefficient to describe complex systems, this does not differ radically from classical phenomenology: what is unusual is that the effective diffusion coefficient vanishes when the probability (or concentration) vanishes. The generalized diffusion equation has formally the same structure as the "porous media equation", but the diffusion coefficient depends on the solution of the equation. This leads to the fact that the diffusion process is classical in the sense that the mean-squared displacement increases linearly with time, but the solutions are not Gaussian: they have the canonical q-exponential form (see Box 1) with $q + \alpha = 2$.

Precursor statistics

From a pragmatic viewpoint, the lattice Boltzmann equation – in particular with the lattice BGK formulation (described above) – can be used to simulate nonequilibrium systems [2]. In contrast to other computational methods, the lattice Boltzmann method offers a mesoscopic approach , which is based on a kinetic theoretical analysis where the macroscopic description (such as given e.g. by the set of hydrodynamic equations) is not pre-established. This approach was used for instance to investigate precursor phenomena in the onset of fingering and the data were analyzed using the generalized diffusion equation [8].

Fingering is a generic phenomenon that results from the destabilization of the interface between two fluids with different

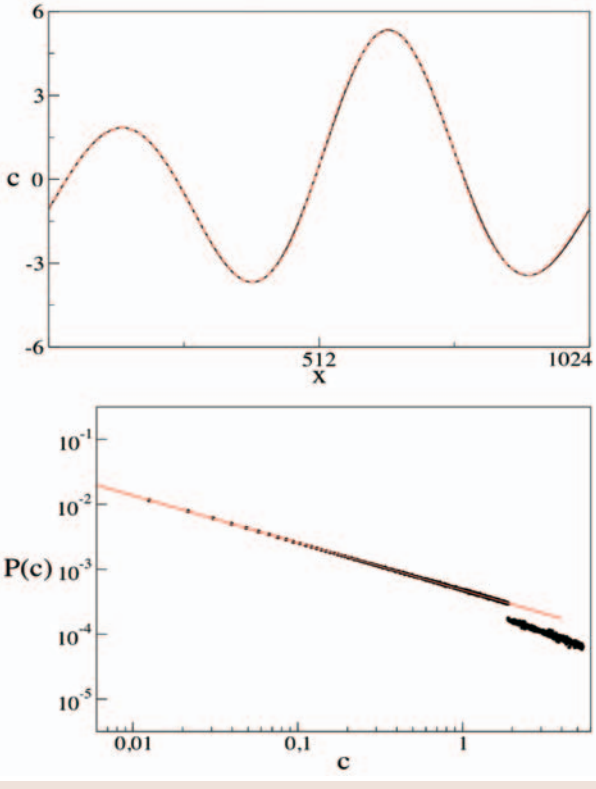

▲ **Fig. 2:** (a) Upper panel: Concentration fluctuations profile (solid line) obtained by a section plane cut through the hills and wells in Fig.1; the dashed line is the q-Gaussian; (b) Lower panel : Concentration fluctuations distribution with power law: $P(c) \propto |c|^{-q}$ with $q = 0.73$ (solid line).

mobilities (because of their differences in viscosity or density) in systems such as a shallow layer or a porous medium, when the fluid with highest mobility is forced through the other fluid. As soon the system responds non-linearly to the driving force, enhanced internal fluctuations (such as concentration fluctuations) are produced characterizing the early stage of the fingering process. If the fluids are miscible, the mixing zone at the interface between the two fluids grows as the fluid with high mobility displaces the other fluid, and there is a dynamical transition where the exponent of the growth of the mixing length of the interfacial zone, $L_{mix} \propto t^{\mu}$, changes from $\mu = 1/2$ (the value typical of a diffusive process) to a larger value. In the diffusive regime (before any fingering pattern becomes visible), the flow produces local concentration gradients which induce mobility fluctuations thereby triggering vorticity fluctuations. The concentration field in Fig.1 shows that a "landscape" of alternating hills and wells has developed. In each "blob", the concentration field exhibits a two-dimensional q-Gaussian profile as illustrated in the upper panel of Fig.2 obtained by a section plane cut through the extrema in Fig.1. Such q-Gaussians are precisely solutions to the generalized diffusion equation. Now the remarkable fact is that the distribution that follows from a q-exponential profile has a power law behavior. In two dimensions and for a q-Gaussian – as for the case of the concentration fluctuations c in the fingering pre-transitional regime – the distribution is simply $P(c) \propto c^{-q}$, as illustrated in Fig.2.

The example presented here is representative of a generic class of driven nonequilibrium systems where q-exponentials and power law distributions are the signature of long-range interactions and whose dynamical behavior is governed by non-linear equations, such as the generalized equation described above.

What has been shown is that during the onset of fingering, one can identify precursors which exhibit statistical features typical of nonextensive statistics. Then the question arises as to whether there is a possible physical interpretation of the origin of *nonextensivity?* The driving force produces a spatial sequence of alternating structures, which, if they were independent, would exhibit an ordinary Gaussian profile originating from local diffusion centers (δ-functions), and would be described by a classical advection-diffusion formulation. However, when growing, these structures develop into overlapping Gaussian blobs, and what the analysis shows is that by renormalizing the overlapping Gaussians, they are recast into a *sum* of scale invariant independent q-Gaussians. Similar statistical properties have been obtained in other nonequilibrium systems which are discussed in companion articles in the present issue.

References

[1] J.-P. Rivet and J.P. Boon, *Lattice Gas Hydrodynamics* (Cambridge University Press, Cambridge, 2001).

[2] S. Succi, *The Lattice Boltzmann Equation for Fluid Dynamics and Beyond* (Clarendon Press, Oxford, 2001).

[3] Y. Qian, D. d'Humières and P. Lallemand, *Europhysics Letters,* **17**, 479 (1992).

[4] B.M. Boghosian, P.J. Love, P.V. Coveney, S. Succi, I.V. Karlin and J. Yepez, *Phys. Rev. E,* **68**, R025103 (2003).

[5] The precise value of q is the solution of a transcendental equation with parameters depending on the spatial dimension, and the set of particle masses and velocities used.

[6] C. Tsallis Physica D, **193**, 3 (2004).

[7] J.F. Lutsko and J.P. Boon, *EuroPhys. Lett.,* **71**, 906 (2005).

[8] P. Grosfils and J.P. Boon, *Physica A,* **358** (2005).

Relaxation and aging in a long-range interacting system

*Francisco A. Tamarit [1] and Celia Anteneodo [2] **

[1]Facultad de Matemática, Astronomía y Física, Universidad Nacional de Córdoba, Ciudad Universitaria, 5000 Córdoba, Argentina

[2]Departamento de Física, Pontificia Universidade Católica do Rio de Janeiro, CP 38017, 22452-970, Rio de Janeiro, Brazil

** tamarit@famaf.unc.edu.ar; celia@cbpf.br*

Complexity refers to the quality that certain systems possess of being intricate and hardly predictable. Ranging from the turbulent flows that form our atmosphere to the human languages, our life has plenty of examples of natural complex behavior. Statistical Mechanics, the area of physics that deals with the problem of explaining the macroscopic world from the dynamics of its components, faces nowadays the challenge of applying the standard reductionist program to all these fascinating systems.

Even when the mathematical equations for describing its time evolution may be only a few, a complex system is composed of a huge number of interacting constituents. These constituents, usually very simple ones, interact giving rise to the emergence of an unexpected collective phenomenology, where cause and effect become subtle and where the long time behaviour is no longer obvious. For succeeding in the plan of explaining complex behavior from first principles, physicists have been looking for simplified models, mathematically tractable and able to catch the essence of complexity.

Suppose you have such a complete knowledge on the microscopic details of certain system that you can write down its Hamiltonian. Now the natural question that arises is the following one: which are the mechanical conditions the system must fulfill in order to guarantee that the statistical mechanics calculations would predict, with an adequate degree of accuracy, the time averaged quantities obtained from a laboratory experiment. And when trying to answer such an apparently simple question, one discovers that even the simplest systems can give place to very intricate behaviour.

Perhaps the simplest Hamiltonian model of interacting particles one can image is the so called *Hamiltonian Mean Field* (HMF) model. Unlike most of the models we are used to deal with when modeling complexity, in this case, not only the dynamical variables but also the interactions among them are extremely simple, lacking any trait of randomness or frustration. The system consists of a set of N interacting particles or *rotators* of unitary mass, each one confined to move around its own unitary circle [1]. Each particle is then mechanically described by an angle θ_i and the corresponding conjugate momentum p_i. The dynamics of the system is ruled by the following Hamiltonian:

$$\mathcal{H} = \frac{1}{2}\sum_i p_i^2 + \frac{1}{2N}\sum_{i,j}\Big[1 - \cos(\theta_i - \theta_j)\Big] \equiv K + V. \quad (1)$$

The first term is the kinetic energy associated with the motion of the particles, while the second one corresponds to the interaction potential (the summation running over all different pairs of particles).

There are a few features of the model that are worth mentioning here. In the first place, it represents a fully connected system, in which each particle interacts with all the others, independently of the distance between them. As it is well known, this unrealistic approach drastically simplifies the mathematical treatment of the thermostatistics of many models, keeping track anyway of its qualitative thermodynamical behavior, at least at high enough dimensionality. Second, the interaction is *ferromagnetic* in nature, in the sense that the potential energy of a pair of interacting particles $[1-\cos(\theta_i-\theta_j)]$ tends to synchronize their movements. Finally, this model can be considered a kinetic version of the *XY* mean field magnetic model, which is without any doubt one of the most studied statistical systems. In fact, we can associate with each particle a two-dimensional local magnetization vector $\vec{m}_i = (\cos\theta_i ; \sin\theta_i)$ and correspondingly a global order parameter:

$$\vec{M} = \frac{1}{N}\sum_i \vec{m}_i \,. \qquad (2)$$

The thermodynamics of this model can be easily solved in the canonical ensemble [1], and this calculation predicts the existence of a continuous phase transition at $T_c = 1/2$ between a *high temperature disordered phase* (characterized by $\vec{M} = \vec{0}$), where rotators uniformly distribute over the circle, and a low temperature ordered phase ($\vec{M} \neq \vec{0}$), where rotators tend to synchronize their movements.

Most of the magnetic models in statistical mechanics do not take into account the kinetic energy. This is mainly because of the well established fact that in any *measure based* statistical theory (microcanonical, canonical or grandcanonical) its contribution to thermodynamical quantities is straightforward (that of a simple ideal gas). However, the inclusion of this term in (1) provides a proper deterministic microscopic dynamics. That is, instead of putting in by hand an external dynamics that would force the system to visit phase space according, for instance, to the usual Boltzmann–Gibbs probability distribution, we can now investigate the true dynamics by simply integrating Newtonian equations

$$\begin{aligned} \dot{\theta}_i &= p_i \\ \dot{p}_i &= M_y \cos\theta_i - M_x \sin\theta_i, \text{ for } 1 \le i \le N \end{aligned} \qquad (3)$$

In doing so, one discovers that, despite its apparent simplicity, this model displays a surprisingly rich variety of complex dynamical behaviour[2].

Let us assume that the system is in thermodynamical equilibrium with a thermal bath at temperature *T*. Then, through the canonical ensemble calculation, we can obtain the mean energy per particle $U/N = \langle H/N \rangle$ by simply assuming, as we learn in any course on Thermostatistics, that the system visits microscopic configurations according to the Boltzmann–Gibbs measure. Alternatively, we may consider a completely isolated system and prepare it initially with a given energy per particle. If we measure the time average of twice the mean kinetic energy per particle $2\bar{K}/N$ along a trajectory, then one would expect this last quantity to coincide with the temperature *T* of the original thermal bath (after suitable transients). This *ergodic* assumption is the master key of the thermostatistics method applied to systems in true equilibrium. But unfortunately complexity seems to occur far away from equilibrium.

There are plenty of physical systems which stay in macroscopic almost stationary states (then, presumably predictable ones) but where the canonical recipe fails. For instance, a window glass or a living cell. Our simple HMF is an excellent prototype for discussing these fascinating questions mainly because, as we will describe in short, the canonical prescription seems to be insuffi- cient to describe its long time behavior. In particular, the HMF is very sensitive to its initial preparation, specially just below the critical point.

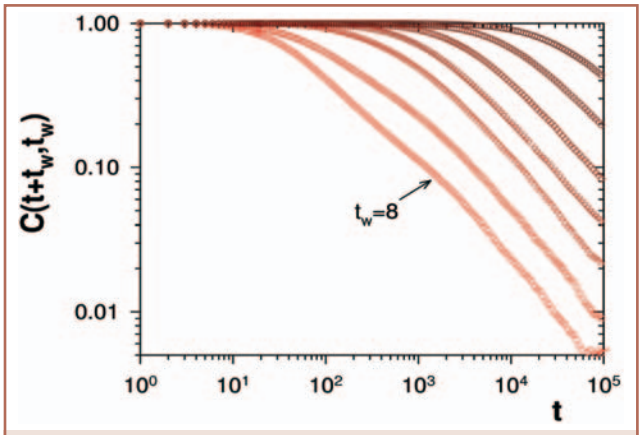

▲ **Fig. 1:** Normalized two-time auto-correlation function of the state variable $(\vec{\theta};\vec{p})$ vs. time, for a value of the total energy (subcritical) and for initial conditions that guarantee that the system will get trapped into a quasi stationary trajectory. Data correspond to averages over 200 of such trajectories. The waiting times are $t_w = 8 \times 4^n$, with $n = 0; \ldots; 6$. The dependence of *C* on both times is evident.

Depending on the initial conditions, the system may become stacked into non-equilibrium long-standing quasi-stationary trajectories. Along these quasi–stationary solutions, whose lifetimes diverge in the limit $N \to \infty$, the time average of any thermodynamical quantity does not coincide with the value predicted by the canonical thermostatistics calculations. The analysis of this complex phenomenology had been the subject of extensive research, including a certain degree of sane controversy [2]. Actually, it presents the kind of drastic slowing down observed in disordered systems, as it happens, for instance, in spin glasses after a sudden quenching into the low temperature phase. Furthermore, the *caloric curve* (the relationship between the internal energy of the system and its temperature), obtained by integrating the equations of motion of the isolated system, strongly disagrees, in the subcritical region, with that expected in the canonical ensemble. Interestingly, this anomalous caloric curve closely resembles the one observed in multifragmentation of clusters of ions or atomic nuclei, where regions with negative specific heat appear. Recently we have shown that this anomalous behavior can be understood in terms of the topology of the potential energy function: the system can not attain true equilibrium because it gets trapped into a sequence of critical points of *V/N* [3], as also verified in many glassy models.

A very simple way of characterizing the relaxation dynamics of a complex system is through the analysis of the two-time auto-correlation function $C(t, t')$, which can exhibit *history-dependent* features, usually referred to as *aging*. For systems that have attained *true* thermodynamical equilibrium, memory effects disappear and only time differences make physical sense. Under these conditions, one expects that $C(t, t') \equiv C(t - t')$. However, for systems exhibiting aging, a much more complex dynamical behavior is observed. (see for instance [4]). Inspired by the strong analogy between the quasistationary trajectories already described and the out of equilibrium states observed in glassy systems, we decided to analyze the behavior of the two-time auto-correlation function of the HMF model [5]. The state of the system in phase space is completely characterized by giving the state vector $\vec{x} \equiv (\vec{\theta}, \vec{p})$. Then, the crude two–time auto-correlation function is

$$C_o(t + t_w, t_w) = \langle \vec{x}\,(t + t_w) \cdot \vec{x}\,(t_w) \rangle, \qquad (4)$$

where $\langle \ldots \rangle$ stands for average over several realizations of the

features

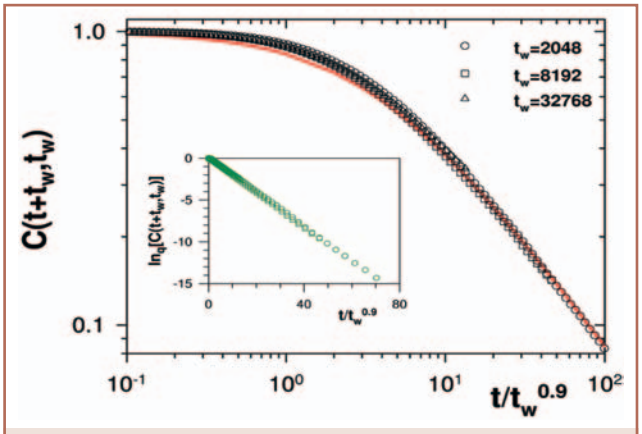

▲ **Fig. 2:** Auto-correlation function vs. scaled time. The data are the same shown in Fig. 1 for the three largest t_w, but suitably scaling the time coordinate makes the data collapse into a single curve. The gray solid line corresponds to a q-exponential fitting. Inset: $\ln_q$-linear representation of the same data, with $q \approx 2.35$. Linearity indicates q-exponential behavior.

dynamics. Afterwards, the auto-correlation function is suitable centered and normalized to remain within the interval [-1, 1].

As we have previously mentioned, because we are dealing with a well defined Hamiltonian system, it is possible to analyze its proper microscopic dynamics. But macroscopic systems always involve such a huge number of interacting particles that the analytical integration of the equations of motion of all the constituents is out of possibility. Then we must be able to integrate their equations of motion with the help of computers (that is what we normally call a numerical simulation). Fortunately, for the system we are interested in, the numerical integration of the coupled equations of motion is a very simple task, which can be carried out even on a modern personal computer, due to its mean-field character. In the cases presented here, the system was always prepared in a "water bag" initial condition, that is, all the angles were set to zero while the momenta were randomly chosen from a uniform distribution with zero mean and such that the system has total energy U. Since for these initial configurations, the total energy is purely kinetic, we emulated the most drastic cooling down compatible with the chosen fixed energy.

In Fig. 1 we plot the normalized two-time autocorrelation function $C(t + t_w, t_w)$, for $U/N = 0.69$, $N = 1000$ and different waiting times (increasing from bottom to top). The value of the specific energy, together with the water bag initial condition, guarantees that, typically, the system will get trapped into a quasi-stationary trajectory as desired. In particular, for the values of U and N chosen, the discrepancy between canonical prediction and microcanonical simulations is the most pronounced one. We clearly note history dependence: for a given fixed t_w, the system remains in a quasi–equilibrium regime with temporal translational invariance up to a time of order t_w. Thereafter, the auto-correlation function presents a slow algebraic decay and a strong dependence on both times. Furthermore, the longer the waiting time t_w, the slower the decay of the correlation.

It is a well established fact that, despite its verified ubiquity in nature, a careful analysis of the aging phenomenology can give valuable information about the microscopic mechanisms involved in the slowing down of the dynamics. In particular, since a general microscopic theory for aging is still lacking, scaling properties can offer a qualitative description of the microscopic phenomenology. Fortunately, a large body of evidence suggests the existence of only a few *dynamical universality classes* associated with the out-of-equilibrium relaxation of a model, as occurs, for instance, in coarsening dynamics or critical phenomena, from which one can extract, by analogy, valuable conclusions. Following these ideas we have looked for the functional dependence of $C(t + t_w, t_w)$ on both times, t_w and t, by trying different data collapses. In Fig. 2 we present the best data collapse obtained for the results of the three largest waiting times displayed in Fig. 1. The resulting scaling law shows that:

$$C(t + t_w, t_w) = f\,(t/t_w^{\beta}) \qquad (5)$$

for the whole range of values of t/t_w considered. Note that, for $t \ll t_w$ it holds that $f\,(t/t_w^{\beta}) \sim (t/t_w^{\beta})^{-\lambda}$. Surprisingly, this kind of scaling behavior is not usual in ordered systems, like the one here studied. Instead, this is the same kind of scaling observed in real spin glasses, which are characterized by the existence of high degrees of randomness and frustration [4]. The solid line corresponds to the best fit of the data with the q-exponential function. This function naturally arises within the generalized thermostatistics introduced by Tsallis [6]. One sees that $q = 1 + 1/\lambda$, yielding $q \approx 2.35$. Notice that the q-exponential allows to fit the whole simulated time span, concluding that:

$$C(t + t_w, t_w) \propto \exp_q\,(-t/t_w^{\beta}) \qquad (6)$$

This affirmation is corroborated by the plot in the inset of Fig. 2, where the same data of the main figure are represented as $\ln_q[C(t + t_w, t_w)]$ vs. t/t_w^{β}, yielding an almost perfect linear behavior. It is worth mentioning that similar fittings were obtained for other system sizes. Later on, these simulations were remade by Pluchino, Rapisarda and Latora [7] who verified that the sub-aging regime observed ($\beta < 1$) is mainly due to the contribution of the momenta. Instead, the contribution of the angles to the correlation function displays the so called *simple aging* regime $C(t, t') \sim t/t_w$, which can be easily understood in terms of the angular coordinates.

Finally, in Fig. 3, we present a further connection between dynamical anomalies and generalized Tsallis thermostatistics. This plot, obtained from [8], presents the probability distribution function (PDF) of the angular position, for a system of $N = 1000$ rotators, initially prepared in the same initial conditions used for analyzing aging, and at different times. It has been reported, some years ago, that, in the quasi-stationary regime, the angles evolve super-diffusively [9] (see also inset of Fig. 3, where the squared deviation is plotted as a function of time). Additional information is obtained looking not only at the squared deviation but at the whole distribution of angles. Curiously, after the meta-equilibrium regime settles, the PDFs can be well described by q-Gaussian shapes. The value of parameter q increases with time reaching a steady value $q \approx 1.5$[8]. The ultimate relationship between this value of q and that obtained previously from the aging curves remains an open question that deserves further analysis [10].

In conclusion, we have discussed two relaxational features (aging and spreading of angles) of the HMF, a paradigm of long-range couplings. Along the quasistationary solutions, both features present traits of generalized exponential behavior. These traits may be a reflection of the complex structure of the phase space regions where quasi-stationary states live. If that were the case, then we would expect that the new generalized thermostatistics introduced by C. Tsallis in 1988 [6], inspired in multifractal geometries, could offer a *novel measure-based* theory for predicting the mean values of a physical system when confined in quasi–stationary long living states. Despite the proper complexity of this enterprise, the manageability of the HMF model invites further and deeper investigations along these lines.

Acknowledgments

We are indebted to Constantino Tsallis for his continuous stimulus along all these years. We thank M. Montemurro and L. Moyano, who are the co-authors of the works here partially described. We finally thank A. Rapisarda and A. Pluchino for helpful discussions and suggestions. The works here described were partially supported by grants from CONICET (Argentina), Agencia C´ordoba Ciencia (Argentina) SECYT-UNC (Argentina) and Brazilian agencies Faperj and CNPq.

References

[1] M. Antoni and S. Ruffo, *Phys. Rev. E* **52**, 2361 (1995).

[2] V. Latora, A. Rapisarda, and S. Ruffo, *Phys. Rev. Lett.* **80**, 692 (1998); C. Anteneodo and C. Tsallis, *Phys. Rev. Lett.* **80**, 5313 (1998); F. Tamarit and C. Anteneodo, *Phys. Rev. Lett.* **84**, 208(2000); V. Latora, A. Rapisarda, and C. Tsallis, *Phys. Rev. E* **64**, 056134 (2001); D.H. Zanette and M.A. Montemurro, *Phys. Rev. E* **67**, 031105 (2003).

[3] F. A. Tamarit, G. Maglione, D. A. Stariolo and C. Anteneodo, *Phys. Rev. E* **71**, 036148 (2005).

[4] J. Hammann, E. Vincent, V. Dupuis, M. Alba, M. Ocio and J.P. Bouchaud, *J. Phys. Soc. Jpn.* **69**, 206 (2000); J.P. Bouchaud, L.F. Cugliandolo, J. Kurchan and M. M´ezard, in *Spin Glasses and Random Fields,* edited by A.P. Young (World Scientific, Singapore, 1998).

[5] M.A. Montemurro, F.A. Tamarit and C. Anteneodo, *Phys. Rev. E* **67**, 031105 (2003).

[6] C. Tsallis, *J. Stat. Phys.* **52**, 479 (1988); *Nonextensive Mechanics and Thermodynamics,* edited by S. Abe and Y. Okamoto, Lecture Notes in Physics Vol. 560 (Springer, Berlin 2001); in *Non-Extensive Entropy-Interdisciplinary Applications,* edited by M. Gell-Mann and C. Tsallis, (Oxford University Press, Oxford, 2004).

[7] A. Pluchino, V. Latora and A. Rapisarda, *Physica A* **340**, 187 (2004); *Physica A* **338**, 60 (2004); *Physica D* **193**, 315 (2004); *Phys. Rev. E* **69**, 056113 (2004).

[8] L. Moyano and C. Anteneodo, in preparation.

[9] V. Latora, A. Rapisarda, and S. Ruffo, P*hys. Rev. Lett.* **83**, 2104 (1999).

[10] C. Tsallis, *Physica A* **340**, 1 (2004); C. Tsallis, M. Gell- Mann and Y. Sato, Proc. Natl. Acad. Sc. USA **102**, 15377 (2005); L.F. Burlaga and A.F. Viñas, *Physica A* **356**, 375 (2005).

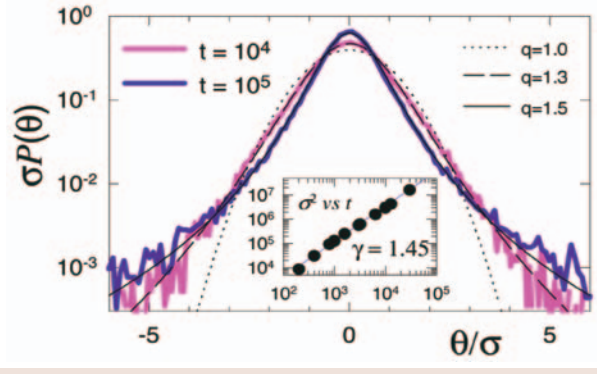

▲ **Fig. 3:** Histogram of normalized angles at different times of the HMF dynamics. Parameters and initial conditions are the same used in previous figures. Notice that at long times, the histogram is of the *q*-Gaussian form. Inset: squared deviation as a function of time. It follows the law $\sigma^2 \sim t^{\gamma}$, with $\gamma > 1$, signaling superdiffusion.

Noise induced phenomena and nonextensivity

Horacio S. Wio *
Instituto de Física de Cantabria, Universidad de Cantabria-CSIC, Santander, Spain
and Centro Atómico Bariloche, S.C. Bariloche, Argentina
* *wio@ifca.unican.es*

During the last few decades of the 20th century the scientific community has recognized that in many situations (and against everyday intuition) noise or fluctuations can trigger new phenomena or new forms of order, like in noise induced phase transitions, noise induced transport [1], stochastic resonance [2], noise sustained patterns, to name just a few examples. However, in almost all the studies of such noise induced phenomena it was assumed that the noise source had a Gaussian distribution, either white (memoryless) or colored (that is, with "memory"). This was mainly due to the difficulties in handling non Gaussian noises and to the possibility of obtaining some analytical results when working with Gaussian noises. In addition to the intrinsic interest in the study of non Gaussian noises, there has been some experimental evidence, particularly in sensory and biological systems, indicating that at least in some cases the noise source could be non Gaussian.

This article is a brief review on recent studies about some of those noise induced phenomena when submitted to a colored (or time correlated) and non Gaussian noise source. The source of noise used in those works was one generated by a *q*-distribution arising within a nonextensive statistical physics framework [3]. In all the systems and phenomena analyzed, it was found that the system's response was strongly affected by a departure of the noise source from the Gaussian behavior, showing a shift of transition lines, an enhancement and/or marked broadening of the systems response. That is, in most of the cases, the value of the parameter q optimizing the system's response resulted $q \neq 1$ (with $q = 1$ corresponding to a Gaussian distribution). Clearly, this result would be highly relevant for many technological applications, as well as for some situations of biological interest.

Non gaussian noise

In order to introduce the form of the non Gaussian noise to be used, we start considering the following form of a Langevin or stochastic differential equation (that is, a differential equation with random coefficients), with additive noise

$$\dot{x} = f(x, t) + \eta(t), \qquad (1)$$

where $\eta(t)$ is the stochastic or noise source. Usually, it is assumed that such noise source corresponds to a Gaussian distributed variable, having a correlation $C(t - t') = \langle \eta(t)\eta(t') \rangle$. If the noise is "white" (a particular form of Markovian or memoryless process), we have $C(t - t') \sim \delta(t - t')$, while for a typical Ornstein-Uhlenbeck process, we have $C(t - t') \sim \exp[-(t - t')/\tau]$, with τ the "correlation time".

However, motivated by previous work based on a nonextensive thermostatistics distribution [3], it was assumed that the noise $\eta(t)$ was a non Gaussian and non Markovian process (that

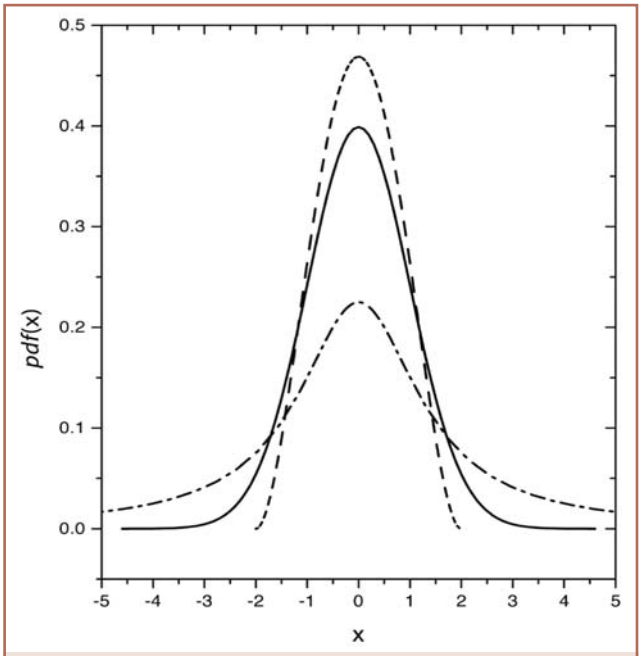

▲ **Fig. 1:** The stationary probability distribution function for the non Gaussian distribution given by Eq. (3), for the value $\tau/D = 1$. The solid line indicates the Gaussian case ($q = 1$); the dashed line corresponds to a bounded distribution ($q = 0.5$); while the dashed-dotted line corresponds to a wide distribution ($q = 2$).

is with "memory"). It was shown that such non Gaussian and non Markovian noise could be generated through the following Langevin equation

$$\dot{\eta} = -\frac{1}{\tau}\frac{d}{d\eta}V_q(\eta) + \frac{1}{\tau}\xi(t); \qquad (2)$$

where $\xi(t)$ is a standard Gaussian white noise of zero mean and correlation $\langle \xi(t)\xi(t')\rangle = D\delta(t\text{-}t')$, while the potential

$$V_q(\eta) = \frac{\mathrm{D}}{\tau(q\text{-}1)}\ln[1 + \frac{\tau}{D}(q\text{-}1)\frac{\eta^2}{2}].$$

As this article is not the appropriate place to refer to all the properties of the process η, we make reference to [4] for details. However, it is instructive to show the stationary probability distribution function, which is given by

$$P_q^{st}(\eta) = \frac{1}{Z_q}\exp_q\left[-\frac{\tau}{D}\frac{\eta^2}{2}\right] \qquad (3)$$

where $\exp_q(x)$ was defined in Box 1 (see the introduction by C.Tsallis and J.P.Boon in this same issue), Z_q being the normalization constant. This distribution can be normalized only for $q < 3$, its first moment is $\langle\eta\rangle = 0$, while the second moment,

$$\langle\eta^2\rangle = \int\eta^2 P_q^{st}(\eta)d\eta = \frac{2\mathrm{D}}{\tau(5\text{-}3q)} \equiv Dq,$$

is finite only for $q < 5/3$. Also, τ_q, the correlation time of the process η, diverges near $q = 5/3$ and can be approximated over the whole range of values of q by $\tau_q \approx 2\tau/(5 - 3q)$. When $q \to 1$ the limit of η being a Gaussian, Ornstein-Uhlenbeck colored noise, is recovered, with noise intensity D and correlation time τ. Furthermore, for $q < 1$, the probability distribution function has a cut-off and it is only defined for $|\eta| < \sqrt{\frac{2D}{\tau(1\text{-}q)}}$. In order to visualize the form of the probability distribution as function of η, in Fig. 1 it is shown for different values of q.

The process η was analyzed in [4], and an *effective Markovian approximation* was obtained via a path integral procedure. Such an approximation allows different (quasi) analytical results to be obtained. Those results and their dependence on the different parameters in the case of a double well potential, were compared with extensive numerical simulations with excellent agreement.

We will now briefly review some of the results obtained when studying a few of the noise induced phenomena indicate above.

Stochastic resonance

The phenomenon of *stochastic resonance* shows the counterintuitive role played by noise in nonlinear systems as it enhances the response of a system subject to a weak external signal [2]. It was first introduced by Benzi and coworkers to explain the periodicity of Earth's ice ages (see [2] and references therein). The study of stochastic resonance has attracted considerable interest due to its potential technological applications for optimizing the response in nonlinear dynamical systems, as well as to its connection with some biological mechanisms. A large number of the studies on stochastic resonance have been done analyzing a paradigmatic bistable one-dimensional double-well potential. In almost all descriptions the transition rates between the two wells were estimated as the inverse of the Kramers' time (or the typical mean passage time between the wells), which was evaluated using standard techniques. In almost all cases, noises were assumed to be Gaussian.

Consider the problem described by Eqs. (1) and (2), where $f(x,t) = -\frac{\partial U(x,t)}{\partial x} = -\frac{\partial U_0(x)}{\partial x} + S(t)$, the external signal is $S(t) \sim A\cos(\omega t)$ and $U_0(x)$ is a double well potential. This problem corresponds (for $A = 0$) to the case of diffusion inside the potential $U_0(x)$, induced by the colored non Gaussian noise η. We will not describe here the details of the *effective Markovian Fokker-Planck equation* (see [4, 5]); but it is worth indicating that such an approximation allowed us to obtain the probability distribution function of the process η, and to derive expressions for the Kramers time. Another useful approximation, the so-called two-state approach [2], was also exploited in order to obtain analytical expressions for the power spectral density and the *signal-to-noise ratio*.

Figure 2 shows some of the main results. In the upper part is depicted the theoretical results: on the left hand part for R – the signal-to-noise ratio – versus D, for a fixed value of the time correlation τ and various q. It is apparent that the general trend is that the maximum of the signal-to-noise curve increases when the system departs from the Gaussian behavior ($q < 1$). The right hand part again shows R vs D, but for a fixed value of q and several values of τ. The general trend agrees with previous results for colored Gaussian noises [2]: an increase of the correlation time induces the maximum of the signal-to-noise ratio decrease as well to shift towards larger values of the noise's intensity. The latter fact is a consequence of the suppression of the switching rate for increasing τ. Both qualitative trends were confirmed by Monte Carlo simulations of Eqs. (1) and (2). The lower part of Fig. 2 show the simulation results. The left hand side corresponds to the same situation and parameters indicated in the upper left part. In addition to the increase of the maximum of the signal-to-noise ratio curve for values of $q < 1$, it is also seen to be an aspect that is not well reproduced or predicted by the effective Markovian approximation: the maximum of the signal-to-noise ratio curve flattens for lower values of q, indicating that the system, when departing from the Gaussian behavior, does not require a fine tuning of the noise intensity in order to maximize its response to a weak external signal. On the right hand side, simulation

results for the same situation and parameters indicated in the upper right part are also shown.

The numerical and theoretical results can be summarized as follows: (a) for a fixed value of τ, the maximum value of the signal-to-noise ratio increases with decreasing q; (b) for a given value of q, the optimal noise intensity (that one maximizing the signal-to-noise ratio) decreases with q and its value is approximately independent of τ; (c) for a fixed value of the noise intensity, the optimal value of q is independent of τ and in general it turns out that $q_{op} \neq 1$.

Using a simple experimental setup, in [6] the stochastic resonance phenomenon was analyzed but using a non Gaussian noise source built up to exploit the form of noise introduced above, for the particular case of non Gaussian white noise. Those results confirmed most of the predictions indicated above.

Brownian motors

Brownian motors or "ratchets" – where the breaking of spatial and/or temporal symmetry, induces directional transport in systems out of equilibrium – is another noise induced phenomenon that attracts the attention of an increasing number of researchers due to both its potential technological applications and its biological interest [1]. The transport properties of a typical Brownian motor are usually studied analyzing the following general stochastic differential or Langevin equation

$$m\frac{d^2x}{dt^2} = -\gamma\frac{dx}{dt} - V'(x) - F + \xi(t) + \eta(t), \qquad (4)$$

where m is the mass of the particle, γ the friction constant, $V(x)$ the (sawtooth-like) ratchet potential, F is a constant "load" force, and $\xi(t)$ the thermal noise satisfying $\langle\xi(t)\xi(t')\rangle = 2\gamma T\delta(t-t')$. Finally, $\eta(t)$ is the time correlated forcing (with zero mean) that keeps the system out of thermal equilibrium allowing the motion to be rectified. For this type of ratchet model several different kinds of time correlated forcing have been considered in the literature [1].

The effect of the class of the non Gaussian noise introduced before on the transport properties of a typical Brownian motor, was analyzed in [7], with the dynamics of $\eta(t)$ described by the Langevin equation (2). As discussed before, for $1 < q < 3$, the probability distribution decays as a power law, that is slower than a Gaussian. Hence, keeping D (the noise intensity) constant, the width or dispersion of the distribution increases with q, meaning that, the higher q, the stronger the "kicks" that the particle will receive when compared with the Gaussian Ornstein-Uhlenbeck process.

By setting $m = 0$ and $\gamma = 1$, the overdamped regime was initially analyzed. The main objective of the studies was to analyze the dependence of the mean current $\left(J = \left\langle\frac{dx}{dt}\right\rangle\right)$ and the efficiency (ε) on the different parameters, in particular, their dependence on q. For the efficiency, defined as the ratio of the work (per unit time) done by the particle "against" the load force F to the mean power injected into the system through the external forcing η, a closed expression using an adiabatic approximation was obtained [7].

Figure 3, on the left hand side, shows typical analytical results - obtained through the adiabatic Approximation - for J and ε as functions of q, together with results of numerical simulations.

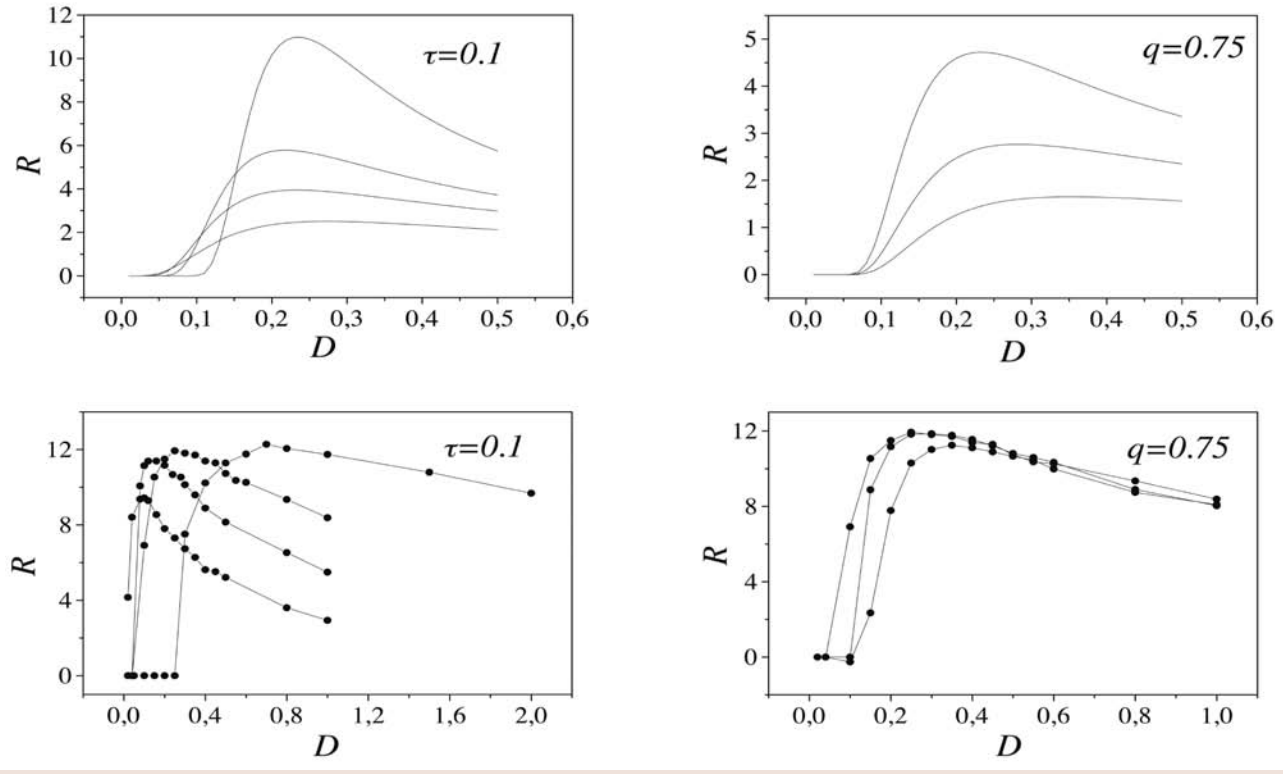

▲ **Fig. 2:** Signal-to-noise ratio (R) vs the noise intensity (D) for the double-well potential $U_0(x) = \frac{x^4}{4} - \frac{x^2}{2}$. Theoretical results are shown in the upper part: on the left hand side for a correlation time $\tau = 0.1$ and different values of the parameter q (that indicates a departure from the Gaussian –q = 1– behavior): (from top to bottom) $q = 0.25, 0.75, 1.0, 1.25$, while on the right hand side for $q = 0.75$ and different values of the correlation time: (from top to bottom) $\tau = 0.25, 0.75, 1.5$. Lower part, Monte Carlo simulation results: left side for $\tau = 0.1$ and (from top to bottom) $q = 0.25, 0.75, 1.0, 1.25$; while on the right side for $q = 0.75$ and (from top to bottom) $\tau = 0.25, 0.75, 1.5$.

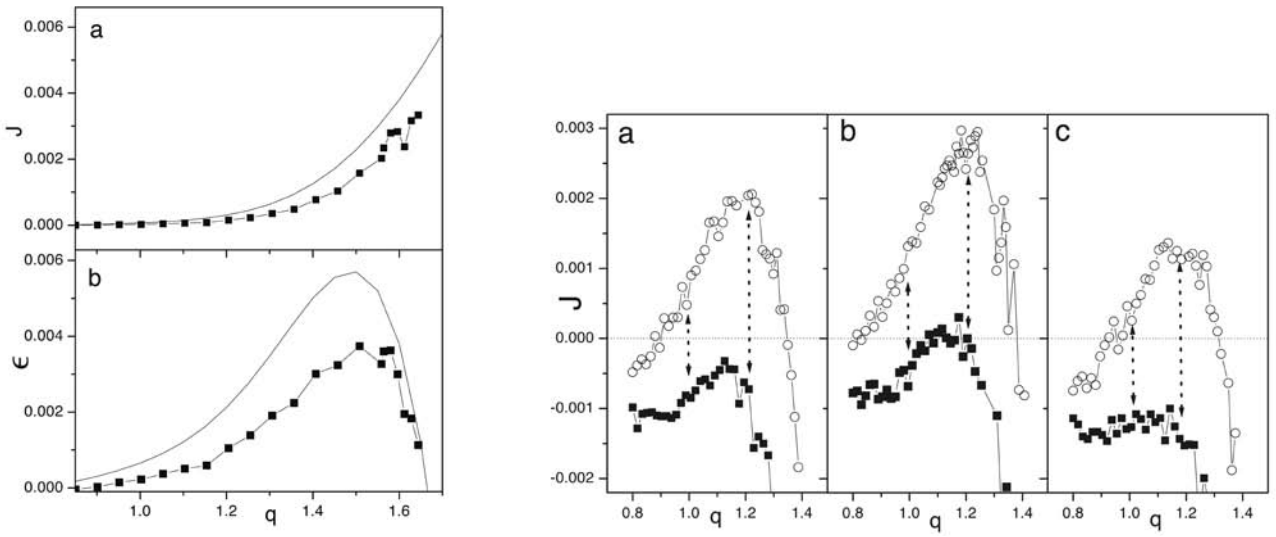

▲ **Fig. 3:** Left hand side: Current (a) and efficiency (b) for the Brownian motor described by Eq. (4), subject to the non Gaussian noise, both as functions of q. The solid line corresponds to an adiabatic approximation while the line with squares shows results from simulations. All calculations are for $m = 0$, $\gamma = 1$, $T = 0.5$, $F = 0.1$, $D = 1$ and $\tau = 100/(2\pi)$. On the right hand side: Separation of masses, results from Monte Carlo simulations for the current as a function of q for particles of masses $m = 0.5$ (hollow circles) and $m = 1.5$ (solid squares). Calculations are for three different values of the load force: $F = 0.025$ (a), $F = 0.02$ (b) and $F = 0.03$ (c). The values of the parameters were fixed at $\gamma = 2$, $T = 0.1$, $\tau = 0.75$, and $D = 0.1875$.

A region of parameters similar to the ones used in previous studies was chosen, but considering a non-zero load force, leading to a non-vanishing efficiency. As can be seen, although there is not quantitative agreement between theory and simulations, the used adiabatic approximation predicts qualitatively very well the behaviour of J (and ε) as q is varied. As shown in the figure, the current grows monotonously with q (at least for $q < 5/3$) while there is an optimal value of q (> 1) giving the maximum efficiency. This fact could be interpreted as follows: when q is increased, the width of the $Pq(\eta)$ distribution grows and high values of the non Gaussian noise become more frequent, leading to an improvement of J. Although the mean value of J increases monotonously with q, the width of $Pq(\eta)$ also grows, leading to an enhancement of the fluctuations around this mean value. This is the origin of the efficiency's decay occurring for high values of q: in this region, in spite of having a large (positive) mean value of the current for a given realization of the process, the transport of the particle towards the desired direction is far from being assured. Hence, the results indicated clearly show that the transport mechanism becomes more efficient when the stochastic forcing has a non Gaussian distribution with $q > 1$.

Regarding the situation when inertia effects are relevant (that is $m \neq 0$), taking into account the results discussed above it is reasonable to expect that non Gaussian noises might improve the capability of mass separation in ratchets. Previous work has analyzed ratchets with an Ornstein-Uhlenbeck noise as external forcing (it is worth emphasising that it corresponds to $q = 1$ in the present case), and has studied the dynamics for different values of the correlation time of the forcing, finding that there was a region of parameters where mass separation occurs. This means that the direction of the current is found to be mass–dependent: the "heavy" species moves in one direction while the "light" one does so in the opposite sense. We have analyzed the same system, but considering the case of non Gaussian forcing, and focusing on the region of parameters where (for $q = 1$) separation of masses was found. The main result was that the separation of masses indeed occurs, that happens in the absence of a load force, and that it is enhanced when a non–Gaussian noise with $q > 1$ is considered. On the right hand side of Fig. 3, part (a) the current J as function of q for $m_1 = 0.5$ and $m_2 = 1.5$ is shown. It is apparent that there is an optimum value of q that maximizes the difference of currents. This value, which is close to $q = 1.25$, is indicated with a vertical double arrow. Another double arrow indicates the separation of masses occurring for $q = 1$ (Gaussian Ornstein-Uhlenbeck forcing). It was observed that, when the value of the load force is varied, the difference between the curves remain approximately constant but both are shifted together to positive or negative values (depending on the sign of the variation of the loading). By controlling this parameter it is possible to achieve the situation shown in part (b), where, for the value of q at which the difference of currents is maximal, the heavy "species" remains static on average (has $J = 0$), while the light one has $J > 0$. In part (c) for the optimal q, the two species move in opposite directions with equal absolute velocity.

Resonant gated trapping

As indicated before, stochastic resonance has been found to play a relevant role in several biology problems. In particular, there are experiments on the measurement of the current through voltage-sensitive ion channels in cell membranes. These channels switch (randomly) between open and closed states, thus controlling the ion current. This and other related phenomena have stimulated several theoretical studies of the problem of ionic transport through biological cell membranes, using different approaches, as well as different ways of characterizing stochastic resonance in such systems. A *toy model,* sketching the behavior of an ion channel, was studied in [8]. Among other factors, the ion transport depends on the membrane electric potential (which plays the role of the barrier height) and can be stimulated by both *dc* and *ac* external fields. This included the simultaneous action of a deterministic and a stochastic external field on the trapping rate of a gated imperfect trap. The main result was that even such a simple (toy) model of a gated trapping process shows a stochastic resonance-like behavior.

The study was based on the so called *stochastic model* for reactions, generalized in order to include the internal trap's dynamics. The dynamical process consists in the opening or closing of the traps according to an external field that has two contributions, one periodic with a small amplitude, and another stochastic whose intensity is (as usual) the tuning parameter. The absorption contribution is modeled as $\sim -\gamma(t)\delta(x)\rho(x, t)$; with ρ the density of the not yet trapped particles, and $\gamma(t) = \gamma^*\theta[B\sin(\omega t) + \eta - \eta_c]$, where $\theta(x)$ – the Heaviside function – determines when the trap is open or closed: if the signal is $B\sin(\omega t) + \eta \geq \eta_c$ the trap opens, otherwise it is closed. The interesting case is when $\eta_c > B$, that is: without noise the trap is always closed. When the trap is open the particles are trapped with a probability per unit time γ^* (i.e. the open trap is "imperfect"). Finally, the colored non Gaussian noise given by Eq. (2) was used for η.

The stochastic resonance-like phenomenon was quantified by computing the amplitude of the oscillating part of the absorption current, indicated by $\Delta J(t)$. The resulting qualitative behavior was as follows: for small noise intensities the trapping current was low (as $\eta_c > B$), hence ΔJ was small too, while for a large noise intensity the deterministic (harmonic) part of the signal became irrelevant and ΔJ was again small. Hence, there was a maximum at some intermediate value of the noise. When compared against the white noise case, an increase in the system response was apparent together with a reduction in the need for tuning the noise, similarly to what was found for the "normal" stochastic resonance: the bounded character of the probability distribution function for $q < 1$ contributed positively to the rate of overcoming the threshold η_c and such a rate remained of the same order within a larger range of values than for the case of η being a white noise [5].

The dependence of the maximum of $\Delta J(t)$ on the parameter q was also analyzed, and the existence of another *resonant-like* maximum as a function of q was observed, implying that it is possible to find a region of values of q where the maximum of ΔJ reaches optimal values (*corresponding to a non Gaussian and bounded* probability distribution function), yielding the largest system response. That is, a *double stochastic resonance effect* exists as a function of both: the noise intensity and q.

Noise induced transition

A system, called the *genetic model,* that when submitted to a Gaussian white noise shows a noise induced transition, was also studied. In previous related works it was shown that, when the noise is an Ornstein-Uhlenbeck one, a re-entrance effect arose (from a disordered state to an ordered one, and finally again to a disordered state) as the noise correlation time τ was varied from 0 to ∞. The same system was studied in [9], but when it was submitted to the non Gaussian noise indicated above. The main result showed the persistence of the indicated re-entrance effect, together with a strong shift in the transition line, as q departed from $q = 1$. The transition was anticipated for $q > 1$, while it was retarded for $q < 1$. A conjecture about a possible re-entrance effect with q was shown to be false.

Final comments

The previously indicated results clearly show that the use of non Gaussian noises in many noise induced phenomena could produce significant changes in the system's response when compared to the Gaussian case. Moreover, in all cases, it was found that the system's response is enhanced or altered in a relevant way, and this occurs for values of q indicating a departure from Gaussian behavior, that is: *the optimum response* happens for $q \neq 1$: Clearly, the study of the variation in the response of other related noise induced phenomena when subject to such a kind of non Gaussian noise will be of great interest.

An extremely relevant point is related to some recent work [10] where the algebra and calculus associated with the nonextensive statistical mechanics has been studied. It is expected that the use of such a formalism could help to directly study Eq. (1), without the need to resort to Eq. (2), and also to build up a *nonextensive path integral* framework for this kind of stochastic process.

To conclude, it is worth commenting on a relevant question: how could it be possible to obtain such a form of noise from, it may be said, *first principles?* It is well known that in dynamical systems with several degrees of freedom evolving with two well separated time scales, Gaussian noises (white or colored) could be obtained through an adequate adiabatic elimination of the fast variables, and assuming some (δ or exponential) correlation properties. It can be conjectured that the form of noise used above could result from the existence of a whole *hierarchy* of time scales and, associated with it, to an adequate *hierarchical adiabatic elimination* of the faster variables. However, the proof or rejection of this conjecture requires some specific work.

About the author

Horacio S. Wio graduated at the Instituto Balseiro, and has been visitor at several institutions in Latin America, Europa and USA. He was Professor at Instituto Balseiro, and Senior Scientist at CONICET and Centro Atómico Bariloche, where he was Head of the Theoretical Physics Division during 1992-1994, and of the Statistical Physics Group during 1986-2002. He is now at the Instituto de Física de Cantabria.

Acknowledgments

The author thanks S. Bouzat, F. Castro, R. Deza, M. Fuentes, M. Kuperman, J. Revelli, A. Sánchez, C. Tessone, R. Toral and C. Tsallis for their collaboration and/or useful discussions. He wants to thank to the European Commission for the award of a *Marie Curie Chair.*

References

[1] R. D. Astumian and P. Hänggi, *Phys. Today* **55** (11), 33 (2002); P. Reimann, Phys. Rep. 361, 57 (2002).

[2] A. Bulsara and L. Gammaitoni, *Phys. Today* **49** (3), 39 (1996); L. Gammaitoni, P. Häanggi, P. Jung and F. Marchesoni, *Rev. Mod. Phys.,* **70**, 223 (1998).

[3] See: M. Gell-Mann and C. Tsallis, Eds., *Nonextensive Entropy - Interdisciplinary Applications* (Oxford U.P, New York, 2004).

[4] M. A. Fuentes, H. S. Wio and R. Toral, *Physica A* **303**, 91 (2002).

[5] M.A. Fuentes, R. Toral and H.S. Wio, *Physica A* **295**, 114 (2001); M.A. Fuentes, C. Tessone, H.S. Wio and R. Toral, *Fluct. and Noise Letters* **3**, 365 (2003).

[6] F.J. Castro, M.N. Kuperman, M.A. Fuentes and H.S. Wio, *Phys. Rev. E* **64**, 051105 (2001).

[7] S. Bouzat and H. S. Wio, *Eur. Phys. J.B.* **41**, 97 (2004), and *Physica A* **351**, 69 (2005).

[8] A.D. Sánchez, J.A. Revelli and H.S. Wio; *Phys. Lett. A* **277**, 304 (2000); H.S. Wio, J.A. Revelli and A.D. S´anchez, *Physica D* **168-169**, 165 (2002).

[9] H.S. Wio and R. Toral, *Physica D* **193**, 161 (2004)

[10] E.P. Borges, *Physica A* **340**, 95 (2004); H. Surayi, in *Complexity, Metastabilty and Nonextensivity,* C. Beck, G. Benedek, A. Rapisarda and C. Tsallis, Eds. (World Scientific, Singapore, 2005).

Nonextensive thermodynamics and glassy behaviour

Andrea Rapisarda and Alessandro Pluchino *
Dipartimento di Fisica e Astronomia and INFN - Università di Catania, 95123 Catania, Italy
** andrea.rapisarda@ct.infn.it, alessandro.pluchino@ct.infn.it*

When studying phase transitions and critical phenomena one usually adopts the canonical ensemble and exploits numerical Monte Carlo methods to predict the equilibrium behaviour. However it is also very interesting to follow the microcanonical ensemble and use molecular dynamics to investigate how the system reaches equilibrium. This is particularly true for finite systems and long-range interaction models since, in this case, extensivity and ergodicity are not assured and deviations from standard thermodynamics are usually found. On the other hand recently many data are available for phase transitions in finite systems, as for example in the case of nuclear multifragmentation or atomic clusters, and there is also much interest in studying plasma and self-gravitating systems [1]. Moreover the generalized thermodynamics introduced by Constantino Tsallis [2] to explain the complex dynamics of nonextensive and non-ergodic systems provides further stimuli and a challenging test in the same direction. In this context an apparently simple but instructive model of fully-coupled rotators, the so-called *Hamiltonian Mean Field* (HMF) model, has been intensively studied in the last decade [3-10] together with a generalized version with variable interaction range [11]. Such Hamiltonians have revealed a very complex out-of-equilibrium dynamics which can be considered paradigmatic for nonextensive systems [4,12]. We will illustrate in this short paper the interesting anomalous pre-equilibrium dynamics of the HMF model, focusing on the novel connections to the generalized nonextensive thermostatistics [5] and the recent links to glassy systems [10].

The HMF model: a paradigmatic example for long-range N-body classical systems

The HMF model has an Hamiltonian $H = K+V$, with the kinetic energy $K = \sum_{i=1}^{N} \frac{p_i^2}{2}$ and the potential one $V = \frac{1}{2N} \sum_{i,j=1}^{N} \left[1 - \cos(\vartheta_i - \vartheta_j)\right]$.

In the latter ϑ_i is the orientation angle of the i-*th* spin $\vec{s_i}$ =(sin ϑ_i, cos ϑ_i) and p_i is the corresponding conjugate coordinate, i.e. the angular momentum or the velocity, since the N spins have unitary mass. All the spins (rotators) interact with each other and in this sense the system is a *mean field model.* The average kinetic term $\bar{K}$ provides information on the temperature of the system, which can be calculated by the relation $T=2\bar{K}/N$. On the other hand, the potential part V is divided by the total number of spins in order to consider the thermodynamic limit. At equilibrium this Hamiltonian has a second order phase transition: increasing the energy density U=H/N beyond a critical point U_C=0.75, characterized by a critical temperature T_C=0.5, the system then passes from a ferromagnetic (condensed) phase to a disordered (homogeneous) one [3]. In correspondence, the order parameter given by the modulus of the total magnetization, i.e. $M = \left|\sum_{i=1}^{N} \vec{s}_i\right|$, goes from 1 to zero. Using standard procedures one can easily obtain the canonical equilibrium caloric curve, given by the relation $U = T/2 + (1 - M^2)/2$. On the other hand, by numerically integrating at fixed energy the equations of motion derived from the Hamiltonian, and starting the system close to equilibrium, the simulations reproduce well the theoretical prediction [3].

However, the situation is quite different when the system is started with strong *out-of-equilibrium* initial conditions, as for example giving to the system all the available energy as kinetic one. One way to do this is by considering all the angles $\vartheta_i = 0$, thus obtaining an initial magnetization M_0=1 and V=0, and distributing all the velocities in an uniform interval compatible with the chosen energy density –*water bag* distribution. Adopting such initial conditions, for an energy density interval below the critical point, i.e. $0.5 \le U \le U_c$, the microcanonical dynamics does have difficulties in reaching Boltzmann-Gibbs equilibrium: in fact, after a sudden relaxation from an high temperature state, the system remains trapped in *metastable long-living Quasi-Stationary States* (QSS) whose lifetime diverges with the system size N [4]. Along these metastable states, the so- called '*QSS regime*', the system is characterized by a temperature lower then the equilibrium one, until, for finite sizes, it finally relaxes towards the canonical prediction T_{eq}. But, if the infinite size limit is taken before the infinite time limit, the system never relaxes to Boltzmann-Gibbs equilibrium and remains trapped forever in the QSS plateau at the limiting temperature T_{QSS}.

The QSS regime is characterized by many dynamical anomalies, such as superdiffusion and Lévy walks, negative specific heat, non-Gaussian velocity distributions, vanishing Lyapunov exponents, hierarchical fractal-like structures in Boltzmann μ-space, slow-decaying correlations, aging and glassy features [3-11].

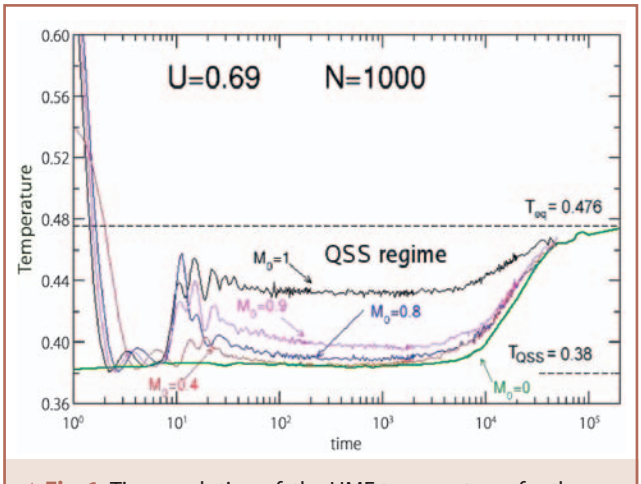

▲ **Fig. 1:** Time evolution of the HMF temperature for the energy density U = 0.69, N = 1000 and several initial conditions with different magnetization. After a very quick cooling, the system remains trapped into metastable long-living Quasi-Stationary States (QSS) at a temperature smaller than the equilibrium one. Then, after a lifetime that diverges with the size, the noise induced by the finite number of spins drives the system towards a complete relaxation to the equilibrium value. Although from a macroscopic point of view the various metastable states seem similar, they actually have different microscopic features and correlations which depend in a sensitive way on the initial magnetization.

These anomalies strongly depend on the initial magnetization M_0. In Fig.1 we show the QSS temperature plateaux for U=0.69 (a value for which the anomalies are more evident), N=1000 and for different out-of-equilibrium initial conditions with $0 \le M_0 \le 1$. The latter are realized by spreading the initial angles ϑ_i over wider and wider portions of the unit circle and using an uniform distribution for the momenta. The system starts from an initial temperature value that rapidly decreases according to the initial magnetization M_0 , until it reaches the metastable QSS. Only for M_0=0, the system already starts from the limiting plateau corresponding, according to the caloric curve, to a temperature T_{QSS}=0.38. In all cases, after a long lifetime, the system relaxes to the equilibrium temperature reported as dashed line. Although the macroscopic metastable states are present for all the initial conditions, from a microscopic point of view the system behaves in a very different way. This is nicely illustrated in Fig.2 where we report, for the energy density U=0.69 and N=10000, the initial time evolution of the μ–space for four different magnetizations. This figure illustrates how structures emerge and persist in the QSS region, but also their dependence on the initial conditions. Fractal-like structures characterize the μ–space for M_0=1 [4]. On the other hand, these features seem to persist, although smoothed, by decreasing M_0 until, for M_0=0, the microscopic configuration of the system remains always homogeneous. For this reason the latter seems to be the only case where an interpretation of metastability in terms of Vlasov equation [7] could likely be applicable. At variance, Tsallis statistics appears to be the best candidate for all the other cases.

Connections to Tsallis thermostatistics

In order to explore the characteristic microscopic dynamics originated by the different initial conditions and its connection with Tsallis thermostatistics, one can focus on the *velocity autocorrelation* function $C(t) = \sum_{i=1}^{N} p_i(t)p_i(0)/N$ [5]. The latter is plotted in Fig.3(a) for U=0.69, N=1000 and several initial magnetizations M_0. The initial fast relaxation illustrated in Fig.1 has been truncated to focus only on the properties of the metastable states and an ensemble average over 500 different realizations was performed. One can see immediately that for $M_0 \ge 0.4$ the correlation functions are very similar, while the decay is faster for M_0=0.2 and even more for M_0=0 [5,10]. These relaxation decays are extremely well fitted by Tsallis' *q-exponential* functions defined as $e_q(z) = [1+(1-q)z]^{1/(1-q)}$, where z = – t/τ, τ being a characteristic time which indicates the bending of the curve, while *q* is the entropic index [2]. Actually, *nonextensive thermostatistics* introduced by Tsallis has been shown to be particularly adequate to generalize the usual Boltzmann-Gibbs (BG) formalism in describing the out-of-equilibrium dynamics of systems that live in fractal regions of phase space [4]. In this new context, the entropic index q is able to quantify the degree of *nonextensivity* and *non-ergodicity* of the dynamics. For q=1 the standard BG statistics is recovered. In Fig.3(a), by means of *q*-exponential fits, we illustrate how one can characterize in a quantitative way the dynamical correlations induced by the different initial conditions: in fact we get a value of q = 1.5 for $M_0 \ge 0.4$, while $q = 1.2$ and $q = 1.1$ for $M_0 = 0.2$ and for $M_0 = 0$ respectively. Thus for $M_0 \ge 0.4$ correlations exhibit a long range nature and a slow long tailed decay. On the other hand they diminish progressively for initial magnetizations smaller than $M_0 = 0.4$, to become almost exponential for $M_0 = 0$. Such a result clearly indicates a different microscopic nature of the QSS in the $M_0 = 0$ case, which is probably linked to the fact that the latter is a stationary solution of the Vlasov equation [7]. On the other hand, Tsallis' generalized formalism is able to characterize the dynamical

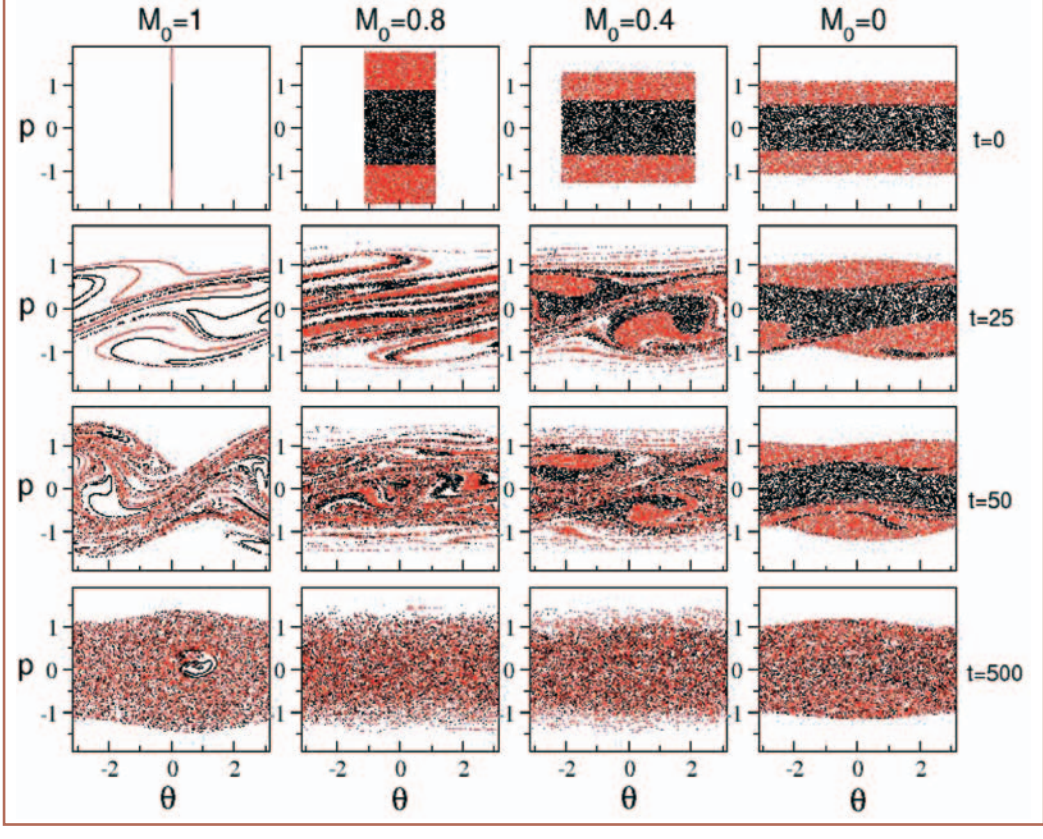

◄ **Fig. 2:** Initial time evolution of the HMF model μ-space at four times (t = 0,25,50,500) and for different initial magnetizations. The energy density is U = 0.69 and the number of spins is N = 10000. The initial fast particles are plotted in red to illustrate the mixing properties of the dynamics in the various cases. Fractal-like structures are formed and persist in the QSS regime for $M_0 > 0$. On the other hand, when the initial magnetization is $M_0 = 0$ the system remains in a homogeneous configuration. In this case microscopic correlations are almost absent and no structure is evident.

features

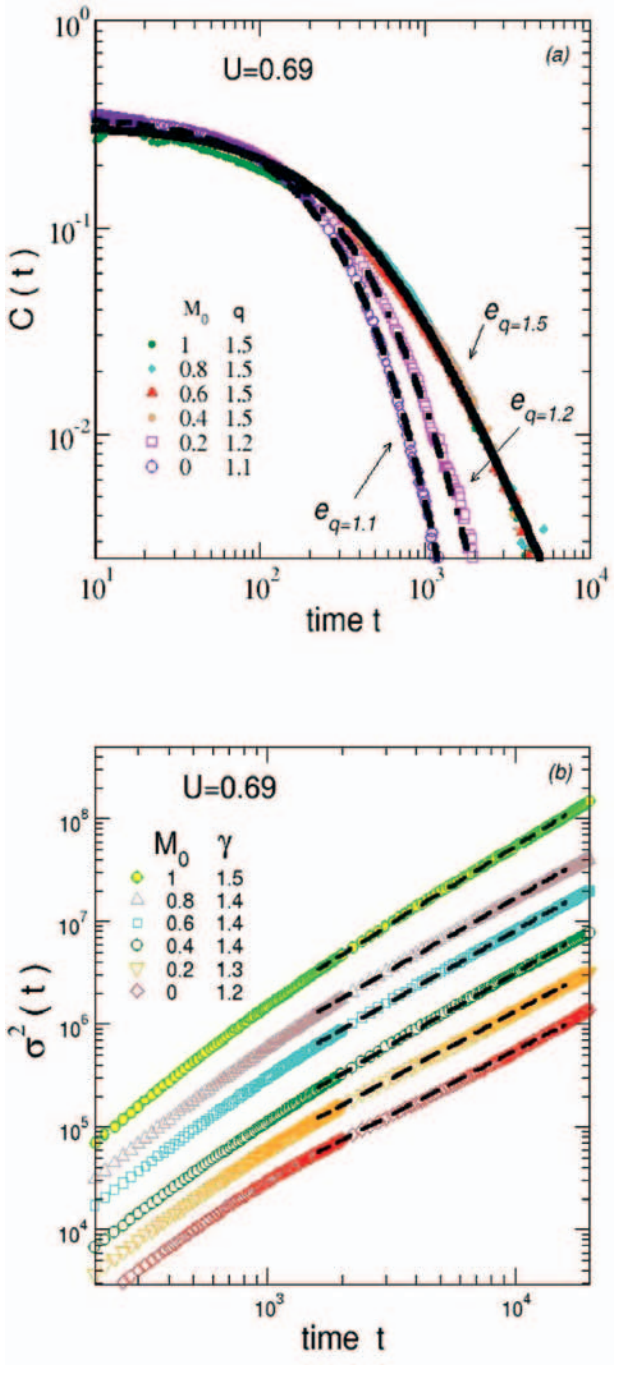

▲ **Fig. 3:** (a) Time evolution of the HMF velocity autocorrelation functions for U = 0.69, N = 1000 and different initial conditions are nicely reproduced by q-exponential curves. The entropic index q used is also reported. (b) Time evolution of the variance of the angular displacement for U = 0.69, N = 2000 and different initial conditions. After an initial ballistic motion, the slope indicates a superdiffusive behaviour with an exponent γ greater than 1. This exponent is also reported and indicated by dashed straight lines. Anomalous diffusion does not depend in a sensitive way on the size of the system. For both the plots shown, the numerical simulations are averaged over many realizations.

anomalies observed not only for $M_0 = 1$ but also for any finite initial magnetization.

Actually there are several other results pointing in this direction and in favour of Tsallis generalized statistics [4-6,12]. In the following, we want to discuss an interesting conjecture that gives further support to this interpretation. It concerns a link between the value of the entropic index q which characterize the velocity autocorrelation decay and the exponent of the anomalous diffusion γ [5].

In order to observe the diffusion process one can consider the *mean square displacement* of phases $\sigma^2(t)$ defined as $\sigma^2(t) = \langle |\theta_i(t) - \theta_i(0)|^2 \rangle$, where the brackets represent an average over all the N rotators. The mean square displacement typically scales as $\sigma^2 \propto t^\gamma$. In general the diffusion is normal when $\gamma = 1$, corresponding to the Einstein's law for Brownian motion, and ballistic (free particles) for $\gamma = 2$. Otherwise, the diffusion is anomalous and in particular one has *superdiffusion* if $\gamma > 1$. In Fig.3(b) we plot the mean square displacement versus time for U=0.69, N=2000 and different initial conditions. One can see that, after the ballistic regime of the initial fast relaxation, in the QSS regime and afterwards the system clearly shows superdiffusion for $0.4 \le M_0 \le 1$ and the exponent γ has values in the range 1.4-1.5. On the other hand, in the case $M_0 = 0$ we get $\gamma = 1.2$. Actually by increasing the size of the system, diffusion tends to become normal ($\gamma = 1$ for N = 10000). Again this case seems to be quite peculiar and microscopically very different from the others studied, where anomalies are much more evident.

Superdiffusion observed in the slow QSS regime seems to be linked with the q-exponential decay of the velocity correlations through the 'γ-q *conjecture*', based on a generalized nonlinear Fokker-Planck equation that generates q-exponential space-time distributions [5]. In this framework the entropic index q is related to the parameter γ by the relationship $\gamma = 2/(3-q)$. Since in diffusive processes space-time distributions are linked to the respective velocity correlations by the well known Kubo formula, one could investigate the γ-q relation considering the entropic index q characterizing the velocity correlation decay in an anomalous diffusion scenario. In Fig.4 we illustrate the robustness of this conjecture by varying not only the initial conditions and the size of the system, but also the range of interaction. These calculations were done by considering the generalized α-XY Hamiltonian, with the parameter α, which modulates the range of the interaction, varying from 0 (HMF model) to 1 [11]. By plotting the ratio $\gamma / [2/(3-q)]$ as a function of γ for various values of N, M_0 and α at U=0.69, one can see that the γ-q conjecture is confirmed within an error of $\pm$ 0.1. This means that knowing the superdiffusion exponent one can predict the entropic index of the velocity correlation decay and viceversa.

The simulations here discussed add an important piece of information to the puzzling scenario of the pre-equilibrium dynamics of the HMF model and its generalizations, which cannot be explained with the standard tools of the BG statistical mechanics. Although these results do not provide a rigorous proof of the applicability of Tsallis generalized statistics, they strongly indicate that this formalism is at the moment the best candidate for explaining the huge number of observed anomalies for a wide class of out-of-equilibrium initial conditions.

Links to glassy systems

The importance of the role of initial conditions in generating anomalous dynamics, together with the discovery of aging and dynamical frustration in the QSS regime [6,10], suggests also

another non-ergodic description of the HMF dynamics complementary to the Tsallis' one, i.e. the so-called *weak ergodicity-breaking* scenario of glassy systems [13]. The latter occurs when the phase space is a-priori not broken into mutually inaccessible regions in which local equilibrium may be achieved, as in the true ergodicity breaking case, but nevertheless the system can remain trapped for very long times in some regions of the complex energy landscape. It is widely accepted that the energy landscape of a glassy system is extremely rough, with many local minima corresponding to metastable configurations surrounded by rather high energy barriers: one thus expects that these states act as traps which get hold of the system during a certain time. In the QSS regime of the HMF model, when the system starts from M_0=1 initial conditions, such a mechanism is reproduced by the existence of a hierarchical distribution of clusters which compete among each other in trapping more and more particles [10]. Such a phenomenon produces a sort of *dynamical frustration* that recalls the pictorial explanation of aging made by the *cage* model for structural glasses [13] and thus could justify the slow relaxation time observed in the velocity autocorrelation function. Recently, the analogy between the HMF model and glassy systems has been extended by introducing a new order parameter, to quantify the degree of freezing of the rotators due to the dynamical frustration. The *elementary polarization* was defined as the temporal average, integrated over an opportune time interval τ, of the successive positions of each spin $\langle \vec{s}_i \rangle = \frac{1}{\tau}\int_{t_0}^{t_0+\tau} \vec{s}_i dt$ with $i = 1, 2, \ldots N$, and t_0 being an initial transient time [10].

Then one can average the module of the elementary polarization over the N spin configurations, to obtain the *polarization p* defined as $p = \frac{1}{N}\sum_{i=1}^{N} |\langle \vec{s}_i \rangle|$. In analogy with the behaviour of the Edwards Anderson order parameter in the Sherrington-Kirkpatrick (SK) model of an infinite range spin-glass [13], in the equilibrium regime of the HMF model the polarization *p* is equal to the magnetization M. On the other hand, in the out-of-equilibrium QSS regime, which plays here the role of the Spin-Glass phase in the SK model, the emerging dynamical frustration introduces an effective randomness in the interactions and quenches the relative motion of the spin vectors. Thus *p* has a non null value as in the equilibrium condensed phase, while magnetization, vanishes with the size N of the system and is zero in the thermodynamic limit.

In Fig.5 we plot the behaviour of *p* and M versus U at equilibrium (a) and vs N in the QSS regime (b), for U=0.69 and the M_0=1 initial conditions. At equilibrium M and *p* assume the

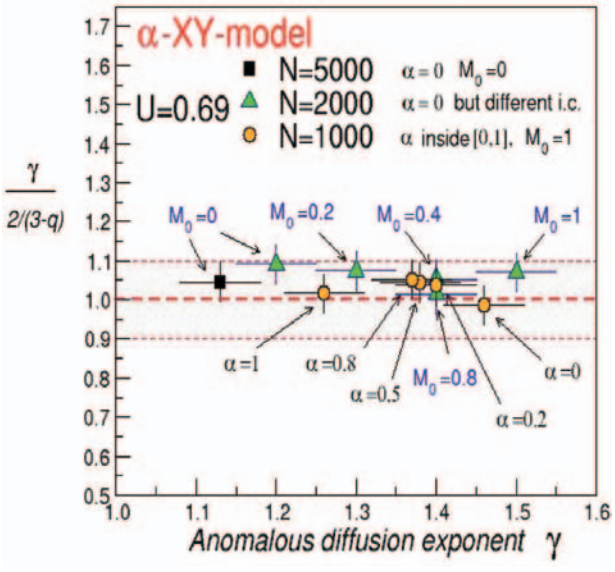

▲ **Fig. 4:** For different system sizes and initial conditions, and for several values of the parameter α which fixes the range of the interaction of a generalized version of the HMF model [11], the figure illustrates the ratio of the anomalous diffusion exponent γ divided by 2/(3-q) vs γ. The entropic index q is extracted from the relaxation of the correlation function (see previous figure). This ratio is always one within the errors of the calculations.

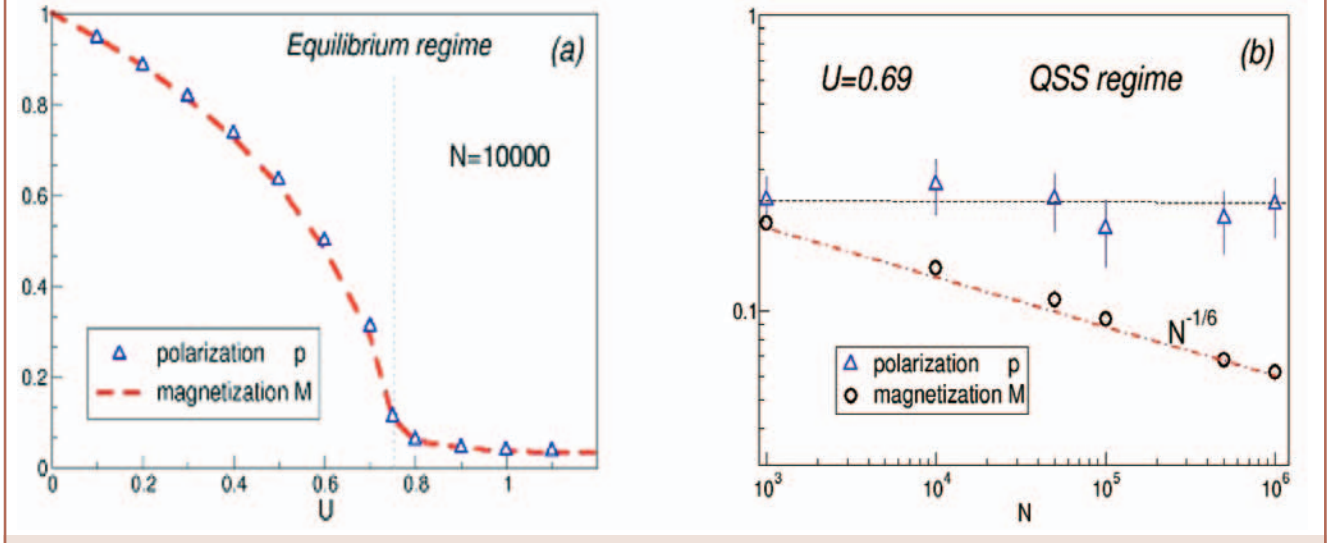

▲ **Fig. 5:** (a) The magnetization M and the polarization p are plotted vs the energy density for N=10000 at equilibrium: the two order parameters are identical. (b) The same quantities plotted in (a) are here reported vs the size of the system, but in the metastable QSS regime. In this case, increasing the size of the system, the polarization remains constant around a value $p \sim 0.24$ while the magnetization M goes to zero as $N^{-1/6}$.

same values for both the ferromagnetic and paramagnetic phase. Instead, in the QSS regime magnetization correctly vanishes with $N^{-1/6}$ while polarization remains constant at a value 0.24 ±0.05. This does strongly indicate that we can consider the QSS regime as a sort of glassy phase for the HMF model. Again, it is important to stress the role of the initial conditions in order to have dynamical frustration and glassy behaviour. Actually, glassy features are very sensitive to the initial kinetic explosion that produces the sudden quenching and dynamical frustration. In particular, reducing M_0 from 1 to 0.95 the polarization effect and the hierarchical clusters size distributions become much less evident, until they completely disappear decreasing further M_0 [10]. In this sense, the M_0=1 initial conditions seems to select a special region of phase space where the system of rotators described by the HMF Hamiltonian behaves as a glassy system. We note in closing that this result gives also a further support to the broken ergodicity interpretation of the QSS regime of Tsallis themostatistics.

Conclusions

Summarizing the HMF model and its generalization, the a-XY model, provide a perfect benchmark for studying complex dynamics in Hamiltonian long-range systems. It is true that several questions remain still open and need to be further studied with more detail in the future. However the actual state of the art favours the application of Tsallis thermostatistics to explain most of the anomalies observed in the QSS regime. The latter seems to have also very interestings links to glassy dynamics.

References

[1] T. Dauxois, S. Ruffo, E. Arimondo, M. Wilkens eds., *Dynamics and Thermodynamics of Systems with Long Range Interactions,* Lecture Notes in Physics Vol. 602, Springer (2002).

[2] Tsallis *J. Stat. Phys.* **52** (1988) 479.

[3] T. Dauxois, V. Latora, A. Rapisarda, S. Ruffo and A. Torcini, in ref.[1] p. 458 and refs. therein.

[4] V. Latora, A. Rapisarda and C. Tsallis, *Phys. Rev. E* **64** (2001) 056134; V. Latora, A. Rapisarda and A. Robledo, *Science* **300** (2003) 249.

[5] A. Pluchino, V. Latora, A. Rapisarda, *Continuum Mechanics and Thermodynamics* 16 (2004) 245 and cond-mat/0507005.

[6] M.A. Montemurro, F.A. Tamarit and C. Anteneodo, *Phys. Rev. E* **67**, (2003) 031106 .

[7] Y.Y. Yamaguchi, J. Barrè, F. Bouchet, T. Dauxois, S. Ruffo, *Physica A* **337** (2004) 36.

[8] H. Morita and K. Kaneko, *Europhys. Lett.* **66** (2004) 198.

[9] P.H. Chavanis, J. Vatterville, F. Bouchet, *Eur. Phys. Jour. B* **46** (2005) 61.

[10] A. Pluchino, V. Latora, A. Rapisarda, *Phys. Rev. E* **69** (2004) 056113, cond-mat/0506665 and A. Pluchino and A. Rapisarda, *Progr. Theor. Phys.* (2005) in press, cond-mat/0509031 .

[11] For a generalization of the HMF model see: A. Campa, A. Giansanti, D. Moroni, *J. Phys. A: Math. Gen*. **36** (2003) 6897 and refs. therein.

[12] F.D. Nobre and C. Tsallis, *Phys. Rev. E* **68** (2003) 036115.

[13] L.F. Cugliandolo in Slow r*elaxation and non-equilibrium dynamics in condensed matter,* Les Houches Session 77, J-L Barrat et al.eds., Springer-Verlag (2003), condmat/0210312 and refs. therein.

Complexity of seismicity and nonextensive statistics

Sumiyoshi Abe [1], Ugur Tirnakli [2] and P.A. Varotsos [3]

[1] Institute of Physics, University of Tsukuba, Ibaraki 305-8571, Japan

[2] Department of Physics, Faculty of Science, Ege University, 35100 Izmir, Turkey

[3] Solid State Section and Solid Earth Physics Institute, Physics Department, University of Athens, Panepistimiopolis, Zografos 157 84, Athens, Greece

Seismic time series is basically composed of the sequence of occurrence time, spatial location and value of magnitude of each earthquake. In other words, seismic moments (their logarithms being values of magnitude) as amplitudes are defined at discrete spacetime points. Seismicity is therefore a field-theoretic phenomenon. However, unlike a familiar one such as an electromagnetic field, it is inherently probabilistic in both magnitude and locus in spacetime. It is characterized by diverse phenomenology, accordingly. Known classical examples are the Gutenberg-Richter law and the Omori law. The former states that the frequency of earthquakes with magnitude larger than M, $N\,(>M)$, is related to M itself as $\log N\,(>M) = A - bM$, where A and b are constants and, in particular, $b \approx 1$ empirically. Magnitude is related to the emitted energy, E, as $M \sim \log E$. The Omori law describes the temporal rate of aftershocks following a main shock. The number of aftershocks between t and $t + dt$, $dN\,(t)$, after a main shock at $t = 0$, empirically decays in time as $(t + t_0)^{-p}$, where t_0 and p are constants with p varying between 0.6 and 1.5 according to real seismic data. It is noticed that both of them are power laws, i.e., they have no characteristic scales, pronouncing complexity and criticality of the phenomenon.

Nonextensive statistics (Tsallis statistics or q-statistics) [1] has been attracting continuous attention as a possible candidate theory of describing statistical properties of a wide class of complex systems. It is a generalization of Boltzmann-Gibbs equilibrium statistical mechanics, and is concerned with nonequilibrium stationary states of complex systems. Since complex systems reside at the edge of chaos in the language of dynamical systems, ergodicity, which is a fundamental premise in Boltzmann-Gibbs statistics, may be broken. That is, at the level of statistical mechanics, long-time average and ensemble average of a physical quantity do not coincide. Clearly, the concept of ergodicity does not apply to seismicity because of the absence of the ensemble notion in its nature.

Though the complete dynamical description of seismicity is still out of reach, some models have been proposed in the literature to explain some features. Among others, the spring-block model, the self-organized criticality model and mean-field models such as the coherent noise model are frequently discussed (the last one will be visited here later).

Criticality and nonergodicity of real seismicity may lead to the question if some of its physical aspects can phenomenologically be described by nonextensive statistics and related theoretical treatments. The answer to this question turns out to be affirmative.

Abe and Suzuki [2] have studied long-time statistics of the spatial distance between two successive earthquakes by using two sets of the data taken in Japan and California. They have found that, over the whole ranges, both of the data are fitted extremely well by the q-exponential distributions with $0 < q < 1$. Here, the q-exponential distributions are the maximum Tsallis entropy distributions [1], where q is the index of the Tsallis entropy [1]. Then, they have further analyzed long-time statistics of the time interval between two successive earthquakes, termed "calm time" (or, interoccurrence time), and have ascertained [2] that, as the spatial distance, the calm time also obeys the q-exponential distributions both in Japan and California with $q > 1$ over the whole ranges. The q-exponential distribution has the form: $\sim \exp_q(-\beta Q)$, where β is a positive constant and Q is a positive random variable, i.e., the distance or the time interval between two successive earthquakes, in the present case [see Box in the Editorial by J. P. Boon and C. Tsallis for the definitions of the q-exponential function, $\exp_q(x)$ and its inverse, the q-logarithmic function, $\ln_q(x)$].

The q-exponential distribution with $q > 1$ is equivalent to the so-called Zipf-Mandelbrot power-law distribution, which is known to be derivable from several independent approaches including the maximum Tsallis entropy principle. On the other hand, the q-exponential distribution with $0 < q < 1$ has a cutoff at a finite value of the random variable under consideration. Simultaneous derivation of both $q > 1$ and $0 < q < 1$ cases is considered to be realized only by the maximum Tsallis entropy principle. Another point of interest is that the sum of the q-indices of the distributions of the spatial distance and the calm time in real seismicity is found to be close to 2, both in Japan and California. In nonextensive statistics, the theories with $q(> 0)$ and $2 - q(> 0)$ are said to be *dual* to each other. Therefore, seismicity exhibits "spatio-temporal duality".

Thus, nonextensive statistics well explains spatio-temporal complexity of real seismicity in its long-time behavior. In the short-time scale, however, the seismic data is nonstationary and highly structured, in general. Such features are mainly due to aftershocks following main shocks. A time interval of the seismic time series, in which the events obey the Omori law for aftershocks, is referred to as "Omori regime". Recently, Abe and Suzuki have discovered [3] that nonstationarity of the time series of aftershocks obeys a peculiar law for event-event correlation. The event-event correlation function proposed in Ref.[3] is given by

$$C(n+n_w, n_w) = \frac{\langle t_{n+n_w} t_{n_w} \rangle - \langle t_{n+n_w} \rangle \langle t_{n_w} \rangle}{\left(\sigma^2_{n+n_w} \sigma^2_{n_w}\right)^{1/2}} \qquad (1)$$

In this equation, t_n is the time when the nth shock after a given main shock occurs. The averages and the variance are defined by $\langle t_m \rangle = (1/M)\sum_{k=0}^{M-1} t_{m+k}$, $\langle t_m t_{m'} \rangle = (1/M)\sum_{k=0}^{M-1} t_{m+k} t_{m'+k}$ and $\sigma_m^2 = \langle t_m^2 \rangle - \langle t_m \rangle^2$, respectively. M is the number of the successive events taken inside the Omori regime under consideration. Comparing Eq. (1) with the ordinary autocorrelation function, one sees that the basic random variable is t_n, which is the occurrence time of the nth event. In other words, n plays a role of a certain time parameter of the discrete time series. Such a time parameter is called "natural time", which has been introduced by Varotsos and his collaborators [4]. Accordingly, n_w in Eq. (1) is termed "natural waiting time".

A striking property reported in Ref.[3] is that event-event correlation of aftershocks exhibits the *aging phenomenon* with respect to the natural waiting time (this phenomenon will be explained below). In addition, it also obeys a definite scaling property. The correlation function in Eq. (1) is found to satisfy the functional relation: $C(n + n_w, n_w) = \tilde{C}(n/f(n_w))$. The relation of this kind is called the scaling relation, and the associated function $\tilde{C}$ of a single argument is termed the scaling function. For earthquake aftershocks, $f(n_w)$ is empirically given by $f(n_w) \sim (n_w)^\gamma$ with a positive exponent γ. It is emphasized that these properties are revealed by the use of the natural time, not the conventional time.

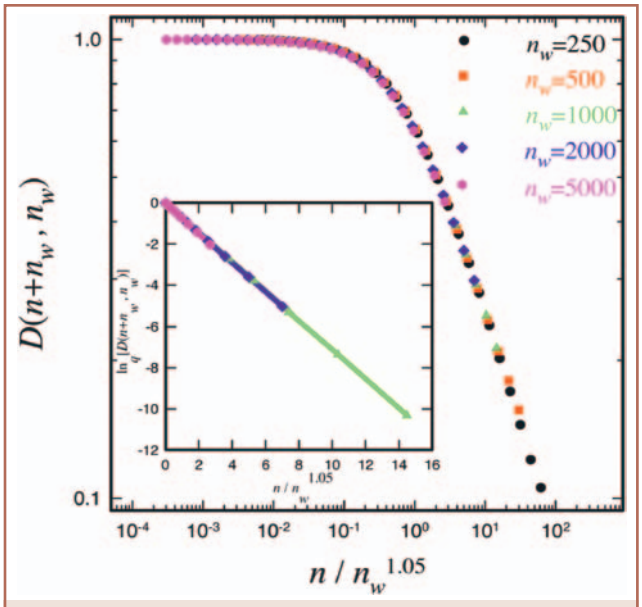

▲ **Fig. 1:** Data collapse of the aging curves of the event-event correlation functions for different values of the natural waiting time. Inset: the semi-q-log plot of the collapsed curve (see Box in the editorial paper for the definition of the q-logarithmic function). The straight line implies that the scaling function is of the q-exponential form with $q \simeq 2.98$. The ensemble average is performed over 120000 numerical runs. All quantities are dimensionless.

The above result sheds new light on the physical nature of aftershocks. The crust has a complex landscape regarding the stress distribution at faults. A main shock can be regarded as a kind of quenching process. Aftershocks following a main shock give rise to nonequilibrium nonstationary process. It is a slow relaxation process due to the power-law nature of the Omori law. Combining these features with the above-mentioned aging phenomenon and scaling relation, one recognizes that the mechanism governing aftershocks may be of *glassy dynamics*. This observation is of particular interest since, according to the recent investigations of Baldovin and Robledo (e-print cond-mat/0504033) and of Pluchino, Rapisarda and Latora (e-print cond-mat/0507005), there is some evidence which suggests the existence of a deep connection between nonextensive statistical mechanics and glassy dynamics.

The Gutenberg-Richter law has been a touchstone for any model of earthquakes. Real seismicity is however characterized by much richer phenomenology. The novel laws, phenomena and relations mentioned above give stringent criteria for modeling. From the physical viewpoint, what is more important is to examine how these properties are universal for complex systems with catastrophes. Model simulation may be useful for this purpose.

Recently, Tirnakli and Abe [5] have numerically reanalyzed a simple mean-field model called the coherent noise model in order to examine if the aftershocks described by it can exhibit the aging and scaling properties. This model is already known to describe both the Gutenberg-Richter law and the Omori law. In the analysis, a main shock is identified and the associated Omori

regime is fixed. As expected, the model is nonergodic and, accordingly, the time average and the ensemble average of a physical quantity are different from each other. We have ascertained that, for the event-event correlation function (defined by the natural-time average) in Eq. (1), the model well reproduces the aging and scaling properties (together with the form of the scaling function, $\tilde{C}$) discovered in Ref.[3] for real seismicity. On the other hand, an intriguing feature was found for the event-event correlation function defined by the ensemble average with respect to numerical runs. To distinguish such a correlation function from the one with the natural-time averages in Eq. (1), it is denoted here by $D(n + n_w, n_w)$. This quantity also turned out to exhibit the aging phenomenon with respect to the natural waiting time, that is, *the smaller the value of the natural waiting time is, the faster correlation decays.* So, the system has an internal clock. Fig. 1 shows that the aging curves become collapsed to a single curve by the rescaling of the natural time: $D(n + n_w, n_w) = \tilde{D}(n/(n_w)^{1.05})$, establishing the scaling property. The inset presents its semi-q-log plot. The straight line there implies that the scaling function, $\tilde{D}$, is given by the q-exponential function.

Now, according to Tsallis [6], there may be "q-triplet" $\{q_{stat}, q_{sen}, q_{rel}\}$ for a system described by nonextensive statistics, where q_{stat} is the entropic index appearing in the maximum Tsallis entropy distribution as well as the Tsallis entropy itself, q_{sen} is the index characterizing sensitivity of a nonlinear dynamical system to the initial condition and q_{rel} controls the rate of relaxation and decay of correlation. In the case of a simple system described by Boltzmann-Gibbs-type statistics, the q-triplet may be given by $\{q_{stat}, q_{sen}, q_{rel}\} = \{1, 1, 1\}$. In the case of a complex system, physical quantities are often expressed empirically in terms of the q-exponential function: e.g., probability distributions (q_{stat}), the distance between two trajectories of a dynamical system (q_{sen}) and relaxation or correlation (q_{rel}), with the values all different from unity. An example is provided by the recent work done by the people from NASA [7], who have discovered a non-Boltzmann-Gibbs case in a single physical setup. Analyzing the fluctuating magnetic field strength observed by Voyager 1 in the solar wind, they have found that $\{q_{stat}, q_{sen}, q_{rel}\} = \{1.75 \pm 0.06, -0.6 \pm 0.2, 3.8 \pm 0.3\}$.

Therefore, the q-exponential scaling function obtained for aftershocks in the coherent noise model, $\tilde{D}$, with $q_{rel} \simeq 2.98$, which is notably different from unity, could be seen as a fingerprint of further relevance of nonextensive statistics.

Science of complexity certainly enables one to reveal novel aspects of real seismicity. Nonextensive statistics is expected to offer a guiding principle for a deeper understanding of complex dynamical systems with catastrophes, in general and complexity of seismicity, in particular.

References

[1] *Nonextensive Statistical Mechanics and Its Applications.* edited by S. Abe and Y. Okamoto (Springer-Verlag, Heidelberg, 2001).

[2] S. Abe and N. Suzuki, *J. Geophys. Res.,* **108** (B2):2113, 2003; S. Abe and N. Suzuki, *Physica A,* **350:** 588-596, 2005.

[3] S. Abe and N. Suzuki, *Physica A,* **332:** 533-538, 2004.

[4] P.A. Varotsos, N.V. Sarlis, and E.S. Skordas, *Phys. Rev. E,* **66:** 011902, 2002.

[5] U. Tirnakli and S. Abe, *Phys. Rev. E,* **70:** 056120, 2004.

[6] C. Tsallis, *Physica A,* **340:** 1-10, 2004.

[7] L. F. Burlaga and A. F. Viñas, *Physica A,* **356:** 375-384, 2005.

S_q entropy and self-gravitating systems

A.R. Plastino [1,2] *

[1] *Departament de Física, Universitat de les Illes Balears, 07122 Palma de Mallorca, Spain.*

[2] *Physics Department, University of Pretoria, Pretoria 0002, South Africa.*

* *arplastino@maple.up.ac.za, vdfsarp9@uib.es*

More than fifteen yeas ago, a generalized thermostatistical formalism (usually referred to as nonextensive statistical mechanics) based on a power-law entropic measure S_q was advanced by Constantino Tsallis [1]. Increasing attention has been paid to the Tsallis proposal in recent years, because it has been hailed by many researchers as a useful tool for the description of certain aspects of physical scenarios exhibiting atypical thermodynamical features due, for instance, to the presence of long range interactions. When the Tsallis formalism appeared in 1988, it was not at all clear what possible physical applications it might have. The first hint pointing towards a relationship between the Tsallis' ideas and the thermodynamics of systems with long range interactions came in 1993 [2], when it was realized that the Tsallis entropic functional is closely related to a family of distribution functions well known by astronomers studying the dynamics of stellar systems: the polytropic stellar distributions. In point of fact, the discovery of the connection between Tsallis entropy and the stellar polytropic distribution constituted the first application of the Tsallis' formalism to a concrete physical problem. Stellar systems, such as stellar clusters or galaxies, are important examples of astrophysical self-gravitating systems, where the gravitational interaction between the constituents of the system play a fundamental role in determining the system's properties. The exploration of the connections between the Tsallis thermostatistical formalism and the physics of self-gravitating systems has been the focus of a considerable research activity in recent years [3-7].

Nonextensive statistical mechanics is built up on the basis of the nonextensive, power-law entropy S_q [1]. The entropic index q (also called the Tsallis' entropic parameter) characterizes the statistics we are dealing with. In the limit $q \to 1$ the usual Boltzmann Gibbs (BG) expression is recovered: $S_1 = S_{BG}$ (for the definitions of the basic quantities associated with the q-entropy see the Box in the editorial introduction by Tsallis and Boon to the present Issue). Optimizing the entropic measure S_q under the constraints imposed by normalization and the mean value of the energy, one obtains the probability distribution associated (in the context of Tsallis' formalism) with the thermal equilibrium or metaequilibrium of the system under consideration. The main property of this q-generalized maximum entropy distribution is that it exhibits a power-law like dependence on the microstate energy ϵ_i, instead of the exponential dependence associated with the standard Boltzmann-Gibbs thermostatistics.

Galaxies can be regarded as self gravitating N-body systems that are trapped for a long time in a non-collisional regime (until collisional effects finally become important) where the stars move under the influence of the mean potential Φ generated by the whole set of stars, Φ being a function of the spatial position $\mathbf{x}$.

The description of a state of any collisionless system is given by a distribution function $F(\mathbf{x}, \mathbf{v}, t)$ in a 6-dimensional phase space where $\mathbf{v}$ is the velocity vector and t the time. The fundamental equation of stellar dynamics is (as far as collisionless systems are concerned) the Vlasov equation

$$\frac{\partial F}{\partial t} + \mathbf{v} \cdot \nabla_x F - \nabla_x \Phi \cdot \nabla_v F = 0, \qquad (1)$$

coupled to an equation relating the distribution function $F(\mathbf{x}, \mathbf{v}, t)$ with the Newtonian gravitational potential Φ,

$$\Phi(\mathbf{x}) = -Gm \int \frac{F(\mathbf{x}', \mathbf{v}')}{|\mathbf{x} - \mathbf{x}'|} d^3\mathbf{x}' d^3\mathbf{v}', \qquad (2)$$

where G is Newton's gravitational constant and m denotes the mass of each individual star. The Vlasov equation can also be written as $(dF/dt)_{\text{orb.}} = 0$, meaning that the total time derivative of the distribution function, evaluated along the orbit of a single star moving in the gravitational potential Φ, vanishes. It has to be stressed that the non-collisional dynamics governed by the Vlasov-Poisson system provides only an approximate description of the behaviour of an N-particle self-gravitating system. However, this approximation is very useful for the study of various stellar systems [8]. A complete (Newtonian) account of the dynamics of a self-gravitating N-particle system is provided by the full set of N coupled (Newtonian) equations of motion of the N-particles. In general, this approach to the dynamics of self-gravitating systems is investigated via numerical N-body simulations (see, for instance, [7]).

The Vlasov equation (1) for self gravitating systems, with the potential Φ given by (2), is nonlinear, since the gravitational potential Φ is given, in a self-consistent way, in terms of the distribution function F. An important feature of the Vlasov-Poisson system is that, given a functional of the form

$$C[F] = \int g(F) d^3\mathbf{x} d^3\mathbf{v}, \qquad (3)$$

the solutions of the Vlasov equation (1) verify $dC/dt = 0$. The total energy of the system, given by

$$E = \frac{m}{2} \int \mathbf{v}^2 F(\mathbf{x}, \mathbf{v}) d^3\mathbf{x}\, d^3\mathbf{v} - \frac{Gm^2}{2} \int \frac{F(\mathbf{x}, \mathbf{v}) F(\mathbf{x}', \mathbf{v}')}{|\mathbf{x} - \mathbf{x}'|} d^3\mathbf{x}\, d^3\mathbf{v}\, d^3\mathbf{x}'\, d^3\mathbf{v}', \qquad (4)$$

is, of course, preserved under the evolution governed by equations (1-2).

When stellar systems relax to an equilibrium (or to a meta-equilibrium) state, one expects them to "forget" all information about their initial conditions with the exception of the conserved quantities. Consequently, if one tries to infer by recourse to a maximum entropy prescription the final relaxed state, it is reasonable to use the conserved quantities as constraints. The natural constraints for spherical stellar systems are the total mass and energy of the system. However, if one tries to maximize the standard Boltzmann-Gibbs entropy of the system under the constraints imposed by the conservation of total mass and energy, one obtains the isothermal sphere distribution, which has *infinite* mass and energy [8].

In [2], it was shown that the extremalization of the non extensive q-entropy under the same constraints leads to the stellar polytropic sphere distributions which, for a certain range of the q parameter, are endowed with *finite* mass and energy, as physically expected. This constituted the first clue suggesting that the generalized thermostatistical formalism based on S_q is relevant for the study of systems exhibiting non extensive thermodynamical properties due to long range interactions.

Stellar polytropic sphere distributions are of the form

$$f(\mathbf{x}, \mathbf{v}) = f(\tilde{\epsilon}) = \begin{cases} A(\Phi_0 - \tilde{\epsilon})^{n-3/2} & \tilde{\epsilon} \leq \Phi_0 \\ 0 & \tilde{\epsilon} > \Phi_0, \end{cases} \qquad (5)$$

where

$$\tilde{\epsilon} = \frac{1}{2}\mathbf{v}^2 + \Phi(\mathbf{x}), \qquad (6)$$

is the total energy (per unit mass) of an individual star, and A, Φ_0, and n (usually called the *polytropic index*) are constants. The quantity $f(\mathbf{x},\mathbf{v}) d^3x d^3v$ denotes the number of stars with position and velocity vectors respectively within the elements d^3x and d^3v in position and velocity spaces. The polytropic distribution (5) exhibits, after an appropriate identification of the relevant parameters, the q-MaxEnt form. The entropic parameter q can be related to index n (see Figure 1) by identifying n-3/2 with $q/(1\text{-}q)$, obtaining [5]

$$\frac{1}{1-q} = n - \frac{1}{2}. \qquad (7)$$

The limit $n \to \infty$ (hence $q = 1$) recovers the isothermal sphere case; $n = 5$ corresponds to the so called Schuster sphere; for $n < 5$ (hence $q < 7/9$), finiteness for mass and energy naturally emerges. The cut-off in the polytropic distribution (5) is an example of what is known, within the field of non extensive thermostatistics, as "Tsallis cut-off prescription", which affects the q-maximum entropy distributions when $q < 1$. In the case of stellar polytropic distributions this cut-off arises naturally, and has a clear physical meaning. The cut-off corresponds, for each value of the radial coordinate r, to the corresponding gravitational escape velocity [8].

Polytropic distributions constitute the simplest, physically plausible models for self-gravitating stellar systems [8]. Alas, these models do not provide an accurate description of the observational data associated with real galaxies. In spite of this, the connection between the S_q entropy and stellar polytropes is of considerable interest. Besides the notable fact that, for a special range of values of q, non-extensive thermostatistics leads to finite stellar systems, the established connection between the S_q entropy and stellar polytropic distributions is interesting for other reasons. Polytropic distributions arise in a very natural way from the theoretical study of self-gravitating systems. The investigation of their properties has constantly interested theoretical astrophysicists during the last one hundred years [8]. Polytropic distributions are still the focus of an intense research activity [3-7], and the study of their basic properties constitutes a part of the standard syllabus of astrophysics students. Now, *polytropic distributions happen to exhibit the form of q-MaxEnt distributions, that is, they constitute distribution functions in the* $(\mathbf{x},\mathbf{v})$ *space that maximize the entropic functional* S_q *under the natural constraints imposed by the conservation of mass and energy [2]*. It is important to remember that the original path leading to the S_q entropic form was not motivated by self-gravitating systems, nor was it motivated by any other *specific* system. The entropic form S_q was proposed by recourse to very general arguments dealing with the consideration of (i) entropic forms incorporating power law structures (inspired on multifractals) and reducing to the standard logarithmic measure in an appropriate limit and (ii) the basic properties that a functional of the probabilities should have in order to represent a physically sensible entropic measure [1]. The q-entropy is a quite natural and, to some extent, unique generalization of the Boltzmann-Gibbs-Shannon measure. Taking this into account, it is remarkable that the extremalization

of the q-measure leads to a family of distribution functions of considerable importance in theoretical astrophysics. In a sense, astrophysicists, when studying Newtonian self-gravitating systems, have been dealing with q-MaxEnt distribution functions for over a hundred years without being aware of it. The link between the Tsallis non extensive q-entropy and stellar polytropic distributions consitutes a clue (among several others) indicating that the entropic measure S_q is not just an ad hoc mathematical construction.

As already mentioned, many interesting contributions have been made in recent years in connection with the application of Tsallis' thermostatistics to self gravitating systems in general, and to the stellar polytropes in particular [3-7]. Sau Fa and Lenzi have obtained the exact equation of state for a two-dimensional self gravitating N-particule system within Tsallis thermostatistics [3]. An interesting analysis of the Jean's gravitational instability of a self-gravitational system characterized by a q-gaussian velocity distribution was done by Lima, Silva, and Santos [4]. A detailed study of the gravothermal catastrophe of self-gravitating systems in conection with Tsallis' q-entropy was performed by Taruya and Sakagami (see [5] and references therein). It has been recently pointed out by Chavanis and Sire [6], that the criterion for nonlinear dynamical stability for spherical stellar systems governed by the Vlasov-Poisson equations resembles a criterion of thermodynamical stability. On the basis of this, it is possible to develop a thermodynamical analogy to study the nonlinear dynamical stability of spherical galaxies. Within this approach, the concepts of entropy and temperature would be essentially effective. In [6], the Tsallis functional is interpreted as a useful H-function connecting continuously stellar polytropes and isothermal stellar systems.

On the basis of long term, N-body simulations of self gravitating systems, Taruya and Sakagami have obtained important numerical evidence for a connection between the physics of self-gravitating systems and the Tsallis formalism [7]. Taruya and Sakagami have shown that the evolution of a stellar system confined within an adiabatic wall (starting with initial conditions away from the Boltzmann-Gibbs distribution, and before the system enters the gravothermally unstable regime and undergoes core collapse) can be fitted remarkably well by a sequence of polytropic distributions (that is, Tsallis' q-maxent distributions) with an evolving polytropic index (i.e., evolving q-parameter). Taruya and Sakagami found that the alluded sequence of polytropic distributions provides a good description both of the density profile, and of the single-particle energy distribution of the transient states of the system. Even more interesting, they also found numerical evidence that the same kind of behaviour occurs if the outer boundary is removed. This suggest that the polytropic distributions may play an important role as quasi-attractors, or quasi-equilibrium states of an evolving self-gravitating system [7].

Summing up, we have seen that the connection between Tsallis entropy and self-gravitating systems has been an active research field in recent years, generating a considerable amount of new results. For sure, there are still several open questions to be addressed. For instance, is there any role to be played here by the super-statistics formalism (see the article by Beck, Cohen, and Rizzo in this Issue)? Another interesting question, in our opinion, concerns the possible relationship between the physics of systems with long range interaction, and the recently advanced proposal by Tsallis, Gell-Mann and Sato [9], that special occupancies of phase space may make the S_q entropy additive.

References

[1] C. Tsallis, *J. Stat. Phys.* **52**, 479 (1988).

[2] A.R. Plastino and A. Plastino, *Physics Letters A* **174**, 384 (1993).

[3] K. Sau Fa and E.K. Lenzi, *J. of Math. Phys.* **42**, 1148 (2001).

[4] J.A.S. Lima, R. Silva, and J. Santos, *Astron. and Astrophys.*, **396** 309 (2002).

[5] A. Taruya and M. Sakagami, *Cont. Mech. and Therm.* **16** 279 (2004).

[6] P.H. Chavanis and C. Sire, *Physica A* **356** (2005) 419.

[7] A. Taruya and M. Sakagami, *Phys. Rev. Lett.* **90**, 181101 (2003).

[8] J. Binney and S. Tremaine, *Galactic dynamics* (Princeton University Press, Princeton, 1987).

[9] C. Tsallis, M. Gell-Mann, and Y. Sato, *Proc. Natl. Acad. Sc.* USA **102**, 15377 (2005).

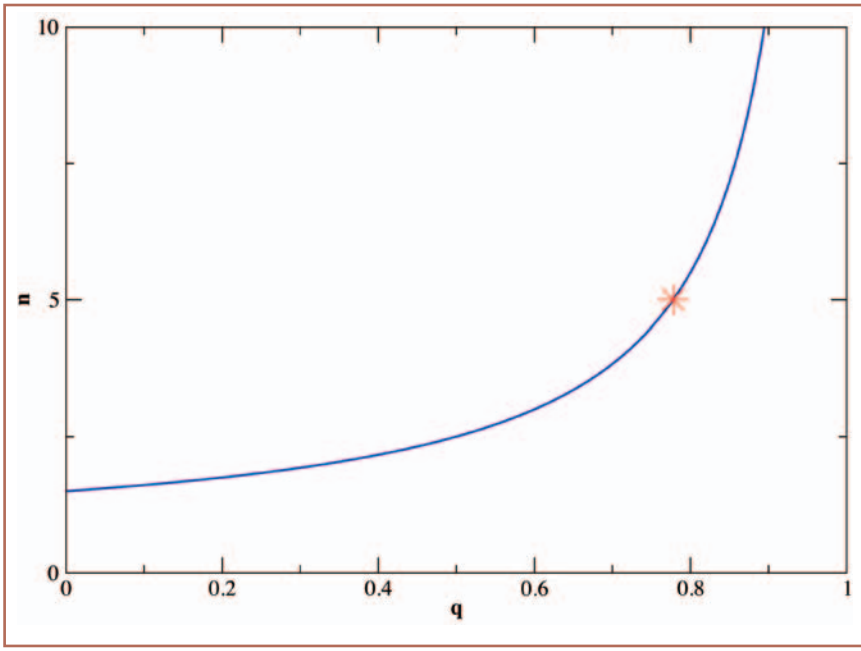

◄ **Fig. 1:** Stellar polytropes are simple models for stellar systems exhibiting a particle density in position-velocity space that is a power-like function of the energy. The conco-mitant exponent is n-3/2, where n is called the polytropic index. This polytropic distribution can be obtained by optimizing the system's q-entropy under the constraints imposed by the system's total mass and energy. The polytropic index n is here plotted as a function of the Tsallis' entropic paramenter q. The red star corresponds to the so called Schuster sphere, with $n = 5$ and $q = 7/9$. For $n < 5$ ($q < 7/9$) the polytropic distributions have finite mass and energy. All the depicted quantities are dimensionless.

Nuclear astrophysical plasmas: ion distribution functions and fusion rates

Marcello Lissia [1,2] *and Piero Quarati* [1,3]
[1] *Istituto Nazionale di Fisica Nucleare (I.N.F.N.) Cagliari*
[2] *Università di Cagliari, Dipartimento di Fisica, S.P. Sestu Km 1, I-09042 Monserrato (CA), Italy*
[3] *Politecnico di Torino, Dipartimento di Fisica, C.so Duca degli Abruzzi 24, I-10129 Torino, Italy*

This article illustrates how very small deviations from the Maxwellian exponential tail, while leaving unchanged bulk quantities, can yield dramatic effects on fusion reaction rates and discusses several mechanisms that can cause such deviations.

Fusion reactions are the fundamental energy source of stars and play important roles in most astrophysical contexts. Since the beginning of quantum mechanics, basic questions were addressed such as how nuclear reactions occur in stellar plasmas at temperatures of few keV (1 keV ≈ 11.6 x 10^6 K) against Coulomb barriers of several MeV and what reactions or reaction networks dominate the energy production. It was soon realized that detailed answers to such questions involved not only good measurements or quantum mechanical understanding of the relevant fusion cross sections, but also the use of statistical physics to describe the energy and momentum distributions of the ions and their screening [1].

Gamow understood that reacting nuclei penetrate Coulomb barriers by means of the quantum tunnel effect and Bethe successfully proposed the CNO and then the pp cycle as candidates for the stellar energy production: this description has been directly confirmed by several terrestrial experiments that have detected neutrinos produced by pp and CNO reactions in the solar core [2].

In the past only a few authors (e.g., d'E. Atkinson, Kacharov, Clayton, Haubold) have examined critically the energy distribution and proposed that such a distribution could deviate from the Maxwellian form. In fact, it is commonly accepted that main-sequence stars like the Sun have a core, i.e. an electron nuclear plasma, where the ion velocity distribution is Maxwellian. In the following, we first discuss why even tiny deviations from the Maxwellian distribution can have important consequences and then what can be the origin of such deviations.

Thermonuclear reaction in plasmas and distribution tails

In a gas with n_1 (n_2) particles of type 1 (2) per cubic centimeter and relative velocity v, the reaction rate r (the number of reactions per unit volume and unit time) is given by

$$r = (1 + \delta_{12})^{-1}\, n_1 n_2 \langle \sigma v \rangle \,, \qquad (1)$$

where $\sigma = \sigma(v)$ is the nuclear cross section of the reaction. The reaction rate per particle pair is defined as the thermal average

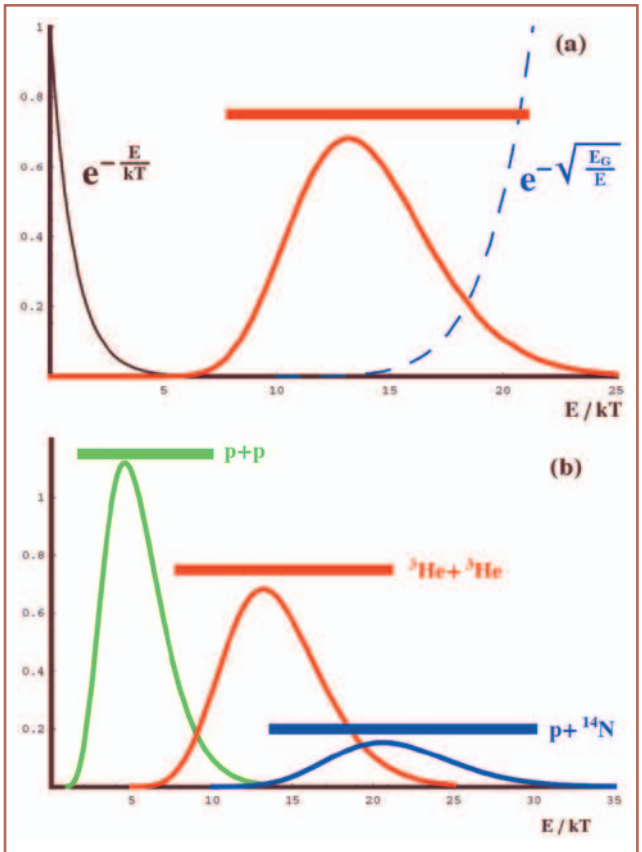

▲ **Fig. 1:** The Gamow peak and energy selection. In the upper panel (a) the exponential thin black curve is the Maxwellian distribution. The rapidly increasing dash blue curve shows the behavior of the penetration factor N x exp (-$\sqrt{E_G = E}$) for the solar reaction ^{3}He + ^{3}He → ^{4}He + 2p (E_G = 11.83 MeV and $N = 10^9$). The red thick curve shows the product of the two curves (Gamow peak) times 10^8. The horizontal red band indicates the energy range of the reacting particles. The lower panel (b) shows how different reactions select different windows of particle energies. The Gamow peak (energy window) moves to higher energies going from $p + p \rightarrow d + \nu + e^+$ (E_G = 493 keV, green), to ^{3}He + ^{3}He → ^{4}He + 2p (E_G = 11.83 MeV, red), and $p + {}^{14}\mathrm{N} \rightarrow {}^{15}\mathrm{O} + \gamma$ (E_G = 45.09 MeV, blue). Correspondingly, the peaks become (much) lower; note that the three curves have been multiplied times 10^5, 10^{17}, and 10^{26}, respectively, to make them visible on the same scale.

$$\langle \sigma v \rangle = \int_0^\infty f(v)\, \sigma v \, dv \,, \qquad (2)$$

where the particle distribution function $f(v)$ is a local function of the temperature [3].

Therefore, the reaction rate per particle pair $\langle \sigma v \rangle$ is determined by the specific cross section and by the velocity distribution function of the reacting particles. When no energy barrier is present and far from resonances, cross sections do not depend strongly on the energy. Most of the contribution to $\langle \sigma v \rangle$ comes from particles with energy of the order of kT, and the dependence on the specific form of $f(v)$ is weak. The same is true for bulk properties that receive comparable contributions from all particles: e.g., the equation of state.

The situation is very different in the presence of a Coulomb barrier, when the reacting particles are charged, as in the fusion

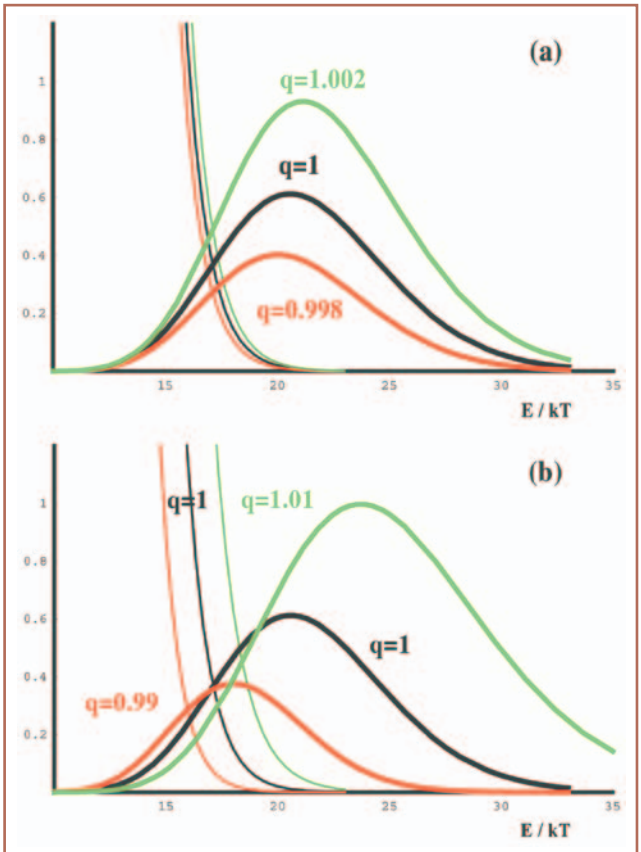

▲ **Fig. 2:** Effects of tiny changes in the tail of the distribution for the reaction $p + {}^{14}N$. Using the parametrization of Eq. (5), the upper panel (a) shows the effect of taking $q = 1.002$ (green) and $q = 0.998$ (red), while the lower panel (b) shows the effect of $q = 1.01$ (green) and $q = 0.99$ (red); black curves correspond to the usual Maxwell distribution ($q = 1$). In the lower panel (b) the green (red) Gamow peak (thick lines) is divided (multiplied) by an additional factor of five. Note that thin curves (exponentials and q-exponentials) have been multiplied by 10^9 to enounce their tiny differences.

reactions that power stars [7]. The penetration of large Coulomb barriers ($Z\alpha/r$ is of the order of thousands in units of kT when r is a typical nuclear radius) is a classically forbidden quantum effect. The penetration probability is proportional to the Gamow factor $\exp[-\sqrt{E_G/E}]$, where the Gamow energy $E_G = 2\mu c^2 (Z_1 Z_2 \alpha\pi)^2$, α is the fine structure constant, μ is the reduced mass, and $Z_{1,2}$ are the charges of the ions. The cross section is exponentially small for $E \ll E_G$ and grows extremely fast with the energy; therefore, one usually defines the astrophysical S factor, whose energy dependence is weaker

$$\sigma(E) = \frac{S(E)}{E} e^{-\sqrt{E_G/E}} \qquad (3)$$

The two factors in the integrand in Eq. (2) that carry most of the energy dependence are the Maxwellian distribution $\propto e^{-(E/kT)}$, which is exponentially suppressed for $E \gg kT$, and the penetration factor $e^{-\sqrt{E_G/E}}$, which is exponentially suppressed for $E \ll E_G$. Contributions to the rate come only from an intermediate region (Gamow peak) around the temperature-dependent energy

$$E_0 = \left(\frac{E_G (kT)^2}{4}\right)^{1/3} \qquad (4)$$

which is called the most effective energy, since most of the reacting particles have energies close to E_0.

Figure 1 gives a pictorial demonstration of how the Gamow peak originates and how different reactions select different parts of the distribution tail and can be used to probe it.

In the upper panel (a) the exponentially decreasing function (thin black curve) is the Maxwellian factor; the rapidly growing function (dash blue curve) is the penetration factor (for graphical reason multiplied by 10^9) of one of the most important reactions in the Sun, ${}^3He + {}^3He \rightarrow {}^4He + 2p$ ($E_G = 11.83$ MeV), which corresponds to a most effective energy $E_0 = (E_G (kT)^2/4)^{1/3} = 17.036\ kT$ for $kT = 1.293$ keV $= 11.6 \times 10^6$ K; the product of the two functions (Gamow peak) is the thick red curve. Note that the Gamow peak, and therefore the rate, is very small (it has been multiplied by an additional 10^8 factor to make it visible on the same scale of the other curves), since at the most effective energy E_0 both the cross section and the number of particles are exponentially small. At this point it is important to remark that the area under the Maxwellian curve for energies within the Gamow peak (the energy window indicated by the red band) is of the order of 0.1% of the total area: only a few particles in the tail of the distributions contribute to the fusion rate.

The fact that the penetration factor effectively selects particles in the tail of the distribution is the more dramatic the larger the charge of the reacting ions: for the $p + {}^{14}N \rightarrow {}^{15}O + \gamma$ (the leading reaction of the CNO cycle, which dominates the energy production in main-sequence stars larger or older than the Sun) the contributing particles are few in a million.

The effect on the Gamow peak when increasing the charges of the reacting nuclei is shown in the lower panel (b) of Figure 1. The green, red, and blue curves show the Gamow peak multiplied by 10^5, 10^{17}, and 10^{26}, respectively, for three fundamental reactions in main-sequence stars: $p + p \rightarrow d + \nu + e^+$ ($E_G = 493$ keV), ${}^3He + {}^3He \rightarrow {}^4He + 2p$ ($E_G = 11.83$ MeV), and $p + {}^{14}N \rightarrow {}^{15}O + \gamma$ ($E_G = 45.09$ MeV)). It is immediately evident that the larger the charges of the ions the higher is the energy of the particles that contribute to the rate, the (much) lower is the peak and, therefore, the (much) smaller is the rate. In fact the maximum of the Gamow peak $E_0 \propto E_G^{1/3} \propto (Z_1 Z_2)^{2/3}$ and its height is proportional to $\exp(-3E_0/kT)$.

A convenient parametrization of deviations from the Maxwell distribution is the deformed q-exponential:

$$\exp_q\left(-\frac{E}{kT}\right) = \left(1-(1-q)\frac{E}{kT}\right)^{1/(1-q)} \qquad (5)$$

which naturally appears in Tsallis' formulation of statistical mechanics [4]. This particular deformation of the exponential has the advantage of describing both longer tails (for $q > 1$) and cut-off tails (for $q < 1$), while reproducing the exponential in the limit $q \rightarrow 1$.

Figure 2 shows the effect of substituting into the Maxwellian distribution $\exp(-E/kT)$ the distribution $N_q \exp_q(-E/kT)$, where N_q is the normalization factor that conserves the total number of particles. We show the effect for the $p + {}^{14}N$ reaction and the values (a) $q = 1 \pm 0.002$ and (b) $q = 1 \pm 0.01$. This reaction determines the rate of energy production from the CNO cycle, dominant at older stages and, therefore, also determines the time of the exit from the main sequence. Black curves refer to the exponential ($q = 1$), red curves refer to the cut-off ($q < 1$) exponential, and green curves refer to the longer-tail ($q > 1$) exponential.

Note that all exponentials have been multiplied times a huge 10^6 factor to emphasise their tiny differences: these values of q produce functions that are almost indistinguishable from the exponential unless one looks very far in the tail.

One can make several remarks:

- Gamow peaks are shifted towards higher energies, when the distribution has a tail longer than the exponential (green curves, $q > 1$); they are shifted towards lower energies for cut-off exponentials (red curves, $q < 1$);
- the effect is larger the larger the deviation from the exponential (the larger $|q - 1|$);
- the peaks (and the rates) become correspondingly higher for $q > 1$ and smaller for $q < 1$;
- the effect on the rate is already large for $|1 - q| = 0.002$, it becomes huge (more than a factor of 10) for $|1 - q| = 0.01$; note that the green (red) peak in lower panel (b) of figure 2 ($|1 - q| = 0.01$) has been divided (multiplied) by five to make them fit on the same scale!

These deviations should be carefully estimated, since reliable calculations of nuclear reaction rates in stellar interiors is fundamental for a quantitative understanding of the structure and evolution of stars. In fact, while the overall stellar structure is rather robust, changes of some of the rates even by few percent can produce detectable discrepancies, when precise measurements are possible, e.g., in the case of the solar photon and neutrino luminosity, and mechanical eigenfrequencies [2]. In quasi-stellar objects like Jupiter, deviations could be even larger and explain their excess energy [5].

As already shown in the recent past, very small deviations from Maxwellian momentum distribution do not modify the properties of stellar core and are in agreement with the helioseismology constraints [6], but may affect the evaluation of the nuclear fusion rates that may be enhanced or depleted, depending on the superdiffusion or subdiffusion properties of the particles [7].

Deviations from Maxwellian distribution

Normal stellar matter, such as that in the Sun, is non-degenerate, i.e., quantum effects are small (in fact, they are small for electrons and completely negligible for ions), is non-relativistic, and is in good thermodynamical equilibrium. On this ground, the particle velocity distribution is almost universally taken to be a Maxwell-Boltzmann (MB) distribution.

Concerning the thermodynamical equilibrium, main sequence stars are more precisely in a stationary state where the luminosity equals the heat production rate. This metastable state has a long life-time, of the order of the star lifetime, and it ends when the nuclear fuel is burned out. In addition, the quasiequilibrium is only local, since the temperature decreases from core to surface. However, nuclear reactions are often, but not always, sufficiently slow on the scale of thermal and mechanical exchanges and take place on such a small scale that spatial and temporal deviations from equilibrium can be neglected to a very good first approximation.

At least in one limit the MB distribution can be rigorously derived: systems that are dilute in the appropriate variables and whose residual interaction is small compared to the one-body energies. In spite of the fact that the effects of the residual interaction cannot be neglected (the electron screening factor is a well-known example of correction due to the astrophysical plasma environment) at zero order the many-body correlations can be neglected and the stellar interior can be studied in this dilute limit. In this limit the velocity distribution is the Maxwellian one.

However, one should keep in mind that derivations of the ubiquitous Maxwell-Boltzmann distribution are based on several assumptions [7]. In a kinetic approach, one assumes (1) that the collision time is much smaller than the mean time between collisions, (2) that the interaction is sufficiently local, (3) that the velocities of two particles at the same point are not correlated (Boltzmann's Stosszahlansatz), and (4) that energy is locally conserved when using only the degrees of freedom of the colliding particles (no significant amount of energy is transferred to collective variables and fields). In the equilibrium statistical mechanics approach, one uses the assumption that the velocity probabilities of different particles are independent, corresponding to (3), and that the total energy of the system could be expressed as the sum of a term quadratic in the momentum of the particle and independent of the other variables, and a term independent of momentum, but if (1) and (2) are not valid the resulting effective two-body interaction is non-local and depends on the momentum and energy of the particles. Finally, even when the one-particle energy distribution is Maxwellian, additional assumptions about correlations between particles are necessary to deduce that the relative-velocity distribution, which is the relevant quantity for rate calculations, is also Maxwellian.

In the following we give arguments and mechanisms that lead to distribution functions that are different from the MB one in a stationary state.

Correlations between particles, so that the probability distribution of the system is not described by the product of independent probabilities of the components, are in general responsible for such more general distributions. The specific microscopic mechanisms that generate these correlations depend on the particular system and there exist many approaches to derive the relevant distributions.

In an approach that uses the Fokker-Planck equation, which takes into account the average effects of the environment through the drift $J(p)$ and diffusion $D(p)$ coefficients, stationary solutions different from the Maxwell distribution (e.g. Druyvenstein or Tsallis like distributions) can be obtained, when $J(p)$ and $D(p)$ include powers of p higher than the lowest order [8]. The presence of higher powers of p, i.e., higher derivative terms, can be interpreted as a signal of non-locality in the Fokker-Planck equation. We stress that these distributions are stationary (stable or metastable) and what counts to decide the distribution is the type of collisions between ions and the dependence on momentum of the elastic collision cross sections (Coulomb, screened Coulomb, enforced Coulomb, among others), or the presence of ion-ion correlations [9].

The presence of random fields (e.g., distributions of random electric micro-fields or, in general, of random forces) introduces in the kinetic equations factors whose effect is to enhance or to deplete the high-momentum tail of the distribution function [7].

Because of the many-body nature of the effective forces, which makes the collisions not independent, the distributions of the relevant degrees of freedom observed, e.g., the ones selected by a fusion reaction, can be different from the distributions of the quasi-particles that describe the plasma. In addition the plasma makes effective interactions time dependent (memory effects) and non-local. These effects depend strongly on the energy of the selected particles and on the collisional frequency.

One important and clear example of this last point is given by the fact that many processes, such as nuclear fusion itself, depend on momentum rather than on energy. This distinction is important because, due to plasma many-body effects, an uncertainty relation holds between momentum and energy [10]. Even when the energy distribution maintains its Maxwellian expression, the

momentum distribution can be different in the high energy tail. In fact, this quantum uncertainty effect (not Heisenberg uncertainty) between energy $\mathcal{E}$ and momentum p, caused by the many-body collisions and described by the Kadanoff-Baym equation, implies an energy-momentum distribution of the form

$$f_Q(\mathcal{E},p) = \frac{1}{\pi} n(\mathcal{E}) \delta_\gamma(\mathcal{E},p) \quad (6)$$

with

$$\delta_\gamma(\mathcal{E},p) = \frac{Im\Sigma^R(\mathcal{E},p)}{(\mathcal{E}-\mathcal{E}_p - Re\Sigma^R(\mathcal{E},p))^2 + (Im\Sigma^R(\mathcal{E},p))^2} \quad (7)$$

where $\Sigma^R(\mathcal{E},p)$ is the mass operator of the one-particle Green function. After integrating in $d\mathcal{E}$ the product of $f_Q(\mathcal{E}, p)$ and the Maxwellian energy distribution, we obtain a momentum distribution with an enhanced high-momentum tail. Although this approach produces a deviation from the MB distribution, the state represented by $f_Q(p)$ is an equilibrium state [11, 12]. The Maxwellian distribution is recovered in the limit when $\delta_\gamma(\mathcal{E}, p)$ becomes a δ function with a sharp correspondence between momentum and energy.

Distributions different from the Maxwellian one can also be obtained axiomatically from non-standard, but mathematically consistent, versions of statistical mechanics that use entropies different from the Boltzmann-Gibbs one [4, 13].

We have argued that it is not sufficient to know that the Maxwellian distribution is a very good approximation to the particle distribution. We must be sure that there are no corrections to a very high accuracy, when studying reactions that are highly sensitive to the tail of the distribution, such as fusion reactions between charged ions. Several mechanisms have been outlined (others need to be studied) that can produce small, but important deviations in the tail of the distribution.

References

[1] R. d.Escourt Atkinson and F. G. Houtermans, *Z. Physik* **54** (1929) 656.

[2] V. Castellani et al, *Phys. Rept.* **281** (1997) 309 [arXiv:astro-ph/9606180].

[3] D. Clayton, *Principles of Stellar Evolution and Nucleosynthesis* (New York: McGraw-Hill Book Company, 1968).

[4] C. Tsallis, *J. Statist. Phys.* **52** (1988) 479.

[5] M. Coraddu et al, *Physica A* **305** (2002) 282 [arXiv:physics/0112018].

[6] S. Degl'Innocenti et al, *Phys. Lett. B* **441** (1998) 291 [arXiv:astro-ph/9807078].

[7] M. Coraddu et al, *Braz. J. Phys.* **29** (1999) 153 [arXiv:nucl-th/9811081].

[8] G. Kaniadakis and P. Quarati, *Physica A* **192** (1993) 677; ibid. 237 (1997) 229.

[9] F. Ferro and P. Quarati, *Phys. Rev. E* **71** (2005) 026408 [arXiv:cond-mat/0407665].

[10] V. M. Galitskii and V. V. Yakimets, *JEPT* **24** (1967) 637.

[11] A. N. Starostin, V. I. Savchenko, and N. J. Fisch, *Phys. Lett. A* **274** (2000) 64.

[12] M. Coraddu et al, *Physica A* **340** (2004) 490 [arXiv:nucl-th/0401043].

[13] G. Kaniadakis et al, *Phys. Rev. E* **71** (2005) 046128 [arXiv:cond-mat/0409683]

Critical attractors and *q*-statistics

A. Robledo
Instituto de Física, Universidad Nacional Autónoma de México, Apartado Postal 20-364, México 01000 D.F. México

The singular dynamics at critical attractors of even the simplest one dimensional nonlinear iterated maps is of current interest to statistical physicists because it provides insights into the limits of validity of the Boltzmann-Gibbs (BG) statistical mechanics. This dynamics also helps inspect the form of the possible generalizations of the canonical formalism when its crucial supports, phase space mixing and ergodicity, break down.

The fame of the critical attractors present at the onset of chaos in the logistic and circle maps stems from their universal properties, comparable to those of critical phenomena in systems with many degrees of freedom. At these attractors the indicators of chaos withdraw, such as the fast rate of separation of initially close by trajectories. As it is generally understood, the standard exponential divergence of trajectories in chaotic attractors suggests a mechanism to justify the property of irreversibility in the BG statistical mechanics [1]. In contrast, the onset of chaos imprints memory preserving properties to its trajectories.

The dynamical nature of trajectories is appraised on a regular basis through the sensitivity to initial conditions ξ_t, defined as

$$\xi_t(x_0) \equiv \lim_{\Delta x_0 \to 0} (\Delta x_t / \Delta x_0),\ t \text{ large}, \quad (1)$$

where Δx_0 is the initial separation of two trajectories and Δx_t that at time t. For a one-dimensional map it has the form $\xi_t(x_0) = \exp(\lambda_1 t)$, with $\lambda_1 > 0$ for chaotic attractors and $\lambda_1 < 0$ for periodic ones. The number λ_1 is called the Lyapunov coefficient. At critical attractors $\lambda_1 = 0$ and ξ_t does not settle onto a single-valued function but exhibits instead fluctuations that grow indefinitely. For initial positions on the attractor ξ_t develops a universal self-similar temporal structure and its envelope grows with t as a power law.

It has been recently corroborated [2]-[5] that the dynamics at the critical attractors associated with the three familiar routes to chaos, intermittency, period doubling and quasiperiodicity [6], obey the features of the q-statistics, the generalization of BG statistics based on the q-entropy S_q [7]. The focal point of the q-statistical description for the dynamics at such attractors is a ξ_t associated with one or several expressions of the form

$$\xi_t(x_0) = \exp_q[\lambda_q(x_0)\, t], \quad (2)$$

where q is the entropic index and λ_q is the q-generalized Lyapunov coefficient. Also the identity $K_1 = \lambda_1$ (where the rate of entropy production K_1 is given by $K_1 t = S_{BG}(t) - S_{BG}(0)$ with S_{BG} the Boltzmann-Gibbs entropy) generalizes to

$$K_q = \lambda_q, \quad (3)$$

where the rate of q-entropy production K_q is defined via $K_q t = S_q(t) - S_q(0)$ [3], [4], [7].

Tsallis *q* index & Mori's *q*-phase transitions

The central issue of research in q-statistics is perhaps to confirm the occurrence of special values for the entropic index q for any given system and to establish their origin. In the case of critical

attractors the allowed values for q are obtained from the universality class parameters to which the attractor belongs. For the simpler cases, the pitchfork and the tangent bifurcations, there is a single well-defined value for the index q [2]. The pitchfork bifurcations form the sequence of period doublings that culminate in the chaos threshold whereas at the tangent bifurcation chaos develops via intermittency. For critical multifractal attractors, as in the period doubling accumulation point and in the quasiperiodic onset of chaos, the situation is more complicated and there appear to be a multiplicity of indexes q but with precise values given by the attractor scaling functions. They come out in pairs and are related to the occurrence of dynamical 'q-phase' transitions [4], and these are identified as the source of the special values for the entropic index q. The q-phase transitions connect qualitatively different regions of the multifractal attractor.

The main quantities in the thermodynamic formalism of q-phase transitions (developed by Mori and colleagues in the late 80's [8]) are the spectral functions $\phi(q)$ and $\psi(\lambda)$, related to each other via Legendre transformation, the function of generalized Lyapunov coefficients $\lambda(q)$, given by $\lambda(q) \equiv d\phi(q)/dq$, and the variance $v(q) \equiv d\lambda(q)/dq$. The functions $\phi(q)$ and $\psi(\lambda)$ are the dynamic counterparts of the multifractal dimensions $D(q)$ and the spectrum $f(\alpha)$ that characterize the geometric structure of the attractor [6]. As with ordinary thermal 1st order phase transitions, a q-phase transition is indicated by a section of linear slope $m_c = 1 - q$ in the 'free energy' $\psi(\lambda)$, a discontinuity at $q = q$ in the 'order parameter' $\lambda(q)$, and a divergence at q in the 'susceptibility' $v(q)$. Actually an infinite family of such transitions takes place but of rapidly decreasing strengths [4], [5].

Tangent & pitchfork bifurcations

The tangent bifurcations of unimodal (one hump) maps of general nonlinearity $z > 1$ display weak insensitivity to initial conditions, i.e. power-law convergence of orbits when at the left-hand side ($x < x_c$) of the point of tangency x_c. However at the right-hand side ($x > x_c$) of the bifurcation there is a 'super-strong' sensitivity to initial conditions, i.e. a sensitivity that grows faster than exponential [2]. The two different behaviors can be couched as a q-phase transition with indexes q and $2 - q$ for the two sides of the tangency point. The pitchfork bifurcations display weak insensitivity to initial conditions.

For the tangent bifurcations one has always $q = 3/2$, while for the pitchfork bifurcation one has $q = 5/3$. Notably, these results for the index q are valid for all $z > 1$ and therefore define the existence of only two universality classes for unimodal maps [2]. The treatment of the tangent bifurcation differs from other studies of intermittency transitions in that there is no feedback mechanism of iterates from an adjacent chaotic region. Therefore, impeded or incomplete mixing in phase space (a small interval neighbourhood around $x = x_c$) arises from the special 'tangency' shape of the map at the transitions that produces monotonic trajectories. This has the effect of confining or expelling trajectories causing anomalous phase-space sampling, in contrast to the thorough coverage in generic states with $\lambda_1 > 0$.

Period-doubling accumulation point

For a unimodal map of nonlinearity $z > 1$ (e.g. the logistic map has $z = 2$) with extremum at $x = 0$ and control parameter μ the onset of chaos is obtained at the accumulation point μ_∞ of the μ values for the pitchfork bifurcations μ_n, $n = 1, 2, \ldots$, [6]. This is often called the Feigenbaum attractor which reappears in multiples together with the precursor cascade of period-doubling bifurcations in the infinite number of windows of periodic trajectories that interpose the chaotic attractors beyond μ_∞. The number of cascades within each window is equal to the period of the orbit that emerges at the tangent bifurcation at its opening. See Fig. 1. The dynamics at the Feigenbaum attractor has been analyzed recently [3], [4]. By taking as initial condition $x_0 = 0$ at μ_∞ it is found that the resulting orbit of period 2^∞ consists of trajectories made of intertwined power laws that asymptotically reproduce the entire period-doubling cascade that occurs for $\mu < \mu_\infty$ (see Fig. 2b) It was established that ξ_t has precisely the form of a set of interlaced q-exponentials, of which the q-indexes and the sets of associated q-Lyapunov coefficients λ_q were determined. As mentioned, the appearance of a specific value for the q index (and actually also that for its conjugate value $Q = 2 - q$) turns out to be

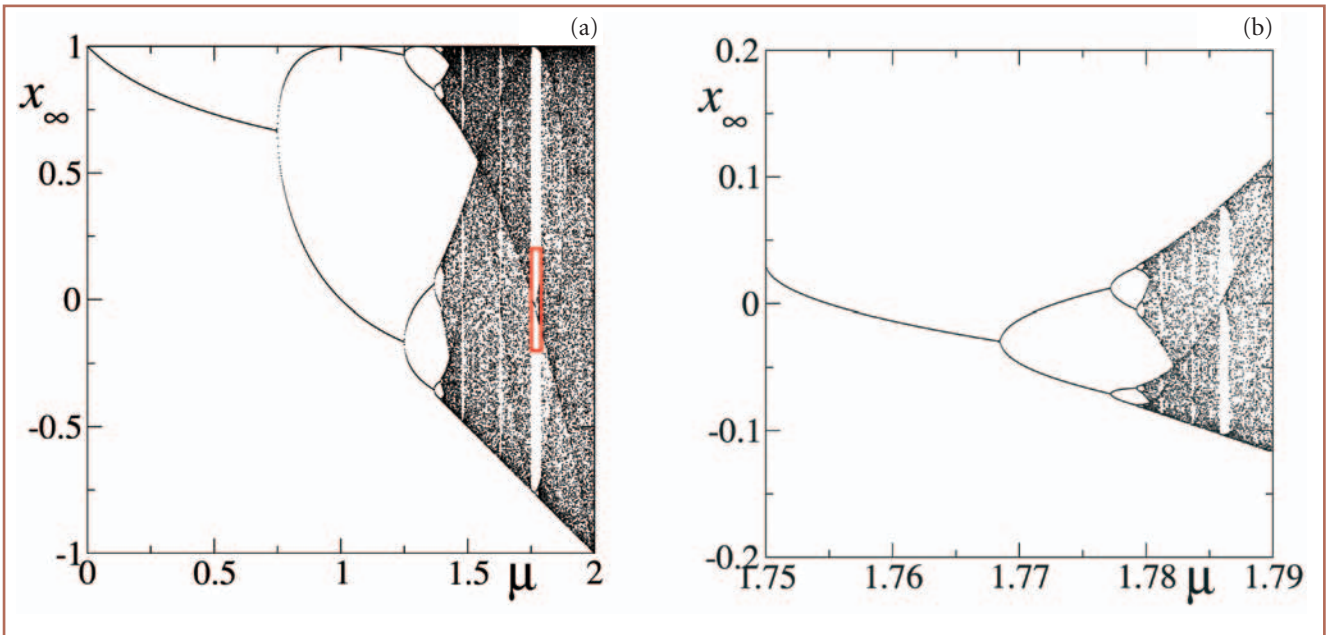

▲ **Fig. 1:** (a) The classic logistic map attractor as a function of control parameter μ. (b) Enlargement of the box in (a).

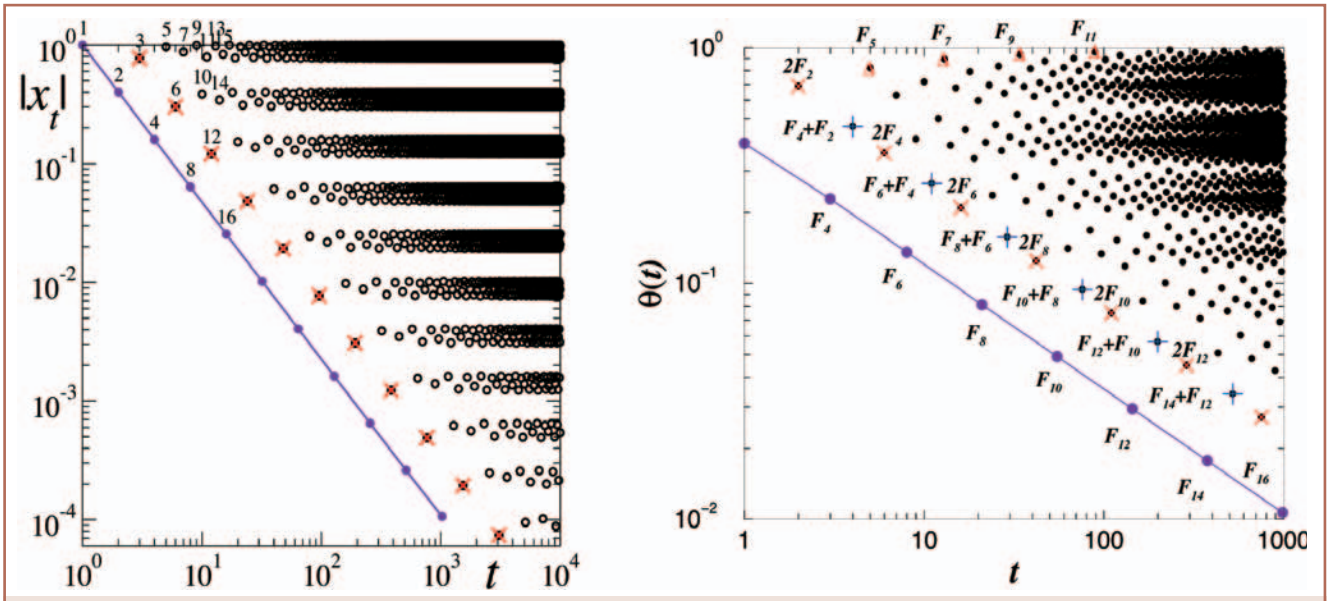

▲ **Fig. 2:** (a) Absolute values of positions in logarithmic scales of the first 10000 iterations for the trajectory of the logistic map at the onset of chaos μ_∞ with initial condition $x_0 = 0$. The numbers correspond to iteration times. The power-law decay of time subsequences mentioned in the text can be clearly appreciated. (b) Positions $\theta(t)$ vs t in logarithmic scales for the orbit with initial condition $\theta(0) = 0$ of the critical circle map for the golden-mean winding number. The labels indicate iteration time t where F_n is the Fibonacci number of order n.

due to the occurrence of q-phase transitions between 'local attractor structures' at μ_∞. The values of the q-indexes are obtained from the discontinuities of the universal trajectory scaling function σ. This function characterizes the multifractal by measuring how adjacent positions of orbits of period 2^n approach each other as $n \to \infty$ [9]. The main discontinuity in σ is related to the most crowded and most sparse regions of the attractor and in this case $q = 1 - \ln 2/(z - 1) \ln \alpha_F$, where α_F is the universal scaling constant associated with these two regions. Furthermore, it has also been shown [3], [4] that the dynamical and entropic properties at μ_∞ are naturally linked through the q-exponential and q-logarithmic expressions, respectively, for the sensitivity ξ_t and for the entropy S_q in the rate of entropy production K_q.

Quasiperiodicity & golden mean route to chaos

A recent study [5] of the dynamics at the quasiperiodic onset of chaos in maps with zero slope inflection points of cubic nonlinearity (e.g. the critical circle map) shows strong parallelisms with the dynamics at the Feigenbaum attractor described above. Progress on detailed knowledge about the structure of the orbits within the golden-mean quasiperiodic attractor, see Fig. 2b, helped determine the sensitivity to initial conditions for sets of starting positions within this attractor [5]. It was found that ξ_t is made up of a hierarchy of families of infinitely many interconnected q-exponentials. Here again, each pair of regions in the multifractal attractor, that contain the starting and finishing positions of a set of trajectories, leads to a family of q-exponentials with a fixed value of the index q and an associated spectrum of q-Lyapunov coefficients λ_q.

As in the period doubling route to chaos, the quasiperiodic dynamics consists of an infinite family of q-phase transitions, each associated to trajectories that have common starting and finishing positions located at specific regions of the multifractal. The specific values of the variable q (in the thermodynamic formalism) at which the q-phase transitions take place are the same values for the entropic index q in ξ_t. The transitions come in pairs at q and $2 - q$ as they are tied down to the expressions for λ_q in ξ_t. Again, the dominant dynamical transition is associated to the most crowded and sparse regions of the multifractal, and the value of its q-index is [5] $q = 1 - \ln w_{gm}/2 \ln \alpha_{gm}$ where $w_{gm} = (\sqrt{5} - 1)/2$ is the golden mean and α_{gm} is the universal constant that plays the same scaling role as α_F.

Structure in dynamics

The dynamical organization within critical multifractal attractors is difficult to resolve from the consideration of a straightforward time evolution, i.e. the record of positions at every time t for a trajectory started at an arbitrary position x_0 within the attractor. In this case what is observed are strongly fluctuating quantities that persist in time with a scrambled pattern structure that exhibits memory retention. Unsystematic averages over x_0 would rub out the details of the multiscale dynamical properties we uncovered. On the other hand, if specific initial positions with known location within the multifractal are chosen, and subsequent positions are observed only at pre-selected times, when the trajectories visit another selected region, a distinct q-exponential expression for ξ_t is obtained.

Manifestations of *q*-statistics in condensed matter problems

There are connections between the properties of critical attractors referred to here and those of systems with many degrees of freedom at extremal or transitional states. Three specific examples have been recently developed (see Table). In one case the dynamics at the chaos threshold via intermittency has been shown to be related to that of intermittent clusters at thermal critical states [10]. In the second case the dynamics at the noise-perturbed period-doubling onset of chaos has been found to show parallelisms with the glassy dynamics observed in supercooled molecular liquids [11]. In the third case the known connection between the quasiperiodic route to chaos and the localization transition for transport in incommensurate systems is analyzed from the perspective of the q-statistics [12].

Critical clusters & intermittency

The dynamics of fluctuations of an equilibrium critical state in standard models of a magnetic or fluid system is seen to be related to the dynamics at a critical attractor for intermittency. The connection can be examined when instead of the entire critical system a single unstable cluster of excess magnetization or density of size R is considered. The analysis, initially developed by Contoyiannis and colleagues [13], has been reconsidered recently in connection with q-statistics [10].

An important element in the analysis is the determination of the order parameter $\phi(r)$ of a large cluster by withholding only its most probable configurations from a coarse-grained partition function Z. The conditions under which these configurations dominate are evaluated as these determine an instability of the cluster. The instability can be expressed as an inequality between two lengths in space. This is $r_0 \gg R$, where r_0 is the location of a divergence in the expression for $\phi(r)$. In a coarse-grained time scale the cluster is expected to evolve by increasing its average amplitude $\bar{\phi}$ and/or size R because the subsystem studied represents an environment with unevenness in the states of the microscopic degrees of freedom (e.g. more spins up than down). Increments in $\bar{\phi}$ for fixed R takes the position r_0 for the singularity closer to R, the dominance of this configuration in Z decreases accordingly and rapidly so. When the divergence is reached at $r_0 = R$ the profile $\phi(r)$ no longer describes the spatial region where the subsystem is located. But a subsequent fluctuation would again be represented by a cluster $\phi(r)$ of the same type. From this renewal process we obtain a picture of intermittency [10].

Amongst the static and dynamical properties for such single critical cluster of order parameter $\phi(r)$ we mention [10]: 1) The faster than exponential growth with cluster size R of the space-integrated ϕ suggests nonextensivity of the BG entropy but extensivity of a q-entropy expression. 2) The finding that the time evolution of ϕ is described by the dynamics of the critical attractor for intermittency which implies an atypical sensitivity to initial conditions compatible with q-statistics. 3) Both, the approach to criticality and the infinite-size cluster limit at criticality manifest through a crossover from canonical to q-statistics.

Glassy dynamics & noise-perturbed Feigenbaum attractor

The erratic motion of a Brownian particle is usually described by the Langevin theory. As it is well known, this method finds a way round the detailed consideration of many degrees of freedom by representing the effect of collisions with molecules in the fluid in which the particle moves by a noise source. The approach to thermal equilibrium is produced by random forces, and these are sufficient to determine dynamical correlations, diffusion, and a basic form for the fluctuation-dissipation theorem. In the same spirit, attractors of nonlinear low-dimensional maps under the effect of external noise can be used to model states in systems with many degrees of freedom. In a one-dimensional map with only one control parameter μ the consideration of external noise of amplitude σ could be thought to represent the effect of many other systems coupled to it, like in the so-called coupled map lattices [9]. The general map formula can be seen to represent a discrete form for a Langevin equation with nonlinear 'friction force' term [11].

The dynamics of noise-perturbed logistic maps at the chaos threshold has been shown to exhibit parallels with the most prominent features of glassy dynamics in, for example, supercooled liquids. In this analogy the noise amplitude σ plays a role similar to the temperature difference from a glass transition temperature. Specifically our results are [11]:

1) Two-step relaxation occurring in trajectories and in their two-time correlations when $\sigma \to 0$.

2) A map equivalent to a relationship between the relaxation time and the configurational entropy.

Route to chaos	Intermittency	Period doubling	Quasiperiodicity
Common properties	Vanishing ordinary Lyapunov coefficient, dynamical phase transitions (Mori's q-phases) power-law dynamics, q-sensitivity, q-Pesin identity		
Distinctive properties	(Also) faster than exponential dynamics	Foam-like phase space	Dense phase space
Applications in condensed matter physics	Critical clusters	Glass formation	Localization
Applications in other disciplines	Information & other flows in networks, ...	Protein folding, vegetation patterns, ...	Mode locking, cardiac cells, Internet TCP, ...

▲ **Table:** Summary. The three routes to chaos, properties and applications.

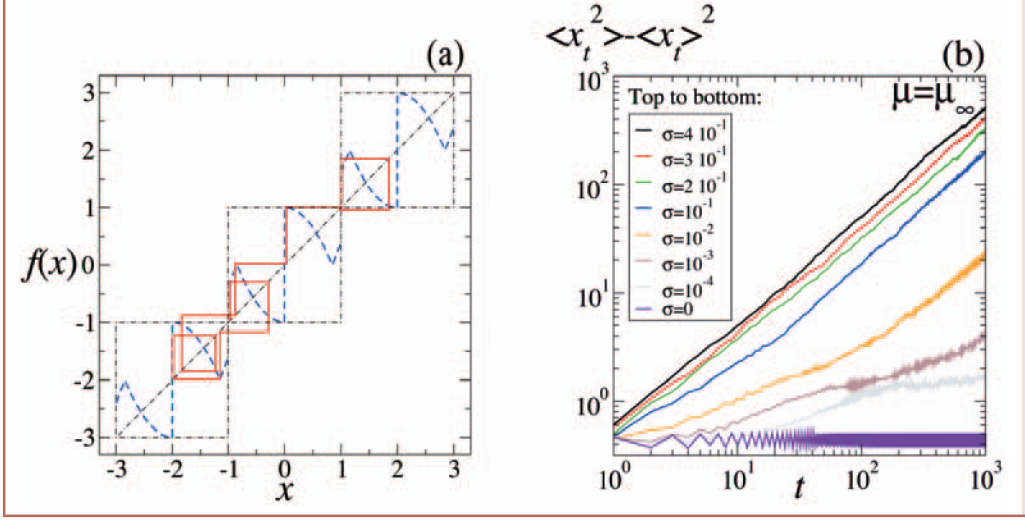

◀ **Fig. 3:** Glassy diffusion in the noise-perturbed logistic map. (a) Repeated-cell map (blue) and trajectory (red). (b) Time evolution of the mean square displacement $\langle x_t^2 \rangle - \langle x_t \rangle^2$ for an ensemble of 1000 trajectories with initial conditions randomly distributed inside [-1; 1]. Curves are labeled by the value of the noise amplitude.

features

3) Both, trajectories and their two-time correlations obey an 'aging' scaling property typical of glassy dynamics when $\sigma \to 0$. 4) A progression from normal diffusiveness to subdiffusive behavior and finally to a stop in the growth of the mean square displacement as demonstrated by the use of a repeated-cell map. (see Fig. 3) The existence of this analogy is perhaps not accidental since the limit of vanishing noise amplitude $\sigma \to 0$ involves loss of ergodicity.

Localization & quasiperiodic onset of chaos

One interesting problem in condensed matter physics that exhibits connections with the quasiperiodic route to chaos is the localization transition for transport in incommensurate systems, where the discrete Schrödinger equation with a quasiperiodic potential translates into a nonlinear map known as the Harper map [14]. In this equivalence the divergence of the localization length corresponds to the vanishing of the ordinary Lyapunov coefficient. It is interesting to note that the basic features of q-statistics in the dynamics at critical attractors mentioned here turn up in the context of localization phenomena.

Acknowledgements

Partially supported by CONACyT and DGAPA- UNAM, Mexican agencies.

References

[1] There are some parallels between the evolution towards an attractor in dissipative maps and the irreversible approach to equilibrium in thermal systems. It should be recalled that for the chaotic dynamics of a conservative system (such as the hard sphere gas) there is no dissipation nor strange attractor. It is of course this dynamics that is relevant to Boltzmann's assumption of molecular chaos.

[2] F. Baldovin and A. Robledo, *Europhys. Lett.* **60**, 518 (2002); A. Robledo, *Physica D* **193**, 153 (2004).

[3] F. Baldovin and A. Robledo, *Phys. Rev. E* **66**, 045104 (2002); E 69, 045202 (2004).

[4] E. Mayoral and A. Robledo, *Phys. Rev. E* **72**, 026209 (2005).

[5] H. Hernández-Saldaña and A Robledo, *Phys. Rev. E* (submitted) and cond- mat/0507624.

[6] See, for example, R.C. Hilborn, *Chaos and nonlinear dynamics,* 2nd Revised Edition (Oxford University Press, New York, 2000).

[7] C. Tsallis, A.R. Plastino and W.-M. Zheng, *Chaos, Solitons and Fractals* 8, 885 (1997).

[8] H. Mori, H. Hata, T. Horita and T. Kobayashi, *Prog. Theor. Phys. Suppl.* 99, 1 (1989).

[9] See, for example, H.G. Schuster and W. Just, *Deterministic Chaos. An Introduction,* 4th Revised and enlarged Edition (John Wiley & Sons Publishers, 2005).

[10] A. Robledo, *Physica A* **344**, 631 (2004); *Molec. Phys.* **103**, 3025 (2005).

[11] A. Robledo, *Phys. Lett. A* **328**, 467 (2004); F. Baldovin and A. Robledo, *Phys. Rev. E* (in press) and cond-mat/0504033.

[12] H. Hernández-Saldaña and A Robledo, in preparation.

[13] Y.F. Contoyiannis and F.K. Diakonos, *Phys. Lett. A* **268**, 286 (2000); Y.F. Contoyiannis, F.K. Diakonos, and A. Malakis, *Phys. Rev. Lett.* **89**, 035701 (2002). 7

[14] J.A. Ketoja and I.I. Satija. *Physica D* **109**, 70 (1997).

Nonextensive statistical mechanics and complex scale-free networks

Stefan Thurner
Complex Systems Research Group HNO, Medical University of Vienna,Währinger Gürtel 18-20, A-1090 Vienna, Austria

One explanation for the impressive recent boom in network theory might be that it provides a promising tool for an understanding of complex systems. Network theory is mainly focusing on discrete large-scale topological structures rather than on microscopic details of interactions of its elements. This viewpoint allows to naturally treat collective phenomena which are often an integral part of complex systems, such as biological or socio-economical phenomena. Much of the attraction of network theory arises from the discovery that many networks, natural or man-made, seem to exhibit some sort of universality, meaning that most of them belong to one of three classes: *random, scale-free* and *small-world* networks. Maybe most important however for the physics community is, that due to its conceptually intuitive nature, network theory seems to be within reach of a full and coherent understanding from first principles.

Networks are discrete objects made up of a set of nodes which are joint by a set of links. If a given set of N nodes is linked by a fixed number of links in a completely random manner, the result is a so-called *random network,* whose characteristics can be rather easily understood. One of the simplest measures describing a network in statistical terms is its degree distribution, $p(k)$, (see box 1). In the case of random networks the degree distribution is a Poissonian, i.e., the probability (density) that a randomly chosen node has degree k is given by $\mathrm{p(k)} = \frac{\lambda^k e^{-\lambda}}{k!}$, where $\lambda = \overline{k}$ is the average degree of all nodes in the network. However, as soon as more complicated rules for wiring or growing of a network are considered,

Some network measures

The degree k_i of a particular node i of the network is the number of links associated with it. If links are directed they either emerge or end at a node, yielding the diction of out- or in-degree, respectively. The degree distribution $p(k)$ is the probability for finding a node with degree k in the network. In (unweighted) networks the degree distribution is discrete and often reads, $p(k) = p(1)e_q^{k/\kappa}q$ with $\kappa > 0$ being some characteristic number of links. Apart from the degree distribution, important measures to characterize network topology are the clustering coefficient c_i, and the neighbor connectivity k_{nn}. The clustering coefficient measures the probability that two neighboring nodes of a node i are also neighbors of each other, and is thus a measure of cliquishness within networks. The neighbor connectivity is the average degree of all the nearest neighbors of node i. When plotted as a function of k, a nontrivial distribution of the average of c allows statements about hierarchic structures within the network, while k_{nn} serves as a measure of assortativity.

the seemingly simple concept of a network can become rather involved. In particular, in many cases the degree distribution becomes a power-law, bare of any characteristic scale, which raises associations to critical phenomena and scaling phenomena in complex systems. This is the reason why these types of networks are often called *complex networks.* A further intriguing aspect of dynamical complex networks is that they can potentially provide some sort of toy-model for 'nonergodic' systems, in the sense that not all possible states (configurations) are equally probable or homogeneously populated, and thus can violate a key assumption for systems described by classical statistical mechanics.

Over the past two decades the concept of *nonextensive statistical mechanics* has been extremely successful in addressing critical phenomena, complex systems and nonergodic systems [1, 2]. Nonextensive statistical mechanics is a generalization of Boltzmann-Gibbs statistical mechanics, where entropy is defined as

$$S_q \equiv \frac{1 - \int_0^\infty dk\,[p(k)]^q}{q-1} \qquad (1)$$

$$\text{with the } q = 1 \text{ limit} \quad S_1 = S_{BG} \equiv -\int_0^\infty dk\, p(k) \ln p(k)$$

where *BG* stands for *Boltzmann-Gibbs.* If – in the philosophy of the maximum entropy principle – one extremizes S_q under certain constraints, the corresponding distribution is the q-exponential (see box in editorial paper by C. Tsallis and J.P. Boon). Another sign for the importance and ubiquity of q-exponentials in nature might be due to the fact that the most general Boltzman factor for canonical ensembles *(extensive)* is the q-exponential, as was recently proved in [3]. Given the above characteristics of networks and the fact that a vast number of real-world and model networks show asymptotic power-law degree distributions, it seems almost obvious to look for a connection between networks and nonextensive statistical physics.

Since the very beginning of the recent modeling efforts of complex networks it has been noticed that degree distributions asymptotically follow power-laws [4], or even exactly q-exponentials [5]. The model in [4] describes growing networks with a so-called preferential attachment rule, meaning that any new node being added to the system links itself to an already existing node i in the network with a probability that is proportional to the degree of node i, i.e. $p_{link} \propto k_i$. In [5] this model was extended to also allow for preferential rewiring. The analytical solution to the model has a q-exponential as a result, with the nonextensivity parameter q being fixed uniquely by the model parameters.

However, it has been found that networks exhibiting degree distributions compatible with q-exponentials are not at all limited to growing and preferentially organizing networks. Degree distributions of real-world networks as well as of models of various kinds seem to exhibit a universality in this respect. In the remainder we will review a small portion of the variety of networks which potentially have a natural link to non-extensive statistics. Even though there exists no complete theory yet, there is substantial evidence for a deep connection of complex networks with the $q \neq 1$ instance in nonextensive statistical mechanics.

Recently in [6] preferential attachment networks have been embedded in Euclidean space, where the attachment probability for a newly added node is not only proportional to the degrees of existing nodes, but also depends on the Euclidean distance between nodes. The model is realized by setting the linking probability of a new node to an existing node i to be $p_{link} \propto k_i / r_i^\alpha (\alpha \geq 0)$, with r_i being the distance between the new node and node i; $\alpha = 0$ corresponds to the model in [4] which has no metrics. In a careful analysis the degree distributions of the resulting networks have been shown to be q-exponentials with a clear α-dependence of the nonextensivity parameter q. In the large α limit, q approaches one, i.e., random networks are recovered in the Boltzmann-Gibbs limit.

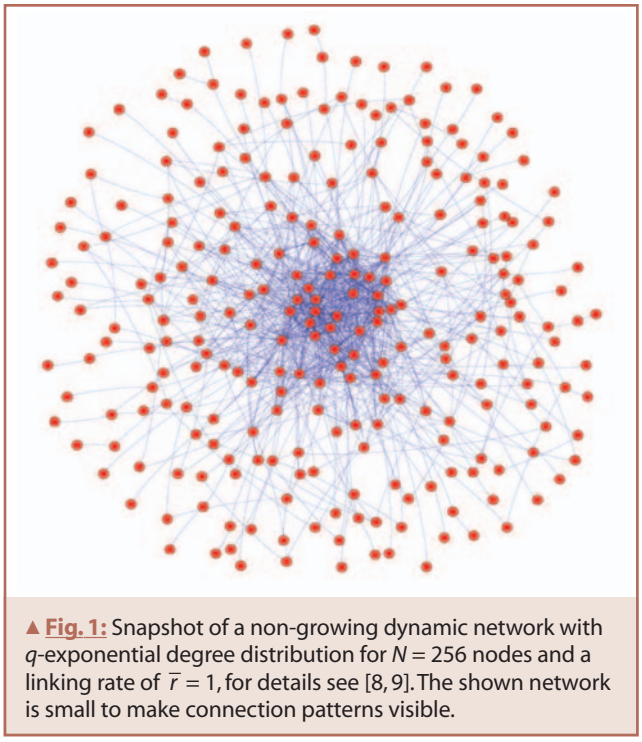

▲ **Fig. 1:** Snapshot of a non-growing dynamic network with q-exponential degree distribution for $N = 256$ nodes and a linking rate of $\bar{r} = 1$, for details see [8, 9]. The shown network is small to make connection patterns visible.

In an effort to understand the evolution of socio-economic networks, in [7] a model was proposed that builds upon [5] but introduces a rewiring scheme which depends on the *internal* network distance between two nodes, i.e., the number of steps needed to connect the two nodes. The emerging degree distributions have been subjected to a statistical analysis where the hypothesis of q-exponentials could not be rejected.

A model for nongrowing networks which was recently put forward in [8] also unambiguously exhibit q-exponential degree distributions. This model was motivated by interpreting networks as a certain type of 'gas' where upon an (inelastic) collision of two nodes, links get transfered in analogy to the energy-momentum transfer in real gases. In this model a fixed number of nodes in an (undirected) network can 'merge', i.e., two nodes fuse into one single node, which keeps the union of links of the two original nodes; the link connecting the two nodes before the merger is removed. At the same time a new node is introduced to the system and is linked randomly to any of the existing nodes in the network [9]. Due to the nature of this model the number of links is not strictly conserved – which can be thought of as jumps between discrete states in some 'phase space'. The model has been further generalized to exhibit a distance dependence as in [6], however r_i not being Euclidean but internal distance. Again, the resulting degree distributions have q-exponential form. In Fig. 1 we show a snapshot of this type of network *pars pro toto* for the many models exhibiting q-exponential degree distributions. The corresponding (cumulative) degree distribution is shown in Fig. 2 in log-log scale, clearly exhibiting a power-law. Figure 3 shows q-logarithms of the degree distribution for several values of q. It is clear from the correlation coefficient of the q-logarithm with straight lines (inset) that there exists an optimal value of q, which makes the q-logarithm a linear function in k, showing that the degree distribution is a q-exponential.

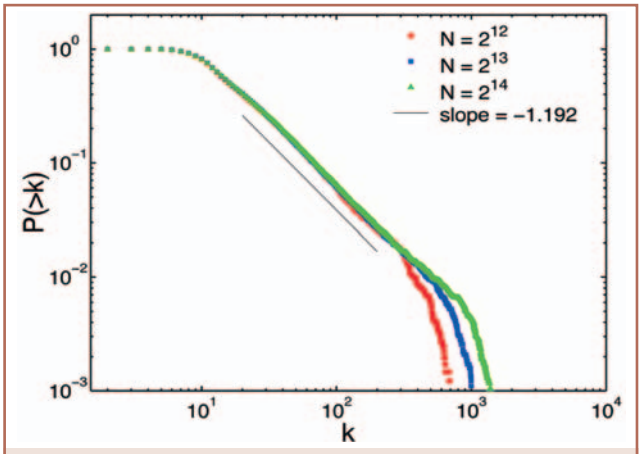

▲ **Fig. 2:** Log-log representation of (cumulative) degree distributions for the same type of network with various system sizes N and $\bar{r} = 8$. The distribution functions are from individual network configurations without averaging over identical realizations. On the right side the typical exponential finite size effect is seen.

A quite different approach was taken in [10] where an ensemble interpretation of random networks has been adopted, motivated by superstatistics [11]. Here it was assumed that the average connectivity λ in random networks is fluctuating according to a distribution $\Pi(\lambda)$, which is sometimes associated with a 'hidden-variable' distribution. In this sense a network with any degree distribution can be seen as a 'superposition' of random networks with the degree distribution given by $p(k) = \int_0^\infty d\lambda \Pi(\lambda) \frac{\lambda^k e^{-\lambda}}{k!}$. In [10] it was shown as an exact example, that a power-law functional form of $\Pi(\lambda)$ leads to degree distributions of Zipf-Mandelbrot form, $p(k) \propto \frac{1}{(k_0+k)^\gamma}$, which is equivalent to a q-exponential with an argument of k/κ and given the substitutions, $\kappa = (1 - q)k_0$ and $q = 1 + 1/\gamma$. Very recently a possible connection between *small-world* networks and the maximum Tsallis-entropy principle, as well as to the hidden variable method [10], has been noticed in [12].

In yet another view of networks from a physicist's perspective, networks have recently been treated as statistical systems on a Hamiltonian basis. It has been shown that these systems show a phase transition like behavior [13], along which network structure changes. In the low temperature phase one finds networks of 'star' type, meaning that a few nodes are extremely well connected resulting even in a discontinuous $p(k)$; in the high temperature phase one finds random networks. Surprisingly, for a special type of Hamiltonian, networks with q-exponential degree distributions emerge right in the vicinity of the transition point [14].

While a full theory of how complex networks are connected to $q \neq 1$ statistical mechanics is still missing, it is almost clear that such a relation should exist. It would not be surprising if an understanding of this relation would arise from the very nature of networks, being *discrete objects.* More specifically, it has been conjectured for nonextensive systems that the microscopic dynamics does not fill or cover the space of states (e.g. Γ-space ($6N$ dimensional phase space) for Hamiltonian systems) in a homogeneous and equi-probable manner [2]. This possibly makes phase space for nonextensive systems look like a network itself, in the sense that in a network not all possible positions in space can be taken, but that microscopic dynamics is restricted onto nodes and links. In this view the basis of nonextensive systems could be connected to a network like structure of their 'phase space'. It would be fantastic if further understanding of network theory could propel a deep understanding of nonextensive statistical physics, and vice versa, making them co-evolving theories.

References

[1] C. Tsallis, *J. Stat. Phys.*, **52**, 479-487, 1988.

[2] M. Gell-Mann and C. Tsallis, eds., *Nonextensive Entropy - Interdisciplinary Applications* (Oxford University press, N.Y., 2004); C. Tsallis, M. Gell-Mann, and Y. Sato, *Proc. Natl. Acad. Sc.* USA **102**, 15377 (2005).

[3] R. Hanel and S. Thurner, *Physica A*, **351**, 260- 268, 2005.

[4] A.-L. Barabasi and R. Albert, *Science*, **286**, 509- 512, 1999.

[5] R. Albert and A.-L. Barabasi, *Phys. Rev. Lett.*, **85**, 5234-5237, 2000.

[6] D. J. B. Soares, C. Tsallis, A. M. Mariz, and L. R. da Silva, *Europhys. Lett.*, **70**, 70-76, 2005.

[7] D. R. White, N. Kejzar, C. Tsallis, J. D. Farmer, and S. White. *A generative model for feedback networks,* Phys. Rev. E (2005), in press cond-mat/0508028.

[8] S. Thurner and C. Tsallis, *Europhys. Lett.*, **72**, 197-203, 2005.

[9] B. J. Kim, A. Trusina, P. Minnhagen, and K. Sneppen, *Eur. Phy. J. B*, **43**, 369-372, 2005.

[10] S. Abe and S. Thurner, *Phys. Rev. E*, **72**, 036102, 2005.

[11] C. Beck and E. G. D. Cohen, *Physica A*, **322**, 267-275, 2003.

[12] H. Hasegawa, *Physica A*, in press, 2005; cond-mat/0506301.

[13] G. Palla, I. Derenyi, I. Farkas, and T. Vicsek, *Phys. Rev. E*, **69**, 046117, 2004.

[14] C. Biely and S. Thurner. *Statistical mechanics of scale-free networks at a critical point: complexity without irreversibility.* cond-mat/ 0507670.

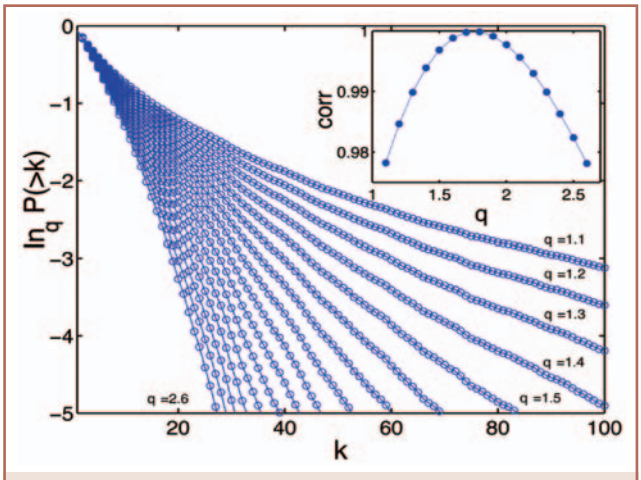

▲ **Fig. 3:** q-logarithm of the (cumulative) distribution function from the previous figure as a function of degree k. Clearly, there exists an optimum q which allows for an optimal linear fit. *Inset:* Linear correlation coefficient of $\ln_q P(\geq k)$ and straight lines for various values of q. The optimum value of q is obtained when $\ln_q P(\geq k)$ is optimally linear, i.e., where the correlation coefficient has a maximum. A linear $\ln_q$ means that the distribution function is a q-exponential; the slope of the linear function determines κ. In this example we get for the optimum $q = 1.84$, which corresponds to the slope $\gamma = 1.19$ in the previous plot.

Nonextensive statistical mechanics : implications to quantum information

A. K. Rajagopal and R.W. Rendell,
Naval Research Laboratory, Washington, DC

The interactions and correlations among the constituents of many-body systems are manifested in characteristic physical properties such as ferromagnetism, superconductivity, etc. A list of some that have been studied in the last century is given in the Box (see below). A parallel development in quantum information was initially slow but over the past two decades progress has been very rapid. Fundamentally this is another aspect of quantum correlations in composite systems arising from the twin features of the superposition principle and the tensor product structure of state space. These features are not utilized in the same manner in quantum many-body physics. In the Box, a corresponding parallel list with properties of many-body systems is given because there has been an interplay between the two research efforts and their understanding. The basic quantum mechanical principles apply to both cases except different aspects are utilized because the goals are different in each.

Both areas of investigation are based on a probabilistic foundation with a variational underpinning founded on an "entropy" maximization, which may be called Quantum Statistical Mechanics [1]. The specific form of the entropy as a functional of the density matrix will be made explicit presently. See Table I for definitions of density matrix and associated quantities.

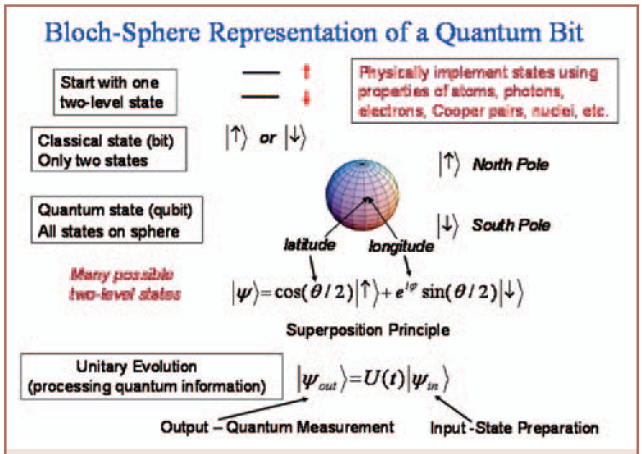

▲ **Fig.1:** Properties and Features of a Single Quantum Bit

The equilibrium properties of the many-body systems are then given by a maximization of von Neumann entropy subject to certain constraints such as the average value of the Hamiltonian of the system - "energy". This leads to the familiar exponential probabilities of the Boltzmann-Gibbs (BG) form. Any non-equilibrium properties are studied by a quantum time evolution equation. Non-equilibrium properties such as the anomalous relaxation in time are often analyzed with the quantum version of the Tsallis entropy with an entropic index, q, which leads to power- law probabilities in contrast to the BG type [2]. (See the Box in the Introduction of Tsallis and Boon).

In quantum information, the maximum entropy scheme is not of use because its origins are elsewhere as will be made clear presently. The evolution is replaced by processing of information

Interplay of Concepts:
Quantum Information and Quantum Many -Body Systems

Quantum Information		Quantum Many -Body Systems	
	1900	1900	
Quanta, (Planck)			Quanta, (Planck)
Quantized atom	1925	1925	Superconductivity Expt .
Quantum Mechanics			BEC Theory Bosons, Fermions
EPR, Nonlocal correlations	1935	1935	Helium atom
Entanglement, Cat States			Superfluidity
(Einstein, Bohm , Schrödinger)			BCS Theory Quasiparticles
	1960	1960	Photons - Laser Aharonov -Bohm Josephson
Bell's Inequalities			
Reversible Computation	1980	1980	
Confirmation of Bell			Quantum Hall Effects
Quantum Simulation			Fractional Charge, Statistics
Quantum Unitary Gates			Composite Fermions, Bosons
Quantum Optics	1990	1990	High -Tc , Cuprates
Quantum Factoring Algorithm			
Quantum Search Algorithm	1995	1995	Atomic Laser Cooling
Quantum Error Correction			Bose -Einstein Condensates
Quantum Cryptography			EIT, "Slow light"
Experimental QI :			BEC – Mott Insulator
Photons, Ions, Atoms, Dots	2005	2005	Quantum Dots

◄ **Box:** Explanation of the terms

EPR – Einstein, Podolsky, Rosen;
QI – Quantum Information;
BEC – Bose – Einstein Condensation;
BCS – Bardeen, Cooper, Schrieffer;
EIT – Electromagnetically Induced Transparency

features

Article available at http://www.europhysicsnews.org or http://dx.doi.org/10.1051/epn:2005613

accomplished by quantum operators, such as unitary or measurement operators, enabling the passage of given initial information to a known destination. The energy level (band-) structure of the states plays the central role in determining the global physical characteristics of the many body system which led to the Silicon-based classical computer. In this development, the classical information structure was sufficient in its construction and operation. In contrast, the quantum information structure exploits the state function of the many-body system and the corresponding development of a quantum computer is presently at an infant stage and it will perhaps be based on quantum optics or state-space aspects of condensed matter. The Box gives a flavor of this mutual relation between many-body systems and information theory, highlighting the twin aspects of the quantum energy level structure and the quantum state.

Classical information theory is a description of communicating information (signals, alphabets, etc. denoted by real numbers x_i, i=1, 2,…N) from one place to another using systems governed by classical physics. It rests on four intuitive ideas: (1) probability structure of a message source, $p(x_i)$; (2) a notion of additive information content, $I(x_i)$= -log $p(x_i)$, where it is the sum of each if there are independent sources; (3) use of a binary arithmetic (see Fig. 1 - yes, no - classical bit), which is sufficient to develop coding, error correction, etc. associated with transmission and reception of information, and a unit of information, the classical bit, log2; and (4) an additive measure of information, which quantifies average information per symbol, the von Neumann entropy, $S = -\sum_{i=1}^{N} p(x_i) \log p(x_i)$. When more than one source is considered, generalization of these concepts lead to the notions of (a) marginal probabilities, (b) conditional probabilities, and related entropies, and (c) relative entropy which enables comparison of two sources. The above description is for digital sources. There are also continuous sources (e.g. light) which describe analog systems. All this changes dramatically when quantum physics is the underpinning structure. To appreciate this change, we first display the foundations of quantum theory that subsumes classical theory (see Table 1 for the relevant definitions).

Quantum theory involves (a) superposition principle, (b) uncertainty principle, and (c) the system density matrix governing the probabilistic description of the system. Physical quantities associated with the system are represented by Hermitian operators whose average values defined in terms of the system density matrix give their measured values. The density matrix replaces the probability of occurrence of events in classical theory. The classical bit now takes on a more general representation, because in the quantum description the superposition principle comes into play. See Fig. 1, for a pictorial representation of a qubit. Conceptually these three features give a more general description of the system than the classical theory. Thus the classical information theory based on probabilities associated with signals and the consequent theoretical structure defining entropy as the information measure, algorithms, coding of information, etc. are all generalized in the quantum version with important consequences. The superposition principle precludes cloning and deletion of information and significantly improves the classical search algorithm. The uncertainty principle places conditions on measurements of a certain class of physical variables of the system and when there is more than one signal or source, gives conditions for "independence" or "separability" of the systems. In fact, classically correlated signals become generalized to include entanglement and other nonlocal features in the quantum context. See Fig. 2 for a description of these concepts in the simple case of two qubits. More precisely, quantum entanglement implies that the parts do not determine the whole. This feature gave rise to dense coding, "teleportation" and novel quantum cryptography that have no classical counterparts. Grover's quantum search algorithm exploits the superposition principle and makes the search faster than the classical version.

A.

Density matrix: $\rho = \sum_i q_i |i\rangle\langle i|; \{q_i\}$, **Probabilities:** $0 \le q_i \le 1$, $Tr\rho \equiv \sum_i q_i = 1$

B.

In general $\rho^2 \le \rho$

Pure state: $\rho^2 = \rho \Rightarrow \rho_P = |\Psi\rangle\langle\Psi|$, $|\Psi\rangle \equiv$ **Pure state of system**

Mixed state: $\rho^2 < \rho$; **Representation as in A.**

C.

Composite system density matrix: $\rho(A,B)$

Marginal density matrices are:

$$Tr_B \rho(A,B) = \rho_1(A),; \quad Tr_A \rho(A,B) = \rho_2(B)$$

D.

Tsallis entropy: $S_q = (q-1)^{-1} Tr\{\rho - \rho^q\}$

von Neumann entropy is obtained when q=1:

$$S(A,B) = -Tr_{A,B}\rho(A,B)\ln\rho(A,B) \ge 0$$

E.

If composite system is uncorrelated i.e., $\rho(A,B) = \rho(A) \otimes \rho(B)$ **then**

$S_q(A,B) = S_q(A) + S_q(B) + (1-q)S_q(A)S_q(B)$ **(NONADDITIVE PROPERTY)**

For q=1 this gives ADDITIVE PROPERTY for the von Neumann entropy.

F.

Comparison of two systems : **Fidelity:** $F = Tr(\rho(A)\rho(B))$

Relative entropy:

$$K(A|B) = Tr\rho(A)[\ln\rho(A) - \ln\rho(B)] \ge 0$$

G.

For a pure state of composite system, $|\Psi(A,B)\rangle$, **marginal density matrices are**

$\rho(A) = Tr_B|\Psi(A,B)\rangle\langle\Psi(A,B)|$, $\rho(B) = Tr_A|\Psi(A,B)\rangle\langle\Psi(A,B)|$ **and if this system is entangled, then the entanglement of formation is given by**

$S(A) = -Tr\rho(A)\ln\rho(A)$.

▲ **Table 1:** Quantum Density Matrix Description

The Shor quantum factorization algorithm is another successful application. For a detailed exposition, one may consult [3].

The hallmark of quantum physics is quantum non- locality which often involves entanglement, whereby distant systems can exhibit random yet perfectly correlated behavior. A fundamental problem in quantum information science is the characterization of entangled states and their measurement. Originally this was stated in terms of a violation of a certain inequality due to Bell by measuring a sequence of correlations that could not be explained by any local realistic model. This violation was taken to indicate quantum non- locality. Experimental tests of the Bell inequality have established this feature of quantum theory. While this violation detects entanglement, it does not quantify it nor is it guaranteed to succeed. Werner defined the separability of states as follows: if the system density matrix, $\rho(A,B)$, of a composite system (AB) (see Table 1) can be written as a sum of the products of the density matrices of its components, $\rho_i(A)$ & $\rho_i(B)$ in the form $\rho(A,B) = \sum_i w_i \rho_i(A) \otimes \rho_i(B)$, $0 \le w_i \le 1$, and $\sum_i w_i = 1$, then the system is separable Those composite systems for which this decomposition does not hold are said to be entangled. A criterion for testing this property was first stated by Peres: if the density matrix of the composite state does not retain its property of positive semi-definiteness under the action of time reversal of one of the subsystems, then the system is entangled. The entanglement measure is often stated in terms of "entropy of formation", originally formulated in terms of the von Neumann entropy for pure states given in Table 1. Since entanglement is due to intrinsic correlations among the parts making up a system, it is not obvious that one could employ an additive measure for this purpose. This point is the subject of discussion to this day [4]. An additive measure of a system is defined by the sum of the corresponding measures of its components (see Table 1). If the system is entangled, it is not clear that additive measures such as von Neumann entropy would be appropriate in general. Anticipating the possibility of a non-additive feature of entanglement, the Tsallis entropy was employed to characterize it. This was shown to be more successful in correctly obtaining the separability criterion of a certain known state where the von Neumann measure gives the wrong answer [5, 6, 7, 8, 9]. Table 2 gives a summary of these results. In this Table, we consider a simple special composite mixed state of two qubits called the Werner state, which is a sum of pure state density matrix and a density matrix representing noise: $(I_2 \otimes I_2)/4$. By noise is meant that all the four states of this system occur with equal probability, 1/4. This state has the interesting property of being an entangled pure state for F=1, but a separable mixed state for certain values of F. The separability condition is deduced by various methods and these are compared with the exact result obtained by the Peres criterion in Table 2.

The Werner state [8] is a mixed state and is given by

$$\rho_W(A,B) = F|\Psi^-\rangle\langle\Psi^-| + \frac{(1-F)}{3}\left(I_2 \otimes I_2 - |\Psi^-\rangle\langle\Psi^-|\right)$$

Here F is a parameter in the range (1/4, 1) and $|\Psi^-\rangle = (|\uparrow\downarrow\rangle - |\downarrow\uparrow\rangle)/\sqrt{2}$

Separability conditions for this state for values of F is determined by various methods:

(a) Peres - Horodecki partial transpose: $F \le 0.5$

(b) von Neumann conditional entropy(q=1): $F \le 0.807$

(c) Bell inequality: $F \le 0.78$

(d) Tsallis conditional entropy: $F \le 0.5$
$\left(\lim_{q\to\infty} S_q(A|B) \ge 0\right)$

This has been extended to a general 3-parameter Werner state by Tsallis et al [8] and to the N-dimensional Werner qubit state by Abe [8]. The Peres-Horodecki condition (a) is known to be exact for two qubits. Thus the non-additive Tsallis approach (d) is found to be better than the additive von Neumann scheme (b) in all forms of the Werner state considered [8].

▲ **Table 2:** Comparison of Separability Criteria of the Werner State

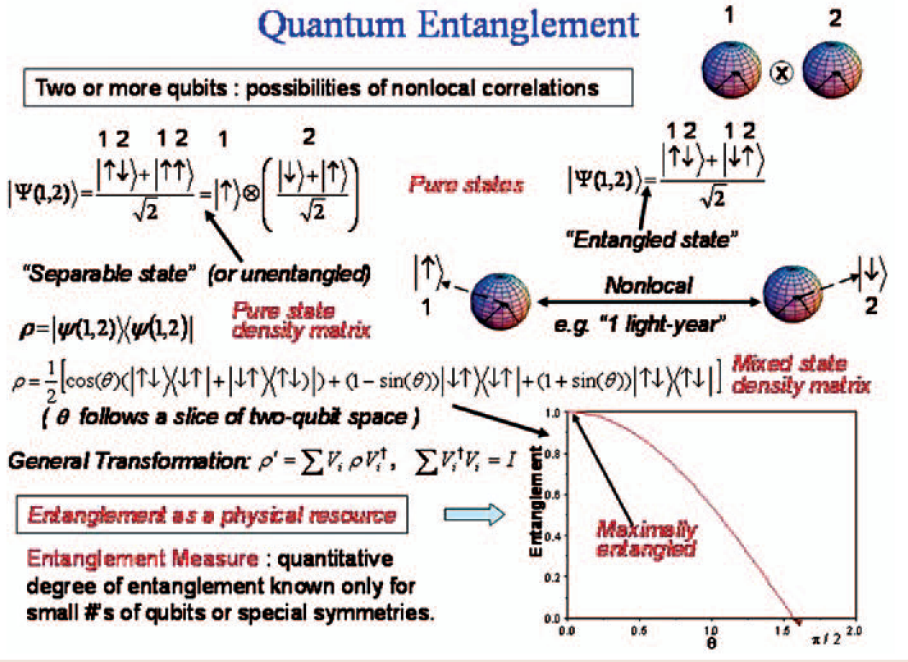

▲ **Fig.2:** Illustration of quantum entanglement based on a single two quantum-bit example. Salient features of pure and mixed state density matrices are also illustrated.

features

Another fundamental issue is the proper discriminating measure when two systems are under consideration. In classical information theory, one employs the Kullback – Leibler relative entropy for this purpose which also has its quantum version. These are also additive measures and the Tsallis counterparts of these have been put forward and employed in the quantum context as well [10, 11]. There is promise in future work using the Tsallis approach to problems arising in quantum information theory, especially in the areas of quantum algorithms and quantum computing.

There has been some discussion of the thermodynamics of information, in particular quantum information. Since there are hints that quantum entanglement may not be additive, and since the concept of entropy has been introduced into the discussion, an examination of maximum Tsallis entropy subject to constraints such as the Bell-Clauser- Horne-Shimony-Holt observable was studied for purposes of inferring quantum entanglement [5, 6].

Acknowledgements

AKR and RWR are supported in part by the US Office of Naval Research and AKR by the Air Force Research Laboratory, Rome, New York.

About the authors

A.K. Rajagopal obtained his Master's degree from the Indian Institute of Science, Bangalore, India and a Doctor's degree from Harvard University, Massachusetts, USA. In the past twenty years he has been a Research Physicist at the Naval Research Laboratory, Washington D. C. Recently the focus of his work has been in Statistical Mechanics and Quantum Information.

R. W. Rendell obtained a PhD in Physics from the University of California at Santa Barbara. For the past twenty years he has been a Research Physicist at the Naval Research Laboratory, Washington D.C. Recently the focus of his work has been in Nanoscience and Quantum Information.

References

[1] A. K. Rajagopal in *Lecture Notes in Physics,* (eds. Sumiyoshi Abe and Yuko Okamoto) Springer-Verlag, New York (2001) gives an account of Tsallis entropy as a unified basis of both quantum statistical mechanics of many-particle systems as well as quantum information. (Lecture series were held during February 15-19, 1999)

[2] M. Gell-Mann and C. Tsallis (eds.) *Nonextensive Entropy – Interdisciplinary Applications,* Oxford Univ. Press, New York (2004); *Physica D* **193**, (2004), Special Issue on Anomalous Distributions, Nonlinear Dynamics and Nonextensivity, edited by H. Swinney and C. Tsallis.

[3] M. A. Nielsen and L.L. Chuang, *Quantum Computation and Quantum Information,* Cambridge Univ. Press, Cambridge (2000)

[4] P. W. Shor, *Commun. Math. Phys.* **246,** 453 (2004)

[5] A. K. Rajagopal, *Phys. Rev. A* **60**, 4338 (1999)

[6] S. Abe and A. K. Rajagopal, *Phys. Rev. A* **60**, 3461 (1999)

[7] A. K. Rajagopal and S. Abe, *Phys. Rev. Lett.* **83**, 1711 (1999)

[8] S. Abe and A. K. Rajagopal, *Physica. A* **289**, 157 (2001); C. Lloyd, and M. Baranger, *Phys. Rev. A* **63**, 042103 (2001); S. Abe, *Phys. Rev. A* **65**, 052323 (2002)

[9] A. K. Rajagopal and R. W. Rendell, *Phys. Rev. A* **66**, 022104 (2002)

[10] S. Abe, *Phys. Rev. A* **68**, 032302 (2003)

[11] S. Abe and A.K. Rajagopal, *Phys. Rev. Lett.* **91**, 120601 (2001)

Entropy and statistical complexity in brain activity

A. Plastino [1,2] and O.A. Rosso [3,4]
[1] Departament de Fisica. Universitat de les Illes Balears. E-070701 Palma de Mallorca, Spain;
*[2] Facultad de Ciencias Exactas and Instituto de Física La Plata Universidad Nacional de La Plata and CONICET, Argentina. C.C. 727, 1900 La Plata, Argentina **
[3] Institut für Mathematik, Universität zu Lübeck, Wallstrasse 40, D-23538 Lübeck, Germany
*[4] Instituto de Cálculo, Facultad de Ciencias Exactas y Naturales, Universidad de Buenos Aires. Pabellón II, Ciudad Universitaria. 1428 Buenos Aires, Argentina. **
** Permanent address*

Electroencephalograms (EEG) are brain-signals that provide us with information about the mean brain electrical activity, as measured at different sites of the head. EEGs not only provide insight concerning important characteristics of the brain activity but also yield clues regarding the underlying associated neural dynamics. The processing of information by the brain is reflected in dynamical changes in this electrical activity. The ensuing activity-variations are found in (*i*) time, (*ii*) frequency, and (*iii*) space. It is then very important to have theoretical tools able to describe qualitative and quantitative variations of these brain-signals in both time and frequency. Epileptic signals (ES) are specially important sources of brain information. We concentrate on ES in this article. The EEG-signal is what mathematicians call a non stationary time-series (ST). Powerful analytical methods have been developed over the years to extract information from ST. The brain ST is contaminated by another body-signals (called artifacts) due mainly to eye movements and muscle activity. Artifacts related to muscle contractions are specially troublesome in the case of epileptic seizures that exhibit rigidity and convulsions (called tonic-clonic seizures). The troublesome artifacts acquire here very high amplitudes that contaminate the whole recording. A drastic way of preventing this contamination is by injecting curare to the patient. The classic work of this type is that of Gastaut and Boughton (GAB) [1], who described the characteristic frequency pattern of a tonic-clonic epileptic seizure (ACES) in patients subjected to muscle relaxation from curarization and artificial respiration. They found that, after a short period characterized by phase desynchronization of the brain' signals, a typical feature appears in the records, baptized by them as an "epileptic recruiting rhythm" (ERR, at about 10 *Hz*). Later, as the seizure ends, they detected a progressive increase of lower frequencies associated with the convulsive phase. The TCES proceeds as follows: about 10 *s* after seizure onset, lower frequencies (0.5-3.5 *Hz*) are observed that gradually diminish their activity. The convulsive activity is associated to generalized polyspike bursts from muscle-jerks. Very slow irregular activity dominates then the EEG, accompanied with a gradual frequency increase of up to (3.5 - 12.5 *Hz*), indicative of the end of the seizure.

In Fig. 1.a we depict a typical EEG signal (sample frequency $\omega_s = 102.4$ *Hz*, for signal acquisition details see Ref. [2]) corre-

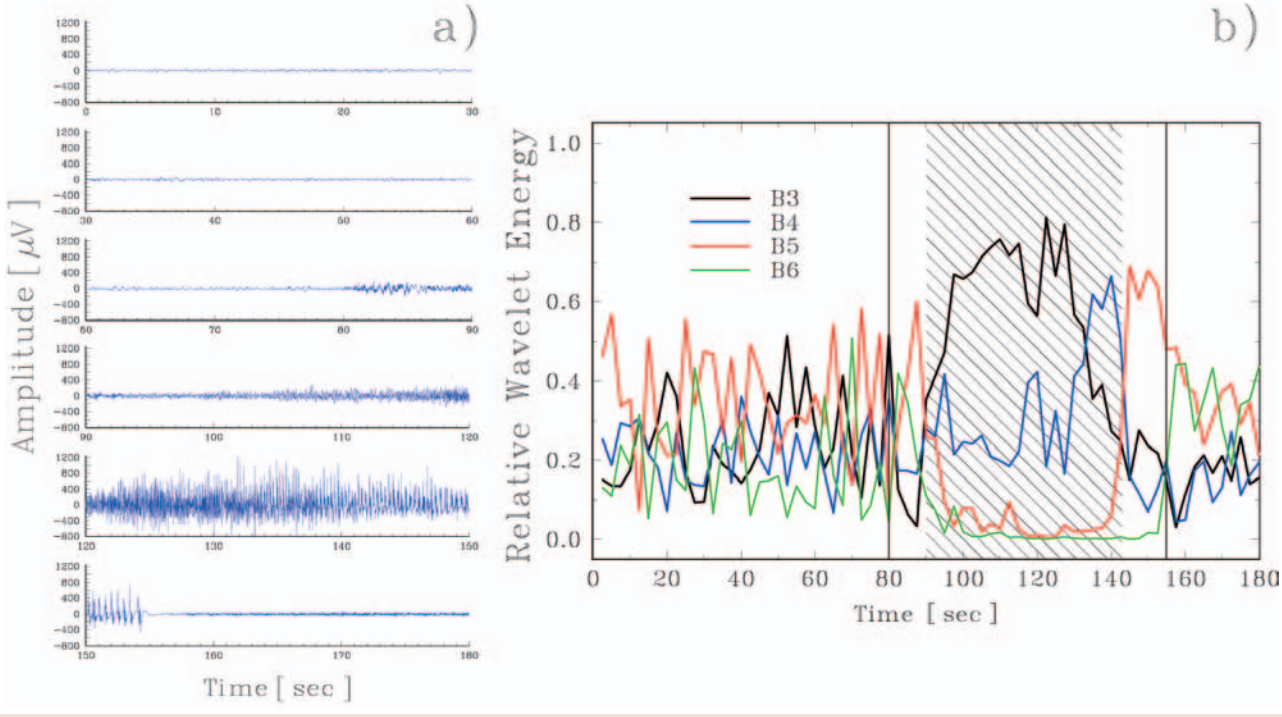

▲ **Fig. 1:** *a)* EEG signal for a tonic-clonic epileptic seizure. The seizure starts at 80 *s* and the clonic phase at 125 *s*. The seizure ends at 155 *s*. Notice that, visually, the dramatic transition from rigidity (tonic stage) to convulsions (clonic stage) around 125 *s* is not clearly discernible. *b)* Time-evolution of the relative wavelet energy corresponding to EEG noise-free signal (without contribution of frequency bands B_1 and B_2, representing frequency contributions > 12.8 *Hz* corresponding mainly to muscular activity that blur the EEG signal). From this figure it is clear that the seizure is dominated by the middle frequency bands B_3 and B_4 (12.8 - 3.2 *Hz*), with a corresponding abrupt activity decreases in the low frequency bands B_6 and B_6 (3.2 - 0.8 *Hz*). This behavior can be associated with the "epileptic recruiting rhythm" - 10 *Hz* (shadowed area in the figure). The vertical lines represent the start and the ending of the epileptic seizure.

sponding to a TCES. Recordings were performed under video control in order to have an accurate determination of the different stages of the seizure. The seizure starts at 80 *s*, with a "discharge" of slow waves superposed by fast ones with lower amplitude. This discharge lasts approximately 8 *s* and has a mean amplitude of 100 μV. Afterwards, the seizure spreads, making the analysis of the EEG more difficult due to muscle artifacts. However, it is possible to establish the beginning of the convulsive phase at around 125 *s*, and the end of the seizure at 155 *s*, where there is an abrupt decay of the signal's amplitude. Notice that it is almost impossible to visually detect the rigidity-to-convulsions (tonic-clonic) transition.

In the mathematical characterization of these brain electrical signals, that one regards as a time-series, we follow what is called a "Wavelet Transform – Information Theory" approach that is able to extract information form signals like that of Fig. 1. The basic elements of the Math we used are called wavelet transform coefficients that we derive from the EEG signal. It was our main idea that of associating a probability distribution (PD) to this time series. If one is in possession of a PD, then the branch of mathematics called Information Theory allows one to evaluate specific quantities, called quantifiers, that contain otherwise inaccessible information. Thus we go from the "bare"-signal of Fig. 1 to quantifiers that can tell us a lot about the EEG. We devised three quantifiers for EEG analysis. For computing these quantifiers we use another Math tool called "wavelet analysis". This is a method which expresses the original signal in terms of what is called a basis of an space of functions. Wavelets are just an appropriate basis, of elements here called $\psi_{j,k}(t)$, and allow for characterizing the signal by the amplitude-distribution in such a basis [3]. The wavelet coefficients represent the elements $C_j(k)$ of this distribution and efficiently provide both full information and a direct estimation of signal-energies at different frequencies. The brain-signal under analysis is given by sampled-values $\mathcal{S} = \{s_n, n = 1, \ldots, M\}$ collected using a uniform time grid. The wavelet-expansion is carried out over all pertinent frequency-resolution levels (denoted by an index j) and writen as $\mathcal{S}(t) = \sum_{j=-N}^{-1} \sum_k C_j(k)\ \psi_{j,k}(t)$, with $N = \log_2(M)$. The wavelet coefficient series $\{C_j(k)\}$ can be interpreted as the local residual errors between successive signal-approximations at scales j and $j + 1$. It contains information on the signal $\mathcal{S}(t)$ corresponding to the frequencies $2^{j-1}\omega_s \le |\omega| \le 2^j\omega_s$.

Since the family $\{\psi_{j,k}(t)\}$ is an orthonormal basis for the space of functions, the concept of energy is linked with the usual notions derived from Fourier's theory for such spaces. The wavelet coefficients are given by $C_j(k) = <\mathcal{S}, \psi_{j,k}>$ and the signal-energy, at each resolution level $j = -1, \ldots, -N$, will be $\mathcal{E}_j = \sum_k |C_j(k)|^2$. The total signal-energy can be obtained in the fashion $\mathcal{E}_{tot} = \sum_{j<0} \mathcal{E}_j$. Finally, we define the normalized ρ_j-values, which represent the *Relative Wavelet Energy* (RWE), $\rho_j = \mathcal{E}_j/\mathcal{E}_{tot}$. This RWE is our *first quantifier*. We decided to regard these ρ_j, at different scales, as a probability distribution for the energy. Clearly, $\sum_j \rho_j = 1$ and the distribution $P = \{\rho_j\}$ can be considered as a time-scale energy probability density that constitutes a convenient tool for detecting and characterizing specific phenomena in both the time and frequency planes [2, 4, 5].

Information theory introduces tools, called entropic information measures, that provide useful criteria for analyzing and comparing different probability distributions. In looking for degrees of "disorder" in our brain-signal, we devised a math-tool, our *second quantifier,* that we call a Generalized Escort-Tsallis Entropy (GWS) [4]. It is written as

$$H_q^{(G)}[P] = \frac{1}{(q-1)} \left\{ 1 - \left[\sum_{j=-N}^{-1} (\rho_j)^{1/q} \right]^{-q} \right\} \Big/ S_q^{max} \quad (1)$$

S_q^{max} is a normalization constant that enforces the convenient inequalities $0 \le H_q^{(G)} \le 1$, that simplify the analysis to be performed.

The GWS is a measure of the degree of order/disorder of the signal and thus yields useful information concerning the underlying dynamical brain-process associated with the signal. Indeed, a very ordered process can be represented by a periodic mono-frequency signal (signal with a narrow band spectrum). A wavelet representation of such a signal will be resolved at just one unique wavelet resolution level *j*, i.e., all relative wavelet energies will be (almost) zero except at the wavelet resolution level *j* which includes the representative signal's frequency. For this special level, the relative wavelet energy will be (in our chosen energy units) almost equal to unity. As a consequence, the GWS will acquire a very small, vanishing value. A signal generated by a totally random or chaotic process can be taken as the representative of a very disordered behavior. This kind of signal will have a wavelet representation with significant contributions coming from all frequency bands. Moreover, one could expect that all contributions will be of the same order. Consequently, the relative wavelet energy will be almost equal at all resolutions levels, and the GWS will acquire its maximum possible value.

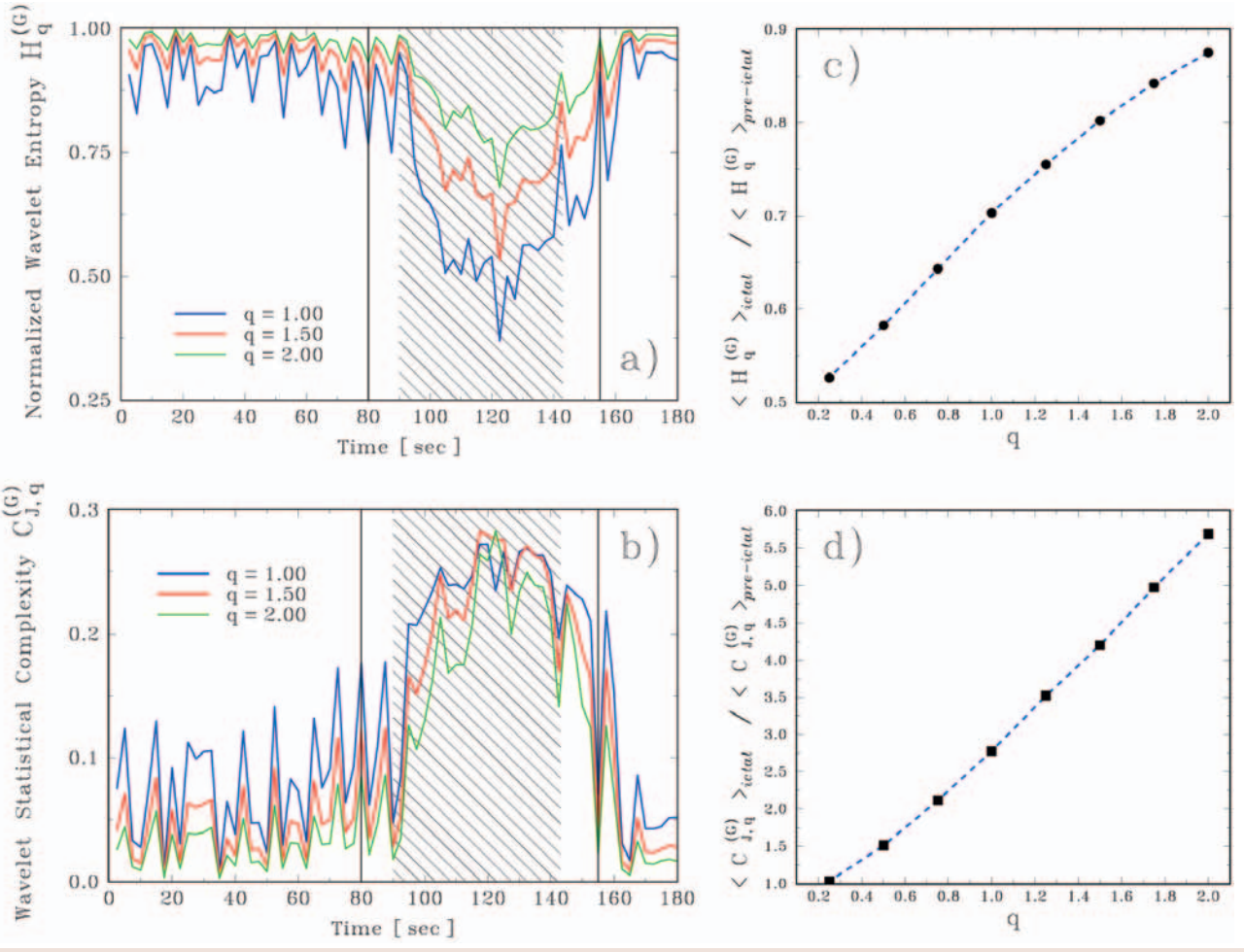

▲ **Fig. 2:** Temporal evolution of two quantifiers *a)* the normalized escort-Tsallis wavelet entropy (GWS) and *b)* Jensen escort-Tsallis wavelet statistical complexity measure (JGWC), corresponding to an EEG noise-free signal (see caption Fig. 1). The behaviour of the GWS clearly varies with *q* (see Figs. 2.a) in the temporal domain. During the pre- and post-ictal stages, these normalized GWS-values acquire a rather regular, constant behaviour, *with a dispersion that diminishes* as *q* grows. For all $q \ge 1$, the normalized GWS (JGWC) values during the ictal stage are much smaller (greater) than those pertaining to the pre-ictal stage. This difference is better appreciated in the time range corresponding to the "epileptic recruiting rhythm" (represented by a shadowed area in the figure). These features suggest that the escort-Tsallis entropy measure constitutes the appropriate tool for characterizing the tonic and clonic stages. The minimum absolute value of the normalized entropy is to be found in the vicinity of ~ 125 s, in agreement with the medical diagnosis: in that neighbourhood one encounters the tonic-clonic "phase transition". *c)* Ratio between the temporal mean value corresponding to ictal and pre-ictal epochs as function of the parameter *q* for the normalized escort-Tsallis wavelet entropy (GWS). *d)* Same for Jensen-escort-Tsallis wavelet statistical complexity measure (JGWC). This behaviour clearly illustrates the superiority of the $q > 1$ techniques that magnify differences between ictal and pre-ictal stages, critical for clinical purposes.

Ascertaining the degree of unpredictability and randomness of a system is not automatically tantamount to adequately grasping all the correlational structures that may be present, i.e., to be in a position to capture the relationship between the components of the pertinent physical system (here, the brain) [5, 6, 7]. Randomness, on the one hand, and structural correlations on the other one, are not totally independent aspects of the accompanying physical description. Certainly, the opposite extremes of perfect order and maximal randomness possess no structure to speak of (zero complexity). In between these two special instances a wide range of possible degrees of physical structure exists that should be reflected in the features of the underlying probability distribution P (here, that for the EEG). A new notion has been recently introduced in this respect, called "complexity". Complexity is a measure of off-equilibrium "order". It refers to non-equilibrium structures that arise spontaneously in certain situations. This type of "order" is not the one associated, for instance, with crystal structures, for which the entropy is very small. Biological life is a typical example of the kind of "new" order one has in mind here, associated with relatively large entropic values.

We adopt the following functional form for the "statistical complexity measure" (SCM) introduced by López-Ruiz, Mancine and Calbet [7] for a given probability distribution P:

$$C[P] = H[P] \cdot Q[P] \,, \qquad (2)$$

where Q stands for the so-called "disequilibrium" and H (defined above) represent the amount of "disorder". The quantity $Q[P] = Q_0 \cdot \mathcal{D}[P, P_e]$ is defined as a distance from the *uniform* distribution P_e among the accessible states of the system, and Q_0 is a normalization constant ($0 \le Q \le 1$). $Q[P]$ tells us just "how far" our P is located (in this space) from the uniform distribution P_e. The disequilibrium Q would reflect on the systems's "architecture", being different from zero if there exist "privileged", or "more likely" states among the accessible ones. Here we choose $\mathcal{D}[P, P_e]$ as the Jensen-escort-Tsallis divergence [8] given by

$$\mathcal{D}[P, P_e] = \frac{1}{2}\, \mathrm{K}_q^{(G)}\left[P \,\middle|\, \frac{P+P_e}{2}\right] + \frac{1}{2}\, \mathrm{K}_q^{(G)}\left[P_e \,\middle|\, \frac{P+P_e}{2}\right] \qquad (3)$$

where $\mathrm{K}_q^{(G)}[P_1|P_2]$ represent the q-Kullback escort-Tsallis entropy of P_1 with respect to P_2 (both discrete distributions) given by

$$\mathrm{K}_q^{(G)}[P_1|P_2] = \frac{1}{(q-1)} \sum_{j=1}^{N} \frac{p_j^{(1)}}{(A[P_1])^q} \cdot \left\{ \left[\frac{\left(p_j^{(2)}\right)^{1/q}}{A[P_2]} \right]^{1-q} - \left[\frac{\left(p_j^{(1)}\right)^{1/q}}{A[P_1]} \right]^{1-q} \right\} \qquad (4)$$

and $A[P] = \sum_{j=1}^{N} (p_j)^{1/q}$. The corresponding *Jensen-escort-Tsallis wavelet statistical complexity measure* (JGWC), $C_{J,q}^{(G)}$ is in this way obtained if we consider for the complexity evaluation (Eqs. (2) to (4)) that distribution P given by the RWE. The JGWC is our *third quantifier.*

For EEG-work six frequency bands are important for an appropriate wavelet analysis [3]. We denote these 6 band-resolution levels by Bj ($|j| = 1, \ldots, 6$), and proceed as follows in the evaluation of the three quantifiers that we have introduced above: RWE, GWS and JGWC, we ignore the contributions from the B_1 and B_2 bands (> 12.8 *Hz*) that contain high frequency artifacts related to muscular activity that blur the EEG [2]. Once the high frequency artifacts are eliminated, we can analyze the time evolution of the above listed three wavelet quantifiers for the "remaining" signal. For this purpose the signal is divided into epochs of lengths $L = 2.5$ *s* each ($M = 256$ *data*).

Figure 1.b displays the quantifier RWE corresponding to the EEG signal (Fig. 1.a) without contaminant artifact-contributions (B_3 to B_6). (The following, detailed description of the signal-analysis can be omitted in a first reading.) We see that the initial (called pre-ictal) phase is characterized by a dominance of low rhythms (pre-ictal: $[B_5 + B_6] \sim 50\%$). The seizure starts at 80 *s* with a discharge of slow waves superimposed on low voltage fast activity. This discharge lasts approximately 8 *s* and produces a marked "activity-rise" in the frequency bands B5 and B6, which reaches 80% of the RWE. Starting at 90 s, the low frequency activity, represented in our analysis by B_5 and B_6, decreases abruptly to relative values lower than 10%, while the other frequency bands become more important. We also observe in Fig. 1.b that the start of the convulsive (clonic) phase is correlated with increased activity in the B_4 frequency band. After 140 *s*, when clonic discharges become intermittent, the B_5 activity rises up again till the end of the seizure, when the B_6 frequency activity also increases in very rapid fashion and both frequency bands become clearly dominant. The B_5 and B_6 frequency bands maintain this predominance throughout the post-ictal phase. We conclude from this example that the seizure is dominated by the middle frequency bands B_3 and B_4 (12.8-3.2 *Hz*), with a corresponding abrupt activity decrease in the low frequency bands B_5 and B_6 (3.2-0.8 *Hz*). Clearly, this behavior can be associated with the above described epileptic recruiting rhythm (ERR) [1] (shadowed area in the figure). We emphasize the fact that our results were obtained without the use of curare or any filtering method.

The other quantifiers, GWS and JGWC, as a function of time, are depicted in Figs. 2.a and 2.b. In their evaluation we ignore contributions due to contaminant high frequency bands (B_1 and B_2). The behavior of the GWS clearly varies with q (see Figs. 2.a) in the temporal domain. During the pre- and post-crisis (ictal) stages, these normalized GWS values acquire a rather regular, constant behavior, *with a dispersion that diminishes* as the Tsallis' q grows (see Figs. 2.a and 2.c). For all $q \ge 1$, the normalized GWS values during the ictal stage are much smaller than those pertaining to the pre-ictal stage. This difference is better appreciated in the time range corresponding to the ERR (represented by a shadowed area in the figure). One may therefore suggest that the escort-Tsallis entropy measure, that we use here, constitutes the appropriate tool for characterizing the tonic and clonic stages of the epileptic crisis.

The minimum absolute value of the normalized entropy is to be found in the vicinity of ~ 125 *s*, in agreement with the medical diagnosis: in that neighbourhood one encounters the tonic-clonic "phase transition", that one can detect by looking at the patient but not by inspection of the bare record of Fig. 1. Two relative maxima are observed at ~145 s and ~ 155 *s*. As stated above, these times are associated with the ends of (*i*) the ERR and (*ii*) the epileptic seizure, respectively. Changes in the EEG series around 125 *s* (transition from tonic to clonic stage) are the result of a mechanism entirely different from the one that produces variations at 145 and 155 *s* (neuronal "fatigue", a decrease of the neuronal firing rate with preponderance of inhibition factors, is largely responsible for originating the end of the seizure).

Our JGWC-quantifier numerical results also depend upon the Tsallis' q. In fact, we see from Figs. 2.b and 2.d that the JGWS yields values *with a dispersion that diminishes* as q grows (in particular for the pre- and post-ictal periods). This behaviour can be clearly appreciated in Figs. 2.c and 2.d, where the ratio between the temporal mean values corresponding to ictal and pre-ictal epochs as function of the parameter q for GWS and JGWC is shown. That is for $q < 1$ the fluctuations in these quantifiers increase and for $q > 1$ decrease, specially in pre-ictal period. This fact (*i*) emphasizes the difference between the mean values corresponding to pre-ictal and ictal stages (increase of statistical significance); (*ii*) clearly illustrates the superiority of the $q > 1$ Tsallis-techniques that magnify such

differences, that are critical for clinical purposes. However, the mean JGWS values are significatively larger in the ictal than in the pre- and post-ictal epochs for all $q \geq 1$.

The present article described informational tools derived from the orthogonal discrete wavelet transform and their application to the analysis of brain electrical signals. The quantifier (relative wavelet energy) RWE provides information concerning the relative energy associated with different frequency bands that are to be found in the EEG and enables one to ascertain their corresponding degree of importance. Our second quantifier, normalized wavelet entropy (GWS), carries information about the degree of order/disorder associated with a multi-frequency signal response. Finally, our third quantifier, the statistical wavelet complexity (JGWC), provides us with a measure that reflects the intricate structures hidden in the brain-dynamics.

In particular, it becomes clear that the ERR behavior reported by Gastaut and Broughton [1] for generalized TCES is accurately described by the RWE quantifier. Moreover, the reported study does not require the use of curare or of digital filtering. In addition, a significant decrease in the entropy was observed in the recruitment epoch, indicating a more rhythmic and ordered behavior of the EEG signal, compatible with a dynamical process of synchronization in the brain activity. In addition the recruiting phase also exhibits larger values of statistical complexity.

It is well established that an EEG is directly proportional to the local field potential recorded by electrodes on the brain's surface. Furthermore, one single EEG electrode placed on the scalp records the aggregate electrical activity from up to 6 cm^2 of the brain surface, and hence from many millions of neurons. With such large numbers, is seems quite natural to model the neocortex as a continuous sheet of neurons (neuronal matter) whose activity varies with time. Taking into account the available results for (*i*) the chaoticity index (the largest Lyapunov exponent with stationary constraints removed) as a function of time and (*ii*) the largest Lyapunov exponent for selected portions of the EEG signal, one can confidently assert that a chaotic behavior can be associated with the whole EEG signal. This chaoticity becomes smaller during the recruiting phase [2]. As pointed out by many authors (see for instance [9]), the coexistence of chaos with ordering and increasing complexity for extended system is a manifestation of self-organization. We can thus suggest, on the basis of experimental EEG data and using appropriate statistical tools, that in the case of tonic-clonic epileptic seizures, the epileptic focus triggers a self-organized brain state characterized by both order and maximal complexity.

References

[1] H. Gastaut and R. Broughton, *Epileptic Seizures.* Charles C. Thomas, Springfield, 1972.

[2] O. A. Rosso, M. L. Mairal, *Physica A* **312** (2002) 469.

[3] S. Mallat, *A Wavelet Tour of Signal Processing,* Academic Press, San Diego, 1999.

[4] O. A. Rosso, M. T. Martin, A. Plastino. *Physica A* **313** (2002) 587.

[5] O. A. Rosso, M. T. Martin, A. Plastino. *Physica A* **320** (2003) 497.

[6] P. W. Lamberti, M. T. Martin, A. Plastino, O. A. Rosso, *Physica A* **334** (2004) 119.

[7] R. López-Ruiz, H. L. Mancini, X. Calbet. *Phys Lett A* **209** (1995) 321.

[8] P. W. Lamberti, A. P. Majtey. *Physica A* **329** (2003) 81.

[9] H. Haken, *Information and Self-Organization,* Springer–Verlag, Berlin, 2000.

Long-range memory and nonextensivity in financial markets

Lisa Borland
Evnine-Vaughan Associates, Inc., 456 Montgomery Street, Suite 800, San Francisco, CA 94104, USA
lisa@evafunds.com

Perhaps one of the most vivid and richest examples of the dynamics of a complex system at work is the behavior of financial markets. The price formation process of a publicly traded asset is clearly the product of a multitude of evasive interactions. Individuals around the globe post orders to buy or sell a particular stock at a particular price. Transactions are cleared at a certain price at a given time, either by passing through the hands of a specialist on the trading floor, or automatically on the many electronic markets which have flourished along with technological advances over the past few years (Fig. 1). Apart from fundamental properties of the company whose stock is being traded, factors such as supply and demand clearly must affect the price of stocks, as well as general trends in the particular industry in question. Stock specific events, such as mergers and acquisitions, have a big impact, as do world events, such as wars, terrorist attacks and natural disasters.

Time series of financial data exhibit highly nontrivial statistical properties. What is quite fascinating is that many of these anomalous properties appear to be universal, in the sense that they are present in a variety of different asset classes, ranging for example from commodities such as wheat or oil, to currencies and individual stocks. Furthermore they are present across the geographical borders, and can be observed among others in US, European and Japanese markets.

Finding a somewhat realistic model of price variations that can capture the spectrum of interesting statistical features inherent in real data is a challenging task, important for many real-world reasons, such as risk control, the development of trading strategies, option pricing and the pricing of credit risk to name a few. Bachelier's random walk model in 1900 was the first attempt of a mathematical model of price variations. While a century ago this Gaussian stochastic process was state-of-the-art, and indeed lies at the bottom of the celebrated Black-Scholes option pricing formalism, we now know Figure 2: The empirical distribution of daily returns from the stocks comprising the SP 100 (red) is fit very well by a q-Gaussian with $q = 1.4$ (blue). that it is way too simple to describe the properties of real data. In fact, during the past decade, there has been an increasing and widespread access to data extracted from financial markets. This includes for example every single trade and quote of all stocks traded on the New York Stock Exchange, records from various electronic markets, the entire order book data from the London stock exchange, to name just a few sources. These vast amounts of historical stock price data have helped establish a variety of so-called stylized facts [1, 2], which can be seen as statistical signatures, of financial data.

The best known stylized fact is perhaps the distributions of returns (defined as logarithmic relative price changes). On time scales ranging from minutes to weeks these have fat tails, exhibiting

power-law decay and are modeled quite well by the Tsallis or Student form [1] (Fig. 2).As the time-scale over which one calculates the price changes increases to months or years, the distribution does become closer to a Gaussian. In addition, there is a long range memory in volatility fluctuations, evident because the autocorrelation of the volatility decays only slowly as a power law. This leads to bursts of higher or lower volatility in the time series of returns, a phenomenon also referred to as volatility clustering, and furthermore the distribution of the instantaneous volatility is close to log-normal. Also, there are certain asymmetric correlations in that large past price changes imply large future volatilities, an effect called leverage. In addition to these stylized facts, are also more subtle ones which have been elucidated in recent years. Examples are multifractal scaling, a financial analogue of the Omori law for earthquakes (in other words, large volatility shocks tend to be followed by after-shocks decaying in magnitude according to a power law), as well as the statistical asymmetry under time reversal, implying the rather obvious fact (which however is not present in most models of price fluctuations!) that financial time series differentiate the past from the future.

Several different models have been proposed [3] in an attempt to capture fat tails and volatility clustering which don't exist in the Gaussian Bachelier model. Popular approaches include Levy processes, which induce jumps and thus fat tails on short time-scales, but convolve too quickly to the Gaussian distribution as the time-scale increases and do not present volatility clustering. Stochastic volatility models, such as the Heston model where the volatility is assumed to follow its own mean-reverting stochastic process, reproduce fat tails, but not the long memory observed in the data. The same holds true for the simplest of Engle's Nobel prize winning GARCH models in which the volatility is essentially an autoregressive function of past returns. Multifractal stochastic volatility models (similar to cascade models of turbulent flow) are another promising candidate (cf [2]), reproducing many of the stylized facts, lacking mainly in that they are strictly time reversal symmetric in contrast to empirical evidence.

In addition, most of the above mentioned models are difficult if not impossible to deal with analytically. Analytic tractability is desirable for reasons such as efficiently calculating the fair price of options or other financial derivatives which in their own right are traded globally in high volumes. They fill important financial functions with respect to hedging and risk control, as well as offer purely speculative opportunities. In short, options are financial instruments which depend in some contingent fashion on the underlying stock or other asset class. The simplest example is perhaps the European call option. This is the right (not obligation) to buy a stock at a certain price (called the strike) at a certain time (called the expiration) in the future. Contracts similar to options were exploited already by the Romans and story has it that Thales, the Greek mathematician, used call options on olives to make a huge profit when he had reason to believe that the harvest would be particularly good. In Holland in the 1600s, tulip options were traded quite a bit by speculators prior to the famous tulip bubble. But it wasn't until 1974 that the fair price of options could be calculated somewhat reliably with the publication of the Nobel-prize winning Black-Scholes formula. This is still the most widely used option pricing model, not because of its accuracy (since it is based on a Gaussian model for stock returns which, as we discussed above, is unrealistic) but rather due to its mathematical tractability (which exists due to the same Gaussian assumptions). In fact, an impressive school of mathematical finance has been developed over the past three decades, and is based largely on notions stemming from the famous Black-Scholes paradigm.

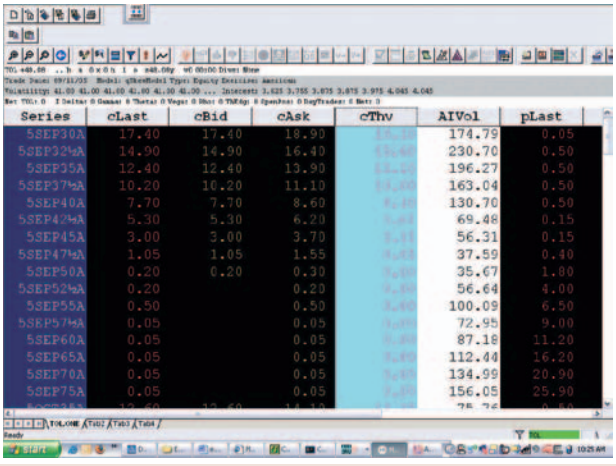

▲ **Fig.1:** A typical electronic trading screen. Here, live quotes on options are fed in from the market and the trader can execute electronically.

Because real stock returns exhibit fat tails, yet the Black-Scholes pricing formula is based on a Gaussian distribution for returns, the probability that the stock price will expire at strikes far from its current price will be underestimated. Traders seem to correct for this intuitively; for the Black-Scholes model to match empirical option prices, higher volatilities must be used the farther away the strike price is from the current stock price value. A plot of these Black-Scholes implied volatilities as a function of the strike price is thus not constant but instead most typically a convex shape, often referred to as the volatility smile. This way of representing option prices in terms of the Black-Scholes volatility is so widely used that prices are often quoted just in terms of this quantity, most often referred to simply as *the vol*.

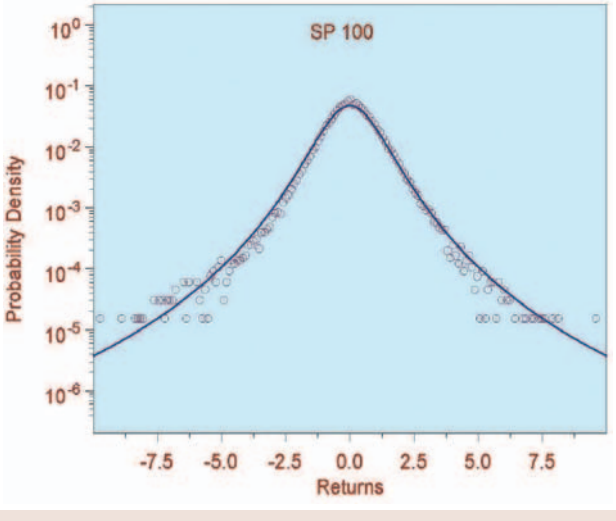

▲ **Fig.2:** The empirical distribution of daily returns from the stocks comprising the SP 100 (red) is fit very well by a *q*-Gaussian with $q = 1.4$ (blue).

[1] The Tsallis distribution (also referred to as a q-Gaussian) is equivalent to the Student distribution whenever q is a rational of the form $(3 + n)/(1 + n)$, where n is a positive integer denoting the number of degrees of freedom.

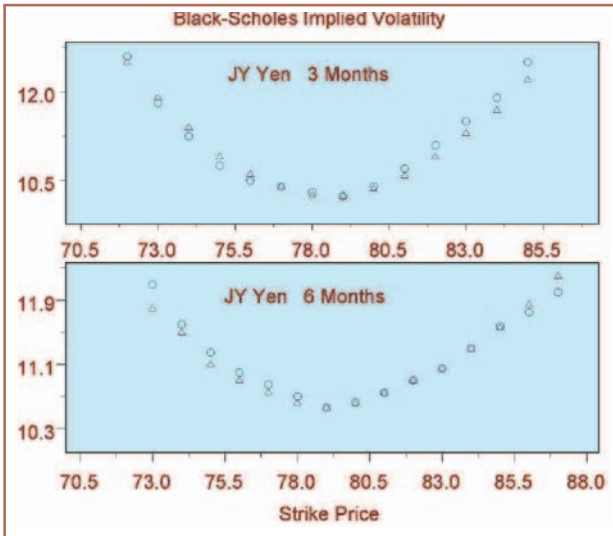

▲ **Fig.3:** Theoretical implied Black-Scholes volatilities from the $q = 1.4$ model (triangles) match empirical ones (circles) very well, across all strikes and for different times to expiration.

From all that has been said up to now, it is really quite clear that the *true* model of stock price fluctuations has many challenging statistics to reproduce, in addition to correctly pricing derivative instruments. Furthermore, it would be desirable that the mechanisms of such a model are somewhat intuitive. With these goals in mind, the field of nonextensive statistical mechanics has made some progress in recent years although of course there is still a long way to go both within and beyond this framework.

As already mentioned in passing, returns (once demeaned and normalized by their standard deviation) have a distribution that is very well fit by q-Gaussians with $q \approx 1.4$ [4], only slowly becoming Gaussian ($q \to 1$) as the time scale approaches months or years. Another interesting statistic which can be modeled within the nonextensive framework, is the distribution of volumes, defined as the number of shares traded. A q-exponential multiplied by a simple power of the volume presents power laws at both high and low volumes and fits very well to the data [4]. These results are encouraging, albeit they are macroscopic descriptions of the data and a dynamical description of the underlying processes is of course desirable. For the volumes, such a model was recently proposed. For stock prices, a class of models that has had some success in option pricing was introduced a few years ago [5], based upon a statistical feedback process. Recently, that model was extended to incorporate memory over multiple time-scales [6] (recovering a class of long-ranged GARCH models [7]) and seems to reproduce most of the stylized facts of financial time series. Other interesting models related to the nonextensive thermostatistics include an ARCH process with random noise distributed according to a q-Gaussian as well as some state-dependent additive-multiplicative processes [8]. These models do capture the distribution of returns, but not necessarily the empirical temporal dynamics and correlations.

In the statistical feedback model, price fluctuations are assumed to evolve such that the Tsallis entropy is maximized. This leads to an instantaneous volatility which is proportional to a power of the probability of the most recent price: It is large when price moves are exceptionally large (or rare); conversely, the volatility is smaller if the price moves are more moderate (or common). This mechanism is an attempt to model the collective behavior of market players. The statistical feedback tries to reflect market sentiment. Mathematically, it leads to a non-linear diffusion equation for the price. Exact time-dependent solutions to this equation can be found resulting in a Tsallis distribution for price changes at all times, and volatility clustering is also present. The entropic index q which characterizes the resulting distribution depends on the power of the statistical feedback term. If $q = 1$, the power vanishes so there is no statistical feedback and the standard Gaussian model is recovered. If $q > 1$, the power is negative and fat tails are present. This model has been quite successful for the purpose of option pricing, again largely due to the fact that one can actually calculate a lot of things analytically, and in particular one obtains closed-form solutions for European options.

Since a value of $q = 1.4$ nicely fits real returns over short to intermediate time horizons (corresponding to 4 degrees of freedom with the Student formulation), this model is clearly more realistic than the standard Gaussian model. Using that particular value of q as calibrated from the historical returns distribution, fair prices of options can be calculated easily and compared with empirical traded option prices, exhibiting a very good agreement. In particular, while the Black-Scholes equation must use a different value the volatility for each value if the option strike price in order to reproduce theoretical values which match empirical ones, the $q = 1.4$ model uses just one value of the volatility parameter across all strikes. One can calculate the Black-Scholes implied volatilities corresponding to the theoretical values based on the $q = 1.4$ model, and a comparison of with the volatility smile observed in the market will reflect how closely the $q = 1.4$ model fits real prices (Fig. 3).

Although quite successful, this model is not entirely realistic. The main reason is that there is one single characteristic time in that model, and in particular the effective volatility at each time is related to the conditional probability of observing an outcome of the process at time t *given what was observed at time* $t = 0$. For option pricing this is perfectly reasonable; one is interested in the probability of the price reaching a certain value at some time in the future, based entirely on one's knowledge now. But this is a shortcoming as a model of real stock returns; in real markets, traders drive the price of the stock based on their own trading horizon. There are traders who react to each tick the stock makes, ranging to those reacting to what they believe is relevant on the horizon of a year or more, and of course, there is the entire spectrum in-between. Therefore, an optimal model of real price movements should attempt to capture this existence of multiple time-scales and long-range memory.

Indeed, by including a kind of statistical feedback over multiple timescales a model is obtained which seems to account for most stylized facts of financial time series (Fig. 4). The distribution of returns are fit well by Tsallis-Student distributions. As the time horizon of returns increase, the distribution approaches Gaussian in the same way as empirical data. Long range volatility clustering is present, with a decay that matches real data. The distribution of instantaneous volatility is close to log normal. Subtle effects like the multifractal spectrum and Omori analogue are reproduced. In particular, the time-reversal asymmetry is inherent. Although some of these statistics can be calculated analytically, most are obtained through numerical simulation. In principle, the model can be used for option pricing via Monte-Carlo simulations, but analytic option pricing formulae would be very welcome. Obtaining these is still an open problem.

A final interesting remark on the implications of this model is that the parameters which calibrate to empirical data put the model close to an instability. This suggests that the dynamics of financial markets are operating on the brink of non-stationarity. In fact, this mathematically perhaps undesirable property is

philosophically quite desirable; in reality, financial markets indeed appear only quasi-stationary and as we have seen historically, they can completely break down and crash. Another implication of the model is that it predicts a large correlation between the present volatility and past price changes, which was verified empirically. This questions the efficient market hypothesis which states that all information relevant to the stock is immediately absorbed and reflected in the price and that the past price history can have no influence on investor behavior. The long-memory volatility model states otherwise however.

To bring an analogue to physics, this fact is in a sense akin to the notion that Boltzmann-Gibbs statistical mechanics works well for systems with short-range interactions and short-term memory. If long-range interactions or long-memory is present, one must go beyond the standard framework. In a similar fashion, the long-memory in financial markets forces us beyond the standard paradigm and we must perhaps rethink some very well-established ideas in a new light.

References

[1]] V. Plerou, P. Gopikrishnan, L.A. Amaral, M. Meyer, H.E. Stanley, *Phys. Rev. E* **60** 6519 (1999);

[2] J.P. Bouchaud and M. Potters, *Theory of Financial Risks and Derivative Pricing,* Cambridge University Press, 2004.

[3] For reference see e.g. J. Hull, *Futures, Options and other Financial Derivatives,* Prentice Hall, 2004.

[4] Cf. M. Gell-Mann and C. Tsallis, *Nonextensive Entropy - Interdisciplinary Applications,* Oxford University Press, NY, 2004.

[5] L. Borland, *Quantitative Finance* **2**, 415-431, (2002).

[6] L. Borland and J.P. Bouchaud, *On a multi-timescale statistical feedback model for volatility fluctuations,* physics/0507073 (2005).

[7]] G. Zumbach, P. Lynch, *Quantitative Finance*, **3**, 320, (2003).

[8] S.M. Duarte Quieros, C. Anteneodo, C. Tsallis, *Power-law distributions in economics: a nonextensive statistical approach, in Noise and Fluctuations in Econophysics and Finance,* eds. D. Abbot, J.-P. Bouchaud, X. Gabaix and J.L. McCauley, Proc. Of SPIE 5848, 151 (SPIE, Bellingam, WA 2005). [physics/0503024].

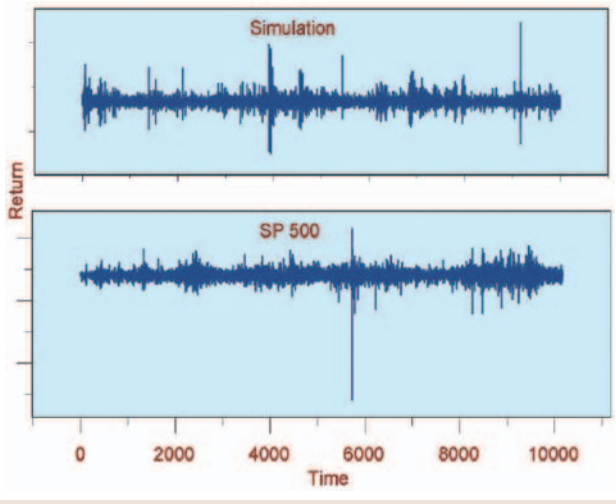

▲ **Fig.4:** A time series of returns simulated with the long-memory multiple time-scale feedback model (top) and the daily returns since 1965 of the SP 500. The simulated series reproduces most of the stylized facts of the real data.

2006 Europhysics Conferences

Atmospheric Science Conference
8 - 12 May 2006 • Frascati, Italy
Contact: Prof. Claus Zehner, ESA/ESRIN,
Via Galileo Galilei, CP 64 • IT-00044 Frascati, Italy
Tel: +39 06 94180 544 • **Fax:** +39 06 94180 552
Email: czehner@esa.int
Website: http://earth.esa.int/atmos2006

18th European Conference on Atomic and Molecular Physics in Ionized Gases • ESCAMPIG-18
12 - 16 July 2006 • Lecce, Italy
Contact: M.Cacciatore, CNR-IMIP c/o Department of Chemistry
University of Bari • IT-70126 Bari, Italy
Tel: +39 08 05442101 • **Fax:** +39 080 5442024
Email: mario.cacciatore@ba.imip.cnr.it
Website: http://escampig18.ba.imip.cnr.it

GIREP 2006 Modeling in Physics and Physics Education
20 - 26 August 2006 • Amsterdam, The Netherlands
Contact: Prof. Ton Ellermeijer,
Amstel Institut, Kruislaan 404
NL-1098 SM Amsterdam, The Netherlands
Tel: +31 20 525 5963 • **Fax:** +31 20 525 5866
Email: ellermei@science.uva.nl
Website: www.girep2006.nl

2006 Sponsored Conferences

European XRay Spectrometry Conference • EXRS2006
19 - 23 June 2006 • Paris, France
Contact: EXRS 2006 Secretariat
Laboratoire National Henri Becquerel, CEA Saclay
F-91191 Gif-sur-Yvette, France
Fax: +33 1 69 08 26 19 • **Email:** exrs2006@cea.fr
or Dr. Alexandre Simionovici
ENS-Lyon, 46 allée d'Italie • 69007 Lyon, France,
Tel: +33 472 72 86 97 • **Fax:** +33 472 72 86 77
Email: alexandre.simionovici@ens-lyon.fr
Website: www.nucleide.org/exrs2006

2nd International Workshop on Physics and Technology of Thin Films • IWTF2
26 - 30 June 2006 • Prague, Czech Republic
Contact: Dr. Zdenek Chvoj,
Institute of Physics AV CR, Na Slovance 2
CZ-182 21 Praha 6, Czech Republic
Tel: +420 220 318 530 • **Fax:** +420 233 343 184
Email: chvoj@fzu.cz
Website: www.fzu.cz/activities/workshops/iwtf2

10th International Conference on the Structure of Non-Crystalline Materials • NCM10
18-22 September, 2006 • Praha, Czech Republic
Contact: Prof. Ladislav Cervinka,
Chairman of the NCM10 Conference,
Institute of Physics,
Academy of Sciences of the Czech Republic, Strizkovska 78
CZ-180 00 Praha 8 - Liben, Czech Republic
Tel: +420-28484 2448 • **Fax:** +420-28484 2446
Email: L.Cervinka@icaris.cz
Website: www.icaris.info/NCM10

1 J.P. Ansermet, M.C.E. Huber, C. Rossel and Ingrid Kissling-Näf
2 M. Gell-Mann receiving the Einstein medal at the opening ceremony
3 World Year of Physicss 2005 flag floats over Bern
4 The editors: G. Morrisson and Claude Sébenne at work
5 The magnetic cannon of Europhysics Fun
6 The main building at the University of Bern

2

4

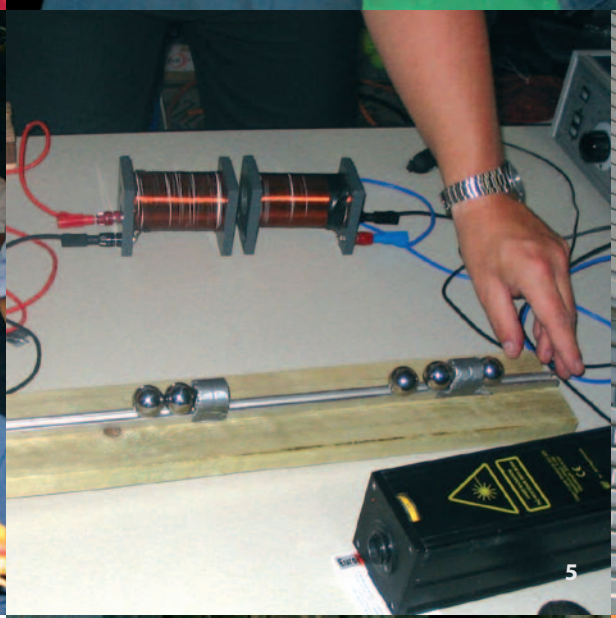

5

6

8

9

7 S. Bagayer and R. Apanasevitch at the Council 2005 dinner
8 P. Melville at the Jungfraujoch
9 The past and present President: M.C.E. Huber and O. Poulsen